ISAS - INTERNATIONAL SCHOOL FOR ADVANCED STUDIES

January 1994

Chemical Abundances in Three Population II Stars

Thesis submitted for the degree of

"Doctor Philosophiae"

Candidate

Piercarlo Bonifacio

Supervisors

Prof. Dennis W. Sciama

Prof. Margherita Hack

TRIESTE

SISSA - SCUOLA INTERNAZIONALE SUPERIORE DI STUDI AVANZATI
TRIESTE
Strada Costiera 11

January 1994

Chemical Abundances in Three Population II Stars

Thesis submitted for the degree of

"Doctor Philosophiae"

Candidate

Piercarlo Bonifacio

Supervisors

Prof. Dennis W. Sciama

Prof. Margherita Hack

INDEX

Acknowledgements:

The work presented in this thesis was developed in a time span of over five years, it would therefore be impossible to adequately thank all of the people, of the Trieste astronomical community, who have helped me through small and big difficulties and have taught me astronomy as well as physics and a bit of understanding of human nature. To them I dedicate this work.

I am indebted with Dr. R.L. Kurucz for hospitality during a short visit at CfA and continuous encouragement and support in using his codes and data. I also wish to thank the Director and staff of Observatoire de Haute–Provence for warm hospitality and precious assistance during the observational runs at that observatory. This work has made use of the SIMBAD data base which is operated by CDS at Strasbourg.

Introduction

The purpose of this thesis is to describe the abundance analysis of three Pop II stars. Chapter one is a historical review aimed at illustrating how the present–day concepts on stellar populations and the formation of the chemical elements came about. Chapter 2 describes the current views on the chemical an dynamical history of the Galaxy. Chapter 3 contains a brief description of two classes of Pop II stars: blue HB stars and extremely metal–poor G–type stars.

The stars which are the object of this thesis belong to these two classes. Feige 86 is a field HB star which has an anomalous chemical composition. We shall argue, in chapter 6, that it represents a Pop II analogue of the Pop I CP stars. Instead CS 22881-39 and CS 22885-96 are "normal" G–type giants whose peculiarity is that the iron abundance is some two orders of magnitude *below* that of the most metal poor globular clusters. This metal deficiency is taken as evidence that these stars were formed out of extremely metal–poor gas, and is not attributed to some sort of atmospheric peculiarity as is the case for the anomalous abundances of Feige 86.

Chapter 4 reviews some of the methods used to fix the atmospheric parameters of B–type and G–type stars. Chapter 5 is devoted to the study of the far UV spectrum of the Pop I B–type star ι Her . The reason for performing this study, and for including it in this thesis, is to provide a "standard" spectrum against which the spectrum of "peculiar" objects, such as Feige 86, may be compared. This "standard" spectrum also provides an ideal test ground for the spectrum synthesis code used throughout this work.

Chapter 6 describes the abundance analysis of Feige 86. Chapter 7 describes the abundance analysis of CS 22881-39 and CS 22885-96. In the appendices we provide plots of the UV spectra of ι Her and Feige 86.

Chapter 1

Stellar Populations and Chemical Elements

1.1 Baade's populations: high and low velocity stars

It was Baade in 1944 who was the first to suggest that the stars in our Galaxy ought to be divided into two distinct populations: the first, which he called Type I gave rise to an ordinary H–R diagram, whereas the other, which he called Type II, gave rise to an odd–looking H–R diagram in which the Hertzsprung gap was populated by stars lying on a horizontal branch extending to the blue up to late B–type. This situation is typical of globular clusters. Baade observed that the stars in the bulge of the Andromeda nebula, had an H–R diagram which was kin to that of globular clusters in our own galaxy.

When Baade wrote his paper it had been known for almost twenty years that the kinematics of the stars in the galaxy suggested a two component system. Oort (1926) studied the distribution of radial velocities of stars and showed this to be a gaussian up to about 60 kms^{-1}, but above that velocity the number of counts shows a " considerable excess over the gaussian curve and a very much lower decrease". Oort also produced a catalogue of high velocity stars with reasonably well known parallaxes and kinematic data, whose absolute space velocity was greater than 62 kms^{-1}(where he set the boundary between high and low velocity stars). He used this catalogue to investigate the properties of high–velocity stars. His findings may be summarized as follows:

1. Highly luminous O and B stars are not found among high–velocity stars;
2. The mean absolute magnitude of dwarfs of a given spectral type is the same for both types of stars;
3. The percentage of G,K and M giants is higher for high–velocity stars than for low–velocity stars;
4. The percentage of double stars is lower among high velocity stars.

Baade was well aware of Oort's work and did not hesitate, especially on account of points 1. and 3. above, to ascribe high–velocity stars to his Type II. Needless to say that globular cluster stars (Baade's prototypes of galactic Type II stars) are high–velocity.

The different kinematics hinted that the two stellar populations had a different origin and history, yet it gave no clues to explain the difference in the morphology of the H–R diagram. Other astrophysical differences had to be sought for. It was well known, since the twenties that high velocity giants showed weak CN bands and strong CH bands (Lindblad, 1922; Keenan, 1942; Morgan *et al.*,1943). Undoubtedly Baade's work stimulated a lot of further work on the spectra of high–velocity stars, which confirmed the earlier findings on CN and CH bands (Popper,1947; Keenan *et al.*,1948), however there were also hints that the metal content of Type II stars might be lower. Schwarzschild& Schwarzschild (1950) analysed 5 low–velocity and 4 high–velocity F type dwarfs with high resolution spectroscopy and, besides confirming the strengthening of the CH bands in high–velocity dwarfs (as was earlier found in giants), they suggested that the iron over hydrogen ratio "might be lower in the high–velocity dwarfs by a factor of approximately 2 as compared to the low velocity dwarfs". In the same year Roman (1950) showed that among late F and early G type stars there appear to be two distinct groups: weak–line stars and strong–line stars. The kinematics of the two groups was markedly different: the strong–line stars had a smaller mean velocity and velocity dispersion than the weak–line stars.[1]

---

[1] For the reader's curiosity: Roman found a mean velocity of 28.1 $\mathrm{kms}^{-1}$with a velocity dispersion of 13.8 $\mathrm{kms}^{-1}$for strong–line stars and a mean velocity of 43.9 $\mathrm{kms}^{-1}$with a velocity dispersion of 23.9 $\mathrm{kms}^{-1}$for weak–line stars

It was tempting to identify line weakness with low abundance. Many objected to this in view of the theoretical difficulties of treating line formation in a stellar atmosphere. Through a careful analysis of the chemical equilibrium Schwarzschild *et al.*(1951) showed that the weakening of CN and strengthening of CH bands could indeed be ascribed to a diminished metal abundance. These authors suggested that this could be due to the fact that Type I stars were formed in interstellar clouds which were enhanced in metals due to the presence of grains. Spectroscopic analysis by the use of curve of growth methods as well as model atmospheres by Chamberlain and Aller (1951) showed two "A–type subdwarfs" to be markedly deficient in iron and calcium[2]. Further work on F–type subdwarfs by Roman (1954) showed that high velocity stars could be picked up with spectroscopic criteria (weak metal lines for a given effective temperature). Moreover she was able to show, contrary to the claim of Oort (1926), that the absolute magnitudes of F-type high-velocity stars where one to two magnitudes below the main sequence. She also pointed out that high–velocity, weak–line stars have an ultraviolet excess of about 0.2 magnitudes. The existence of this UV excess was later confirmed for globular cluster stars. Many clues suggested that Pop II stars are deficient in heavy elements with respect to the sun. However a detailed spectroscopic study of globular cluster as well as galactic Population II stars, showing the reality of this metal–deficiency had to wait a few more years (Helfer *et al.*1959).

---

[2] The atmospheric parametrs derived by Chamberlain and Aller for the two stars HD 19445 and HD 140283 suggested a spectral type F . They had been classified as A4sp and A5sp in the Mount Wilson Spectroscopic Parallax Catalogue (Adams *et al.*, 1935) based on the weakness of the metallic lines, which Chamberlain and Aller showed to be due to the metal deficiency

That the stars of the globular clusters should be deficient in the metallic elements was also suspected on the basis of the evolutionary tracks computed by Hoyle and Schwarzschild (1955): they could well reproduce the red giant branch of the old galactic cluster M67 with tracks computed assuming solar abundances, but, in order to reproduce the brightest tip of the red giant branch of globular clusters, they had to lower the metallicity of their models by two orders of magnitude. To explain these results it was necessary to understand the origin of the chemical elements.

1.2 The Origin of The Chemical Elements

By the mid–fifties the topic of stellar populations had become intimately related with that of the origin and distribution of the elements. Ever since it was understood that element transmutation could take place, it was clear that the present distribution of the elements should hold memory of the past history of the universe. In one of the earliest papers devoted to the subject Tolman (1922) worked out the thermodynamics of the reaction which led to the formation of He from protons. His result was that, provided equilibrium is attained, hydrogen should completely combine to form He. That H and He coexist in terrestrial and stellar environments is clearly at odds with this conclusion. Tolman did not account for the effect of the Coulomb barrier, which makes the reaction so slow at temperatures typical of a planetary, or stellar, atmosphere environment that equilibrium may not be attained. However at temperatures typical of stellar interiors the reaction rate is high enough that equilibrium is reached and Tolman's thermodynamics may still be held valid, at least qualitatively. Indeed more refined calculations as well as observations do show that under such conditions the He forming reactions will

continue essentially until all the available H is used up, as predicted by Tolman. This was the first suggestion that one should expect a chemical evolution of the universe, at least from a thermodynamical point of view. In the following years the problem was tackled from, essentially, three directions:

1. equilibrium theory;
2. non–equilibrium theory;
3. polyneutron theory.

1.2.1 Equilibrium Theory

Equilibrium theory tried to explain the observed abundances by assuming them to be the result of a statistical equilibrium of nuclear reactions. To my knowledge the first serious attempt in this direction was that of Sterne (1933). The first extensive computations were those of Chandrasekar and Henrich (1942) and Klein *et al.*(1945). The latter authors obtained a good agreement with observations for elements with A $\leq$ 50 but their predicted abundances fell far below the observed values for the heavier elements. The site of these *e–processes* was usually undefined and referred to as the *prestellar state.* Following the authoritative paper of Bethe (1939) the generally held opinion was that the synthesis of elements heavier than helium was negligible in ordinary stars. One therefore had either to postulate the existence of very special stellar types or to seek for a primordial locale for element synthesis. The existence of a state of the universe characterized by high density and temperature, some time back in the past was obviously suggested by the present expansion of the universe. The characterization of this early state was left rather vague. Klein and collaborators had in mind an ensemble of stellar–mass objects in thermal equilibrium with an intense radiation field. A similar picture was envisaged by Beskow and Treffenberg (1947) who considered stellar

models of various masses (39 $M_\odot$, 15 $M_\odot$ and .31 $M_\odot$) embedded in a sea of radiation of temperature 1 MeV. Chandrasekar and Henrich (1942), on the other hand, had in mind a more or less uniform, roughly isothermal, distribution of matter and radiation, which underwent rapid cooling, either due to the expansion of the universe or to some other mechanism, such as energy loss through neutrino emission. It is interesting to quote Chandrasekar and Henrich's concluding remark on the *prestellar state*: "In conclusion, it should perhaps be emphasized that the considerations of this paper should be regarded as of a purely exploratory nature and that such *agreements* as may have been obtained should not be overstressed. It should, indeed, be remembered that we are dealing here with a stage of the universe in which conditions were utterly different from the present conditions. To emphasize this fact, it may be remarked that at an average density of the order of 10^7 g/cm^3 the entire mass in the universe (*ca.* 10^{54} g) may be inclosed in a sphere of radius of the order of 10^{16} cm, i.e. somewhat less than a hundredth of a parsec.". This ought to be a memento, to theoreticians, of the conceptual difficulties involved in extrapolating physical laws outside the known range of applicability.

The main difficulties of equilibrium theories were the formation of the heavy elements and the " freezing–in " mechanism, by which the abundance distribution, determined during the equilibrium state, was maintained when the universe moved away from this state. Related to the latter is the objection raised by Gamow (1946), who noted that when the density of the universe was of the order of 10^6g/cm^3 the expansion of the universe " must have been proceeding at such a high rate, that this high density was reduced by an order of magnitude in only about

one second". While such a rapid expansion could provide an efficient freezing–in mechanism it was doubtful whether this time scale would be long enough for equilibrium to be attained.

1.2.2 Non-Equilibrium Theories

The above considerations led Gamow (1946) to consider non–equilibrium reactions in the "universal prestellar state" , as he called it. He was also the first to take into account neutron capture processes. In the following years non–equilibrium theory was developed to a considerable degree of complexity by Gamow himself in collaboration with Alpher, Herman and Bethe (Alpher *et al.*1948; the notorious $\alpha\beta\gamma$ paper). The theory and main results are reviewed by Alpher and Herman (1950, 1953). The details of the theory depend upon the physical state of the early universe, which, in turn, depends upon a specific cosmological model.

1.2.3 Polyneutron Theory

A totally different attack is provided by the "polyneutron theory" of Mayer and Teller (1949). These authors noted that, while for light elements the most abundant isotopes are the lightest, the reverse is true for heavy elements. They took this as evidence that heavy elements were formed in presence of a neutron excess [3]. Mayer and Teller postulated the existence, in the early universe, of stellar mass bodies composed of a nuclear fluid of neutrons. Such bodies may form droplets of nuclear fluid, due to surface tension. Such droplets may evaporate,

---

[3] incidentally this conclusion is still believed to be valid, the most popular point of view is that heavy elements are formed through neutron capture processes, either slow or rapid, see section 1.3.2.

undergo β decay and, eventually, end up as the heavy nuclei which we observe today.

1.2.4 The role of stars in nucleosynthesis

All three theories had some appealing features, but none succeeded in explaining satisfactorily the observed abundances of the elements. A weak point of all three theories was that each demanded the existence of matter in a particular primordial state, for which no direct evidence was available. On the other hand, in the late forties and early fifties it had become clear that stellar interiors did show physical conditions which would allow synthesis of, at least, the lightest elements. Hoyle (1947), noted also that hydrogen is, by far the most abundant element in the universe, however, from the point of view of nuclear physics, it is also the most unstable, as was correctly predicted by Tolman's (1922) thermodynamics. Thus Hoyle concluded that, some time back in the past history of the universe, it was the only element present. Hoyle tried to explain the abundance distribution starting from three simple hypothesis:

1. initially only H is present in the universe;
2. He is synthetized in ordinary stars;
3. a further process synthesizes the heavy elements.

Hoyle was able to show that a collapsing star could provide a suitable site for the synthesis of the heavy elements. He also envisaged how such a star could cast off chemically enriched material through rotational instability.

In the same year Van Albada (1947) noted that formation of very heavy elements could take place only if the neutron gas was degenerate. If it were not, rapid fission would destroy these elements. On the other hand the theory developed by Chandrasekar (1939) on white dwarfs implied that there existed a limiting mass

for an equilibrium configuration of a degenerate fermion gas. Van Albada claimed that this ruled out the possibility of forming heavy elements in the prestellar stage. He pointed out that degenerate cores of massive stars, on the other hand, could provide a suitable site for heavy elements synthesis. He also realised that the building up of such heavy elements would make the star unstable, so that it would give rise to a supernova outburst. For lighter elements one needs not to worry about the decay through fission, thus, Van Albada argued, they could be synthesised in non-degenerate stellar cores as well as in the early universe.

Both the work of Van Albada and that of Hoyle implied that the chemical composition of stars and interstellar matter should go through an evolution. However at that time evidence for such an evolution was still lacking.

1.3 1957– The Vatican Conference and B^2FH

The year 1957 was a key year both for the studies on the origin of the elements and for that of stellar populations.

1.3.1 The Vatican Conference

In May 1957 a very small number of well–known scientists met at the Vatican City for the "Semain d'Etude" on stellar populations, organized by father O'Connell, then director of the Vatican Observatory. This was rather unlike any of the conferences we are used to. It was designed to review the current understanding on stellar populations and, in a fashion customary to the Roman Catholic Church, to "establish a doctrine"; a point was made that whenever there were two or more discrepant theories or interpretations one should be chosen and if that

were not possible the reasons for this impossibility should be clearly explained. The conference was highly successful, the team of scientists which was invited was, indeed, formidable. Many of the basic concepts which are the common background of present–day astronomers were established at that conference. It would be impossible to summarize in a few pages the wealth of observational data and theoretical understandings which were presented at the conference. The proceedings of the conference make, even today, a very interesting reading. The key points which are of interest to the present thesis are:

1) The populations form a one–dimensional sequence differing in age. It was agreed to divide this sequence into five populations.
2) Population II stars have a roughly spherical distribution, move about the galactic center on highly elliptical orbits and show up in the solar neighbourhood as high velocity stars.
3) The older stars are deficient in metallic elements.
4) The difference in chemical composition may be understood in terms of a building–up process which starting from hydrogen forms all of the heavier elements in stellar interiors. The elements so synthetized are input in the interstellar medium through a number of mechanisms (supernovae, novae, stellar winds...) The subsequent generations of stars which form out of polluted gas show enhanced metal–abundance.

The four above–mentioned points provide the basic framework within which most of subsequent work on stellar populations has been developed. It shows a way to interpret the chemical and kinematical differences of stellar populations in terms of formation and evolution of stars. There were still many bits of observational evidence which did not fit into this framework. The very same year Morgan & Mayall (1957) reported that the spectrum of M31 had cyanogen bands of normal

strength, like that of Pop I stars. This could be reconciled with the orthodox view that Pop II stars have low metal abundance by assuming that the main contribution to the light of M31 was due to Pop I stars. We shall discuss in the next chapter our present understanding of the links between age and metallicity.

1.3.2 B^2FH

Point 4) of the previous section was forcefully put forward at the Vatican Conference by F. Hoyle and R.A. Fowler who, in collaboration with G.R. and E.M. Burbidge had been working on an element formation theory which rendered obsolete all preexisting theories discussed in section 1.2. This theory was presented in a paper which is one of the cornerstones of modern astronomy (Burbidge *et al.*, 1957, universally known as B^2FH) which was published in October that year. The key point was that the elements are synthetized in stellar interiors, this hypothesis had two appealing features: 1) it was not necessary to postulate the existence of some particular *prestellar state* and 2) the inhomogeneities in abundance distribution, such as the differences in chemical composition between Pop I and Pop II stars could be easily accounted for. This last point was fatal for theories which sought a "primordial" origin for the elements. B^2FH identified not less than eight nuclear processes responsible for the current distribution of elements, they also pointed out that the complexity of the theory was a point in its favour, since the abundance curve is complex [4]. The processes invoked were

1) H burning;

2) He burning;

---

[4] this is, epistemologically, a rather unorthodox view, in fact it seems the exact reverse of Occam's razor !

3) α process: this is the process by which α particles are added to Ne^{20} to synthetize the nuclei Mg^{24}, Si^{28}, S^{32}, Ar^{36}, Ca^{40} and probably Ca^{44} and Ti^{48};

4) *e* process: it is an equilibrium process by which, under conditions of extremely high temperatures and pressures, the iron peak elements are synthetized;

5) *s* process: this is the slow neutron capture process, neutrons are captured at a rate which is small compared to the intervening β decays. It takes place on long time scales from 10^2 to 10^5 years;

6) *r* process: this is the rapid neutron capture process, the time scale is short compared to that of intervening β decays, of the order of 10^{-2} to 10 seconds;

7) *p* process: this is the capture of a proton, with emission of a photon or the emission of a neutron, following absorption of a photon;

8) *x* process: this is the collective name by which B^2FH indicate the processes responsible for the formation of the light nuclei, D, Li, Be and B.

Although B^2FH assumed these processes to take place in stars, during various phases of their evolution, from the standpoint of nuclear physics, their processes are applicable also in a primordial environment if temperature and pressure have suitable values.

1.4 Primordial fireballs: the prestellar state, again!

B^2FH were far more successful in predicting the observed abundances of elements than their predecessors, however a large discrepancy remained for He. It turned out that stars were poor producers of He, this led Hoyle and Tayler (1964) to go back to the idea of a primordial synthesis of He or, alternatively, the synthesis by *supermassive objects*, i.e. objects which had a mass in excess of $10^3 M_\odot$.

In 1965 Penzias & Wilson discovered the microwave background radiation which was readily interpreted as the remnant of a primordial fireball (Dicke *et al.*, 1965). This greatly revived the interest in the initial phases of a Friedman universe following the lines earlier drawn by Alpher, Bethe and Gamow (1948, cf. section 1.2.2). The microwave background and the recession of galaxies (Hubble's law) strongly favoured a cosmological model in which the universe was initially hot and dense. Such models are characterized by an initial singularity. Such models are usually referred to as Hot Big Bang models or simply Big Bang models, because of this singularity[5]. This initial condition was a suitable site for primordial nucleosynthesis. The details of this were explored by Wagoner, Fowler and Hoyle (1967) in another fundamental paper. The basic assumptions were:

1) general relativity (with a zero cosmological constant) describes the dynamics of the universe;
2) the universe passed through a phase in which the temperature exceeded 10^{11} K;
3) the universe was approximately homogeneous and isotropic;
4) the electrons were non-degenerate.

A fact which is often forgot by people quoting this paper is that the nucleosynthesis was meant to apply either to the universe in its early stage or *to interiors of stars with masses exceeding* $10^3 M_\odot$. Both sites were considered as likely candidates for the synthesis of He. The results of this paper which will be relevant in the following chapters are:

1) He may be produced in a primordial fireball as well as in massive objects, provided that temperatures of the order of 20×10^9 K are obtained. The He

---

[5] I have not been able to trace back in the literature the first occurrence of this term, it was not used before 1957 and in 1965 it had become a standard notion.

fraction produced is somewhere between 0.2 and 0.3 by mass for the primordial fireball, but can be higher in massive objects;[6]

2) traces of D, He^3 and Li^7 are also produced in primordial fireballs;

3) elements heavier than Li^7 are *not* produced in primordial fireballs;

4) for nuclei with $A \geq 12$ the abundances are nothing like the solar abundances for either primordial fireballs or massive objects.

These correspond to conclusions 1),2),3) and 8) of the paper of Wagoner *et al.*(1967).

1.5 A General framework

We are now in the position to describe the general framework of ideas on stellar populations and nucleosynthesis which emerged in the early seventies and is the starting point for our present understandings.

The standard Big Bang theory (Wagoner *et al.*, 1967) is quite successful in predicting the observed He/H ratio, a feature which other theories on the formation of chemical elements, such as polyneutron theory or equilibrium theory, lacked. However it fails to predict the formation and relative abundances of all other elements. It thus seems that if we accept the Big Bang theory, or some modification of it, we are led to the inescapable conclusion that all elements heavier than He ("metals" in the astronomer's jargon) must have been formed elsewhere, in successive times. The B^2FH paper is still of paramount importance, since it is

---

[6] note that if we were to interpret the He abundance in He strong stars as being primordial this would rule out the primordial fireball, but would leave the door open for synthesis in massive objects

focussed on the nuclear physics of element formation and predicts which reactions will take place under suitable conditions, irrespective of the site where these conditions are fulfilled. Thus B^2FH still provides the basic framework within which we can understand nucleosynthesis.

It is very natural to identify the sites of nucleosynthesis of elements heavier than He with stellar interiors. We find there suitable temperatures and pressures for nuclear reactions to occur. Supernovae provide a viable mechanism to eject the nucleosynthesis products into the ISM, other mechanisms may be sought and may indeed be important, but what is germane here is that there exists at least one obvious way to enrich the ISM with the elements produced in stellar interiors. One should also keep an open mind towards the possible existence of other sites for nucleosynthesis. Until not long ago one of the most popular theories to explain the abundance anomalies in CP stars was nucleosynthesis (Burbidge & Burbidge, 1955) occurring in the *external* layers of the stars. The theory assumed that particles could be accelerated by the betatron mechanism (Swann, 1933 , Riddford & Butler, 1952) to speeds largely exceeding the local thermal speed, thus acquiring enough energy to undergo nuclear reactions. The theory has presently been dismissed, on the account of its failure to produced observed abundance patterns in CP stars, in particular the lack of evidence for an odd–even effect which would be expected if nuclear reactions were involved. It is however interesting to notice how it is possible to conceive physically plausible sites of nucleosynthesis other than stellar interiors.

Chapter 2

The Galaxy and its history

2.1 Introduction

In this chapter we depart from the historical development of the subject and try to describe our present understanding of the past chemical and dynamical history of the Galaxy.

2.2 The Galaxy: a schematic view

In this section we wish to outline schematically the structure of the Galaxy to be used as reference in the subsequent discussion. We shall distinguish 4 or 5 components:

1) extended disk or thin disk/thick disk

2) metal–weak halo

3) central bulge

4) the system of globular clusters

1) The disk is flat (scale height of the order of 200-300 pc) radially extended (of the order of a few kpc) and rotates rapidly (at the galactocentric distance of the sun $v_{circ} \approx 220$ kms^{-1}). There is material which has a larger scale height and velocity dispersion, which was highlighted by Gilmore & Reid (1983), this is usually referred to as the "thick disk" (Gilmore & Wyse, 1985, Wyse and Gilmore ,1986 ; see also Gilmore *et al.* 1989). The existence of such disks with considerable vertical extension was noted for the first time by Van der Kruit & Searle (1982) in external galaxies of Hubble type similar to ours. Whether this is a discrete component or is just the tail of an "extended disk" configuration (Norris & Ryan, 1991) is still open to debate. We shall come back on this point later.

2) We call "metal–weak–halo", following Zinn (1986) and Freeman (1986), all the halo field stars and the globular clusters with [Fe/H]< -1.0. This definition differs from that of "halo" found elsewhere in the literature (e.g. Pagel & Edmunds, 1981) for the exclusion of the metal–rich globular clusters. The halo is a spheroid and is rotating slowly, there have been suggestions that this rotation may be retrograde (Majewski, 1991,1992). The net angular momentum of the halo is essentially zero (Carney, Latham and Laird 1990).

3) The central bulge is relatively little studied, due to the observational difficulties [1]. Its integrated colours are distinctively red and similar to those of globular clusters. On the basis of this evidence Baade classified its stars as Pop II. The study of Rich (1986, 1988) has shown that the bulge stars display a range in metallicities from 1/10 up to 7 times the solar abundance (look at figure 3 of Rich, 1988). The age of the bulge stars is still an open question, it seems possible that the bulge shows an age spread. The presence of RR Lyrae variables implies that at least a part of the bulge population is very old, but the age of these stars relative to globular clusters is uncertain. There have been suggestions that the bulge is a bar as is seen in external barred spiral galaxies (Blitz & Spergel, 1990 ; Whitelock, 1991). Carney, Latham and Laird (1990) suggested that the present–day structure of the bulge may result also from accretion of gas expelled from the halo. What is sure is that the bulge shows a very complex chemical and dynamical structure which may well be the result of a very complex history.

4) The system of globular clusters is not a homogeneous population, in any sense, chemical or dynamical. This had been suspected for a long time and it was

---

[1] the bulge stars are very far away and hence faint and the fields are very crowded, the non–resolved turn–off population provides a high background luminosity which must be subtracted from the observations

Baade himself who, at the Vatican Conference (1957), suggested that the more metal–rich clusters formed a flattened system which rotates faster than the more metal–poor clusters (which we have assigned to the halo population) which have a spheroidal distribution. This was demonstrated observationally by Zinn (1980, 1985) who suggested a subdivision into "inner" and "outer" halo, since the more metal–poor clusters tend to be at larger galactocentric distances.

2.3 Age–metallicity relation and abundance gradients

In the most naïve picture, one should expect that the stars formed more recently, out of enriched material, should have a higher metallicity, therefore metallicity ought to be some monotonically increasing function of time. If we combine this idea with simple concepts of galactic dynamics we can expect also the existence of abundance gradients with galactocentric distances if the time–scale for chemical evolution is shorter than the dynamical time–scale.

Observationally it is difficult to determine the existence, or lack of, both the age–metallicity relation (hereafter AMR) and abundance gradients, since both require the availability of a statistically significant, unbiased sample of stars. The first quantitative studies of the AMR where those of Mayor (1976) and Twarog (1980), who used Strömgren photometry to determine metallicities. The data of Twarog was revised by Carlberg *et al.*(1985) and Nissen *et al.*(1985) to take into account both a revision of the isochrones and a calibration of the (photometric) abundances. A plot of the data from Twarog (1980) and Mayor (1976) may be found in figure 1 of Chiosi & Jones (1983). A general trend of decreasing metal abundance with increasing age is clearly seen in the data of the four above–mentioned papers. However the existence of a one to one relation is questionable.

For the galactic disk the best available data is, presently, that of Edvardsson *et al.*(1993) who give abundances derived from high–resolution, high S/N spectra and model–atmosphere analysis for 189 disk stars with well defined selection criteria based on Strömgren photometry. They also provide accurate space motions and galactic orbital parameters, obtained for an assumed form of the Galactic potential, and ages, derived from isochrone fitting. The picture which emerges from this impressive amount of data is that "there is only a weak correlation between age and metallicity" (Edvardsson *et al.*,1993); moreover these authors have convincingly shown that the scatter in the AMR is real and not due to observational errors. This means that although, generally speaking the young stars are metal–rich, there are some *very old* stars of comparable metallicity. This means that there are parameters other than age which influence the chemical enrichment.

Edvardsson *et al.*(1993) investigated whether a simple age–metallicity relation exists for stars at a given galactocentric distance. They do indeed provide a tentative relation which links [Fe/H], age and galactocentric distance. However a large scatter exists around their relation. The radial abundance gradient which they find is in good agreement with those found by Grenon (1987, 1989). There is a general tendency for metallicity to decrease with increasing galactocentric distance. Note that if a relation of the kind proposed by Edvardsson *et al.* exists then, in order to get meaningful information about abundance gradients, one should measure abundances for stars of the same age.

For the halo the question is considerably more intricate. The pioneering work of Eggen *et al.*(1962, hereafter ELS), suggested that there are correlations between metallicity (as measured by the $\delta(U-B)_{0.6}$ index, for the definition of this index see chapter 4) and the modulus of a star's velocity perpendicular to the galactic plane, the eccentricity of its projected orbit and the angular momentum. This correlation

between chemical and kinematical properties was taken to indicate that the Galaxy formed by collapse from a larger volume with ongoing metal–enrichment and that this led to the formation of the disk through dissipation (Sandage,1986). The original ELS sample was enlarged by Sandage (1981) and Sandage & Fouts (1987) who came to essentially the same conclusions as ELS and claimed that there exists a metallicity gradient in the halo, although their conclusion applies to what they define as "lower halo", i.e. stars whose distance from the galactic plane is always less than 5 kpc.

Tackling the problem of abundance distribution from another point of view, Zinn (1980, 1985) studied the properties of a sample of globular clusters. His result was that there is a metallicity gradient between the "inner halo" ($R \leq 9$kpc) and the "outer halo" (R> 9kpc) and also within the "inner halo". There appears to be a wide range in metallicities in the zone 9kpc $<$ R $\leq$ 40kpc but there is no evidence for a gradient.

A sample of kinematically selected halo stars was presented in a series of papers by Carney and collaborators (Carney & Latham, 1987, Carney *et al.*1987, Laird *et al.*1989, Carney *et al.*1990, Carney, Latham and Laird, 1990 and other papers in the series) who, in one of these papers (Carney *et al.*, 1990), specifically investigated the metallicity gradient in the halo, their result was that there is no gradient. They also gave an explanation for the discordant result of ELS and Sandage & Fouts (1987). According to Carney *et al.*(1990) and also Norris & Ryan (1989) the $\delta(U-B)_{0.6}$ index is not suitable to trace abundances at very low metallicities, essentially because at low metallicities line blanketing becomes negligible. This may give rise to systematic effects which will results in apparent correlations between velocity and metallicity even if none exists (Norris & Ryan, 1989). Another interesting result of Carney *et al.*(1990) is that there exist a small

number of stars with halo kinematics, but almost solar abundances (look at their figure 3).

On the side of the age–metallicity relation Zinn (1980), from the study of HB morphologies of globular clusters, deduced that, for a given type of HB morphology, the more distant clusters are the *youngest*, in spite of the fact that they are more metal–poor. A similar result has more recently been found for *field* HB stars by Preston *et al.*(1991). They have shown that the mean unreddened colour $< B - V >_w$ [2] increases by about 0.025 mag going from 2 kpc to 12 kpc of galactocentric distance. By calibrating HB–morphology against two distinct time–dependent parameters they were able to show convincingly that this colour gradient is an age effect. Their final conclusion was that the mean age of the field population decreases by about 2 Gyr going from 2 kpc to 12 kpc of galactocentric distance.

2.3 Simple ideas on chemical evolution

We now want to understand, at least qualitatively, how chemical enrichment can proceed. Let us assume that the Galaxy was initially metal–free and that it evolves as a closed system. As time increase the gas is used up to form stars which synthetize heavy elements in their interiors, in some cases stars are able to eject these nucleosynthesis products, through supernovae explosions, stellar winds or other mechanisms about which we shall not bother. We ignore the elements which

---

[2] This quantity is defined by Preston *et al.*(1991) as $< B - V >_w = \sum I(B - V)/\sum I$ where I is a correction for incompleteness effect, for each star of magnitude B observed I(B) are present. Preston *et al.* limited their analysis to cases where $I(B) < 5$. The subscript w denotes the colour window defined by Preston *et al.* to isolate blue HB stars: $-0.02 < (B - V)_0 < +0.18$.

are synthetized and locked up in the cores of stars which end their evolution as white dwarfs, since they do not take part in chemical evolution [3]. Let us make the further assumption that the nuclear processing of the gas is instantaneous, thus neglecting finite lifetimes of stars. This is the so–called *instantaneous recycling* hypothesis first put forward by Talbot & Arnett (1971). Under these hypothesis it can be shown (Searle & Sargent, 1972) , that the mass fraction of heavy elements in the ISM, Z at any given time may be expressed as

$$Z = y \log(1 + \frac{\text{mass in stars}}{\text{mass in gas}})$$

where y is called the mean yield and represents the average ratio of the rate at which heavy elements are produced and returned to the ISM, to the rate at which H is used up in the ISM to form stars. If we call μ the ratio $\frac{\text{mass in gas}}{\text{total mass}}$ we may write

$$Z = y \log(\frac{1}{\mu})$$

and the fraction of stars f, which have metallicity $\leq Z$ at the present time is

$$f = \frac{1 - \mu^{Z_1/Z}}{1 - \mu_1}$$

---

[3] One should, however, take into account stars which end up as white dwarfs in binary systems which evolve as novae. In such cases there is the possibility that the elements in the core of the white dwarf are dredged–up, either by diffusion (Prialnik& Kovetz , 1984) or shear instabilities (Kippenhahn & Thomas, 1978), and then ejected into the ISM through thermonuclear runaways. The present estimates of the amount of heavy elements contributed to the ISM by such systems is very low (0.004 $M_\odot yr^{-1}$, Truran, 1986), thus their contribution is usually neglected. These estimates depend, however, on details, such as the duration of the constant bolometric luminosity phase, which are poorly known. Moreover novae are known to be important for the production of specific isotopes, such as ^{13}C,^{15}N and ^{17}O , which are produced in the β limited CNO cycle.

(Adouze& Tinsley, 1976), the subscript 1 denotes the present time value of any quantity.

If we compare this prediction with the observed distribution of G–dwarfs in the solar neighbourhood[4] we find a large discrepancy, in the sense that much fewer metal–poor stars are observed than are predicted. This is the so–called classical G–dwarf problem, first recognized by Van den Bergh (1962) and Schmidt (1963). This refers to the galactic disk, however a similar problem exists in the halo, which shows a lack of giants with [Fe/H]< -3.0 (Bond, 1981; Chiosi & Jones, 1983).

An even more direct line of argument poses a serious difficulty for the simple ideas outlined above: the lifetime of a 0.8 $M_{\odot}$ star exceeds the Hubble time (Bond, 1981) thus a star formed out of "primordial" matter very early in the history of the Galaxy would still be on the MS today. However no zero–metallicity star has so far been detected.

2.4 Simple ideas on dynamical evolution

The first quantitative observational study which tackled the problem of the dynamical history of the Galaxy was, probably, the work of ELS. They determined a correlation between metallicity and kinematical properties which was interpreted as evidence for a rapid collapse of the halo to form the galactic disk. In this picture the dynamical properties would change smoothly from disk to halo. This rapid collapse would leave as a signature a metallicity gradient in the halo as the one found by ELS, Sandage (1981) and Sandage & Fouts (1987). Carney *et al.*(1990)

---

[4] We shall follow Adouze & Tinsley (1976) and define the solar neighbourhood as a "cylindrical cell of about 1 kpc of radial extent". This represents the material with which the "local material has interacted since the Galaxy formed"

noted that four conditions must be satisfied in order to form a chemical gradient in the halo:

1) the random kinetic energy must have been somehow dissipated in order to confine the gas into a smaller volume; the proposed dissipation mechanism is gas–gas collision (Sandage, 1986)
2) the time–scale for chemical enrichment must have been short when compared to the dynamical time–scale.
3) the proto-Galaxy must have been rather homogeneous, since any inhomogeneities would have destroyed the gradient
4) Other phenomena which would have erased a gradient, such as mixing of the halo caused by tidal interaction with another Galaxy or mergers, must have been avoided.

The second of these requirements was, almost certainly, satisfied. In fact, the shortest possible dynamical time–scale is that of free–fall and is of the order of 10^8 yr (Carney *et al.*, 1990), on the other hand the lifetimes of massive stars which evolve as type II SNe is of the order of $10^6, 10^7$ yr.

In the picture of ELS the halo and the disk of the Galaxy share the same origin. This picture was attacked from several points of view and more so in the recent years. Probably one of the first serious attacks came from Searle & Zinn (1978) who found that the distribution of space velocities among stars in different metallicity bins were indistinguishable from each other. This was interpreted as a sign that there was no time for dynamical evolution over the time required for chemical evolution. Searle & Zinn (1978) proposed that the proto–Galaxy was the result of mergers of many small "fragments" each of which had its own chemical history, the "fragments" which formed the present–day halo came into dynamical equilibrium with the disk on a longer time–scale.

Another attack came from Norris *et al.*(1985) and Norris (1986), who used kinematically unbiased samples to show that there exist a significant fraction of metal–poor stars on low projected–eccentricity orbits, i.e. not all metal–poor stars are on plunging orbits, as claimed by ELS. Sandage & Fouts (1987) pointed out that only about 20% of the stars of Norris *et al.*(1985) have this property and they claimed that "80% of [the Norris *et al.*] sample remain with high eccentricity, requiring a rapid collapse for them".

Norris & Ryan (1989b) and Carney *et al.*(1990) also attacked both ELS and Sandage & Fouts (1987) for their use of $\delta(U-B)_{0.6}$ as a metallicity indicator at low metallicities (see previous section). The question is far from settled and still subject to debate.

A separate, but related, issue is the interpretation of the "thick disk" mentioned in section 2.2. There is a general consensus on the existence of this material, however it may be interpreted as a separate discrete component or as an "extended disk" (Norris& Ryan, 1991) of which the hotter and more metal–poor component is the Gilmore & Wyse "thick disk". Norris & Ryan (1991) proposed that the available data is better explained by an extended disk+halo configuration than by a thin disk+thick disk+halo configuration[5]. This led Norris & Ryan (1991) to suggest a specific scenario for the dynamical history of the Galaxy, which requires four interconnected processes:

1) contraction of a rotating gas cloud to form the galactic disk, as proposed by ELS;
2) formation of field stars and clusters from "fragments" which do not take part to the collapse, along the lines proposed by Searle & Zinn (1978);

---

[5] We wish to point out that both configurations predict too many stars in the metallicity interval -1.5<[Fe/H]<-1.0 . Look at figure 3 of Norris & Ryan (1991)

3) gaseous infall which continues long time after the formation of the disk, this allows to solve the classical G–dwarf in a very simple and natural way;
4) Heating and thickening of the disk by stochastic gravitational processes, thus forming the extended disk.

This scenario implies that "the halo of the Galaxy is decoupled (in the sense of being kinematically and chemically distinct) from its disk" (Norris & Ryan, 1991).

Edvardsson *et al.*(1993) note that from their data there is no sign of an increase in velocity dispersion with age in the time–span 3-10 Gyr. On the other hand the "thick disk" is at least 10 Gyr old and has a much larger velocity dispersion. Thus either there is an extra source of heating or the stars of the thick disk were formed with this vertical velocity dispersion.

Although the issue on the formation of the halo and its relation to the disk is far from being settled in the light of the presently available observational material we have an inclination in favour of a Searle & Zinn (1978) type of scenario. The following points favour it versus the ELS rapid collapse scenario:

a) The age effect detected by Zinn (1980) for globular clusters and by Preston *et al.*(1991) for field HB stars, may not be explained in a collapse scenario, but may come about naturally in a merger scenario;
b) the absence of a metallicity gradient in the halo;
c) the existence of stars which are as metal–rich as the disk but have a halo kinematics;

Burkert *et al.*(1992) presented a chemodynamical model for the collapse of the Galaxy to form the galactic disk. The starting point of their calculation was, however, not a spherical, cold, zero–metallicity halo, but a hot proto–disk which had already a metallicity of [Fe/H]=-1.5. This model or others like it may still

be applicable to a merger scenario, but the question of the formation of this hot proto–disk then remains open, since it cannot have any relation to the present–day halo.

Chapter 3

Two classes of Pop II stars

3.1 Introduction

It has become evident in the previous chapter that detailed spectroscopic investigation of Pop II stars is important for several reasons. In the first place it allows to determine atmospheric parameters such as surface gravity and effective temperature which may be compared with predictions from evolutionary theories. In the second place the determination of abundances is, by itself, an issue which may put constraints on theories concerning chemical and dynamical evolution of the Galaxy. Another important application is to determine sets of standard stars against which photometric or low–resolution spectroscopic indices may be calibrated.

The problem with detailed spectroscopic analysis is that it is time consuming. The following chapters of this thesis contain a description of detailed investigation of three Pop II stars and one Pop I star. The reason which motivated the study of the Pop I star ι Her was to provide a reference star for the study of Feige 86. It must be regarded as a necessary tool, and for this reason it is included in this thesis. The Pop II stars which are described in chapters 6 and 7 are of a very different nature: Feige 86 is a blue HB star while CS 22881-39 and CS 22885-96 are evolved G–type giants. Some of the methods employed in the two studies are similar, while some are very different. I this chapter I wish to outline briefly some of the properties of these two kind of objects.

3.2 Blue HB stars

We already mentioned in chapter one that the H–R diagram of globular clus-

ters is characterized by a horizontal branch which populates the Hertzsprung gap. Modern evolutionary theory has allowed to identify this horizontal branch (hereafter HB) with the locus occupied by stars which have a double source of energy: He burning in the core and H burning in a shell. These are stars which have already gone through the red–giant phase. The He burning phase is the second longest in a star's lifetime after the H–burning phase and is of the order of 10^8 yr (Chiosi *et al.*1992).

On closer inspection one realizes that different clusters exhibit different HB morphologies. In the first place the absolute magnitude of the cluster is different from cluster to cluster. In the second place the extent to the blue of the HB varies considerably. Another point worth mentioning is that in some cases the HB runs through the RR Lyrae "gap". This corresponds to an instability strip in the H–R diagram where RR Lyrae variable are found. It is not a "gap" in the sense of being an underpopulated region in the H–R diagram. It appears as a gap in the published colour–magnitude diagrams of globular clusters because, usually, not enough observations are available to determine the periods and mean magnitudes of these variable stars. However their presence and variability may be detected from a few frames only.

Theoretical investigations (e.g. Rood, 1970; Gross, 1973; Caloi *et al.*, 1978 Sweigart, 1987) have allowed to determine several parameters which affect HB morphology: He content, metallicity, age, rotation etc... The main parameter affecting the luminosity of the HB is the He content (Chiosi *et al.*1992). Also metallicity has an important effect: the lower the metallicity the bluer the HB. However it was discovered long time ago that some metal–poor clusters show a very red HB (Sandage & Wildey, 1967; Van den Bergh, 1967). The reverse also happens like in the case of M13, which has a very blue HB and intermediate metal–abundance.

This fact is usually referred to as the "second parameter phenomenon". That is to say that there must be some parameter other than metallicity at play, in order to explain the differences between clusters. Likely candidates for the "second parameter" are age, He content, abundances of C, N and O relative to iron (see Renzini, 1977 for a review).

Cluster HB stars have apparent magnitude in the range $B \approx 15$ to $B \approx 17$ (see e.g. Sanduleak, 1989). Thus only the brightest are accessible to spectroscopic investigation, and they require large telescopes and modern solid–state detectors. Twenty years ago, with photographic techniques, they were beyond the reach of even the largest telescopes. It was natural, then, to look for analogs of globular cluster HB stars among the brighter field stars. Two pioneering papers were published some twenty years ago by Newell (1973) and Greenstein & Sargent (1974), both papers were centered on the study of "blue halo stars" many of which were expected to be the field counter–parts of globular cluster HB stars. Two results of the above–mentioned papers are of interest here:

1) Newell noticed that the distribution of field blue stars in the $(U-B),(B-V)$ plane was not smooth but was characterized by the presence of two gaps.

2) Greenstein& Sargent confirmed the presence of Newell gap 1 (although they found no evidence for his gap 2) and showed that the HR diagram for field blue stars showed an HB which extended to higher effective temperatures than that of globular clusters. They called this the Extended Horizontal Branch (EHB).

In the following years it was realized that these two features are shared by many globular clusters. The classical and, perhaps, best studied example is NGC 6752 (Cannon, 1981, Heber *et al.*1986, Glaspey *et al.*1989). This globular cluster displays an EHB which is separated by a gap from the normal HB.

Theoretically it is possible to understand EHB stars as HB stars which have an envelope of negligible mass, Caloi (1989). This was already suggested by Greenstein & Sargent (1974). Note that in such models the luminosity of the H–burning shell is negligible. Contrary to what happens in normal HB models, in which the luminosity of the H-shell equals or even exceeds that of the He core. The structure of an EHB is therefore similar to that of an He MS star.

This interpretation, however, still leaves us with the problems of how stars with such a low envelope mass are formed, why they show up in some globular clusters and not in others and, even more important, why should the EHB be separated from the HB by a gap. For a discussion of the causes which may result in bimodality the reader is referred to Crocker *et al.*(1988). An interesting result was found by Norris (1981), who showed that NGC 6752 and M4, both of which have a bimodal distribution of stars along the HB, also have a bimodal distribution of cyanogen on the red–giant branch. This led Norris to formulate the working hypothesis that these bimodalities have the same cause, which he identified as a spectrum of core rotational velocities in the MS stars of globular clusters [1].

As far as the abundances are concerned stars in the HB and EHB display a bewildering array of peculiarities. One of the main anomalies noted is He abundance.

---

[1] "Beyond some critical value of the rotational velocity, a star will mix some of the products of the CN cycle into its outer layers, while still on or near the main sequence. The distribution of chemical peculiarities is thus dependent on the initial velocity distribution. The range in angular momentum leads in a range in luminosity at which helium flash occurs and, thereby, to a range in total and core mass on the horizontal branch which is also dependent on the initial velocity distribution. Both the distribution of the products of mixing in the red giants and that of stars along the horizontal branch are thus determined by the spectrum of angular velocities in the cluster stars" (Norris, 1981)

He is found to be underabundant in some stars (He-weak stars) and overabundant in others (He strong stars). It is generally understood that these anomalous He abundances do not reflect the star's "intrinsic" abundance, but rather, are the result of some atmospheric phenomenon (Greenstein *et al.*1967). The most successful theory to explain He anomalies is diffusion (Michaud, 1970; Michaud *et al.*, 1979). However, in general, parameter–free diffusion models fail to predict all of the observed abundance patterns (Michaud *et al.*, 1989). The question on the origin of these peculiar abundances is not yet settled. The greatest difficulty for diffusion is the very low diffusion velocities predicted (of the order of a few cm s^{-1}) it is clear that even a very modest turbulent velocity (undetectable spectroscopically) would erase anomalous patterns formed by diffusion.

3.3 Extremely Metal Poor Stars

We saw, in the previous chapter, that in the framework of standard Big Bang cosmology, one expects the first generation of stars to have formed out of metal–free gas. Low mass stars formed at that time would still be on the main sequence today. The fact that we have, so far, not detected any such star needs to be explained.

Several ways to circumvent this problem have been suggested:

a) an inhomogeneous Big Bang (Applegate *et al.*1988) in which nucleosynthesis may occur in the neutron–rich environment of a high entropy bubble left over from the cosmic quark–hadron transition. Enough ^{14}N should be produced to be observed in stellar atmospheres. Very heavy elements may be created in a cosmological r–process;

b) Cayrel hypothesis (Cayrel, 1986): when a primordial cloud suffers gravita-

tional collapse the first step is the formation of a dense core which starts producing very massive ($\approx 50 M_{\odot}$) stars before low–mass stars. These very massive stars explode as supernovae and pollute the atmospheres of the other stars with heavy elements;

c) Very Massive Objects (VMO, Carr *et al.*, 1984): objects formed before the formation of the Galaxy in the mass range $10^2 - 10^5 M_{\odot}$, they would have a very rapid evolution at the end of which they would go pair unstable leading to an explosion by which the gas, which would later on form the Galaxy, would be polluted;

d) cut off in the IMF (Jones, 1985): the first generation of stars did not contain objects of mass less than, about, one solar mass, probably due to the lack of efficient cooling of the primordial clouds, owing to the lack of metals;

e) alternative cosmological theories: if the universe, after all, is not evolving but is in a stationary state, then there is no reason why metal–free gas should have existed at all. The stationary state cosmology, proposed by Bondi, Gold and Hoyle in 1948 has long since been abandoned, however some of its ideas have recently been revived by Hoyle, Burbidge and Narlikar (1993) in what they call Quasi Steady State Cosmology (QSSC), this requires that matter is created (to maintain density constant, despite of the expansion of the universe) in several events, which they call "mini–bangs". A major such event is identified with the Big Bang, but the same process should go on, on a smaller scale, and be manifest as quasars, QSO's and active galactic nuclei, in general. The temperature, density and time–scale of the creation events proposed by Hoyle *et al.*(1993) are quite different from those encountered in the standard Big Bang and may result in the production of heavy elements, thus the gas would be created with non–zero metallicity, eliminating the need for Pop III stars.

Table 3.1

Star	T_{eff}	log g	M_V	V	B.C.	[Fe/H]
G64-12	6350	4.00	4.55	11.43	-0.262	-3.52[1]
CD-38245	4700	1.40	-0.60	12.00	-0.526	-4.50[2]
CS22876-32	5900	4.00	3.68	12.80	-0.300	-4.29[3]
CS22881-39	6000	1.00	0.60	15.12	-0.227	-3.53[4]
CS22885-96	4900	1.00	0.89	13.31	-0.530	-4.21[4]
CS22891-209	4737	1.00	-0.48	13.46	-0.531	-3.42[5]
CS22848-66	5257	1.50	0.13	13.46	-0.354	-3.36[5]
CS22897-8	5045	1.50	-0.11	13.31	-0.428	-3.56[5]
CS22968-14	5010	1.50	0.40	13.70	-0.428	-3.72[5]
CS22884-108	6250	4.0	3.70	14.24	-0.268	-3.27[6]

[1] Carney & Peterson (1981)

[2] Bessel & Norris (1984)

[3] Molaro & Castelli (1990)

[4] Molaro & Bonifacio (1990)

[5] Molaro *et al.*(1993)

[6] Norris *et al.*(1993)

The search for stars of very low metallicity resulted in the discovery of a few stars with [Fe/H] below -3.0. In table 3.1 we give the data for the 10 of these stars studied with high resolution spectroscopy. CS 22876-32 is a known spectroscopic binary star (Nissen 1989). Unfortunately the period is not known, nor is any photometric variability. It would be, of course, of great interest to derive masses for this system.

One reason to study abundances and abundance ratios in these stars is to

understand where the nucleosynthetic events responsible for their enrichment took place. The abundance pattern in a Pop I star, like the sun, is the result of a complicated evolution to which several mechanisms have contributed. We expect the chemical history of these extremely metal poor stars to be much simpler, possibly the result of a single enrichment event (Molaro *et al.*, 1993).

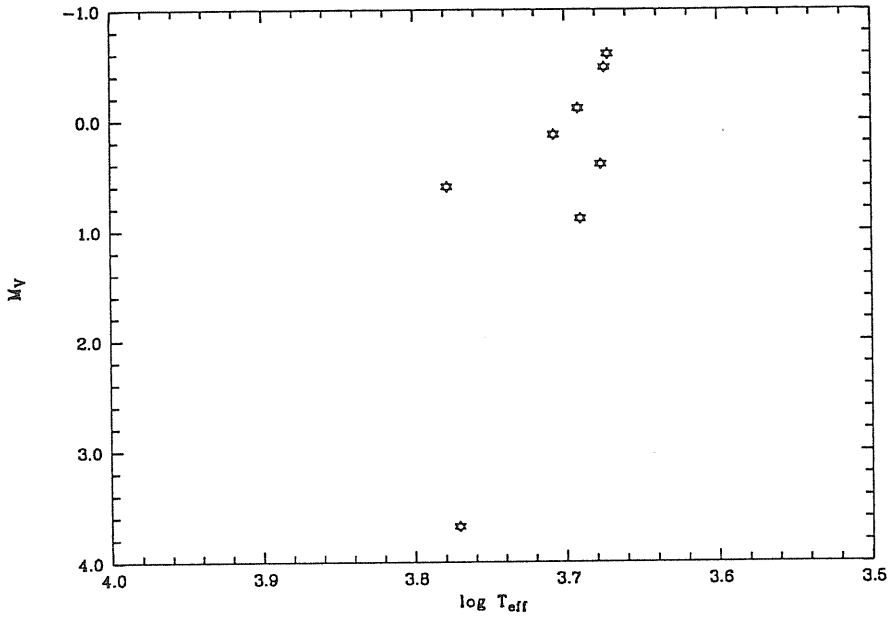

Fig. 3.1 The HR diagram for the most metal–poor stars

Chapter 4

Determination of atmospheric parameters

4.1 Introduction

The first step in the analysis of a stellar spectrum is to select or compute a model–atmosphere representative of the star. We always use Kurucz model–atmospheres, that is either taken from the grid distributed by R.L. Kurucz on magnetic tape or computed with some version of the ATLAS code. These model atmospheres are characterized by four input parameters: effective temperature, surface gravity, microturbulence and chemical abundances. In this chapter we shall deal with surface gravity and effective temperatures.

The methods we shall describe always rely on the comparison of observed and computed quantities. A general discussion of all methods available is beyond the scope of this chapter, I shall give only a brief outline of some of the methods used for B and G stars, since these are the types of stars which we shall study in chapters 5,6 and 7.

4.2 Reddening

Several of the methods described in the following sections rely on fluxes or colours, these are affected by the effect of interstellar reddening. I wish to discuss here the effect of reddening on observed colours from a rather general point of view. I shall follow closely the treatment of the book of Cester (1984), although the notation used here is somewhat different.

Consider the electromagnetic radiation emerging from a stellar atmosphere, and denote the flux per unit wavelength at the stellar surface by F_λ^0. Assume that the intervening interstellar medium is

1. isotropic
2. void of sources of radiant energy

Denote by $\tau_\lambda = -\int_0^D \kappa_\lambda \rho dr$ the optical depth of the interstellar medium, at a distance D from the star's surface(κ_λ is the mass absorption coefficient and ρ the mass density, r is a space coordinate). Then the flux received at earth, per unit solid angle will be simply

$$f_\lambda = \frac{F_\lambda^0 e^{-\tau}}{4\pi D^2} \tag{4.1}$$

(compare with formula (18.1) of Cester (1984, p.6)) If we denote by m_λ the apparent magnitude per unit wavelength at wavelength λ and by M_λ the absolute magnitude, expressing D in parsecs one has from Pogson relation and equation (4.1)

$$m_\lambda = M_\lambda + 5 - 5\log D + 1.086\tau_\lambda \tag{4.2}$$

Using the isotropy hypothesis one may factor out of the integral defining the optical depth the term κ_λ and what is left is

$$m_\lambda = M_\lambda + 5 - 5\log D + 1.086\kappa_\lambda C(D) \tag{4.3}$$

where C(D) is the mass column density.

The term $1.086\kappa_\lambda C(D)$ is called A_λ and represents the effect of the interstellar medium on the star's radiation. Consider next a colour index formed by taking the difference between two magnitudes at λ_1 and λ_2. One has, changing slightly the notation ($m(\lambda) = m_\lambda$)

$$m(\lambda_1) - m(\lambda_2) = M(\lambda_1) - M(\lambda_2) + 1.086(\kappa(\lambda_1), -\kappa(\lambda_2))C(D) \tag{4.4}$$

the last term on the righthandside is just $A(\lambda_1) - A(\lambda_2)$ and is called the colour excess. It is usually denoted as $E(\lambda_1 - \lambda_2)$. If we now consider the ratio between

two colour excesses $\frac{E(\lambda_1-\lambda_2)}{E(\lambda_3-\lambda_4)}$ (the four wavelengths are not necessarily all different) we find that it is independent of D and of the path taken by the light, in fact it is only a function of $\lambda_1, \lambda_2, \lambda_3, \lambda_4$, i.e. *of the photometric system employed.* Such a ratio is often denoted by r and is called reddening slope. It is care of the people who establish a photometric system to find the value of the reddening slope for a pair of conveniently chosen colour indices. Well known examples are: in the Johnson system the reddening slope $\frac{E(\mathrm{U-B})}{E(\mathrm{B-V})} = 0.72$ and in the Strömgren system $\frac{E(\mathrm{u-b})}{E(\mathrm{b-y})} = 1.56$. Let ζ and η denote a pair of colour indices in any photometric system; ζ_0 and η_0 be the corresponding colours corrected for reddening; retain the previously made assumptions on the interstellar medium and let r be the reddening slope, i.e.

$$\frac{(\zeta_0 - \zeta)}{(\eta_0 - \eta)} = r \tag{4.5}$$

It is trivial to prove that the parameter $\chi \stackrel{\text{def}}{=} \zeta - r\eta$ is reddening free. In fact it is sufficient to prove that $\chi_0 = \zeta_0 - r\eta_0 = \chi$.

$$\Leftrightarrow \chi - \chi_0 = 0$$

$$\Leftrightarrow \zeta - r\eta - \zeta_0 + r\eta_0 = 0$$

$$\Leftrightarrow \zeta - \zeta_0 = r(\eta - \eta_0)$$

The righthandside is non-zero by (4.5).

$$\Leftrightarrow \frac{(\zeta - \zeta_0)}{(\eta - \eta_0)} = r$$

The last equation is true by (4.5).

All which has been said so far is always assumed any time the formulas which we shall derive below are used, but seldom these assumptions are stated.

So far we dealt only with monochromatic magnitudes, however all which has been said remains valid for polychromatic magnitudes if we replace wavelength by effective wavelength. There is one important difference: effective wavelength, as well as the mean mass absorption coefficient, depend upon the flux distribution, i.e. on the spectral type. As a consequence of this fact we expect slightly different reddening slopes for stars of different spectral types. Well known reddening–free parameters are Johnson's Q or [c1], [m1] and [u-b] of Strömgren photometry. Heintze (1973) gives the different values of the reddening slope in the (B-V),(U-B) diagram. In order to use these reddening–free parameters to correct the observed colour indices one needs to know a relation between the dereddened colours, of the form $G(\zeta,\eta) = 0$. Such a relation may be either theoretical or empirical, it is usually expected theoretically (when designing a photometric system) and established empirically. A local relation is sufficient, that is to say that it may be valid only for a limited domain of the (ζ,η) plane. By using the definition of χ, the fact that it is reddening free and this relation one may set up two equations in two unknowns and deduce the values (ζ_0,η_0) from the observed values (ζ,η).

For the Johnson system this procedure leads to the relations

$$(\mathrm{B}-\mathrm{V})_0 = 0.277\mathrm{Q} - 0.045 \tag{4.6}$$

$$(\mathrm{U}-\mathrm{B})_0 = 1.175\mathrm{Q} - 0.036 \tag{4.7}$$

these are the relations given by Heintze (1973), which supersede the earlier results of Johnson (1958). Note that these equations imply a linear relationship between (U-B) and (B-V), however, since the intrinsic relation between (U-B) and (B-V) becomes flat around A0 these relations cease to be valid for cooler stars.

For the Strömgren system one may use the relations given by Crawford (1978)

$$(u-b)_0 = 1.13[u-b] - 0.186 \tag{4.8}$$

$$[u-b] = (u-b) - 1.5(b-y) \tag{4.9}$$

It is clear that all these formulas are not valid in the case the interstellar medium is not isotropic. Since the observational evidence is against isotropy we must conclude that *different stars have different reddening slopes.* This means that in general r is a function of both angular coordinates and distance, therefore two stars which are angularly near on the sky, but at different distances will have different reddening slopes. According to Mathis (1990) the value of R_V =A(V)/E(B-V) ranges from 3.1 to 5.0, the lower value is appropriate for diffuse dust, while the higher value is appropriate for high density dust, called by Mathis *outer-cloud dust.* Observationally this is reflected by the fact that the reddening–free parameters are not truly unaffected by reddening, we may just hope that the dependence is weak.

We studied in detail the problem of determining reddening for A and B type stars. The results have been presented at IAU Colloquium 138 (Bonifacio & Castelli ;1992) were we have shown that the slope of the Paschen continuum is very sensitive to reddening. By considering the theoretical fluxes we showed this slope to be very nearly independent of effective temperature. Thus by comparing the observed spectral energy distribution with the theoretical fluxes one may derive a value of E(B-V) accurate to about 0.02 mag, if the error in the measured flux distribution is of this order of magnitude.

4.3 Effective temperature and gravity for B–type stars

I discussed this topic in chapter 6 of my *Magister* thesis so I shall give here only brief summary and mention some results which appeared in the literature since 1991.

4.3.1 Flux distribution

The flux distribution may be used to determine the effective temperature of B–type stars, however, the temperature–sensitive part of the spectrum is the Balmer continuum, as mentioned in the previous paragraph. So in the case of ground–based scanner observations only the points bluewards of the Balmer jump are relevant. Since most of the flux in B–type stars is carried out in the far UV it is the flux in this spectral region which is best suited for temperature determination (see, e.g. Heber *et al.* 1984, Heber *et al.* 1986, Heber 1986). Low resolution flux–calibrated IUE spectra have often been used for this purpose.

4.3.2 Broad–band photometry

The reddening free parameter Q of Johnson photometry may be used as a temperature indicator, see, for example, the calibration of Schild *et al.*(1977). Since broad–band photometry is easily available Q is often used to provide a first guess of $T_{\rm eff}$.

4.3.3 Itermediate–band photometry

Intermediate–band photometry generally provides more information. In particular Strömgren photometry has the great advantage that the u filter samples the spectrum on the blue side of the Balmer jump, while the the b does the same on the red side. Thus one may have a precise measurement of the size of the Balmer jump itself, which is a powerful temperature indicator. Within the Strömgren system one may form three indices which measure the balmer jump

$$c1 = (u - v) - (v - b)$$

$$[c1] = c1 - 0.2(b - y)$$

$$[u - b] = (u - b) - 1.56(b - y)$$

The latter two indices are reddening–free. while $c1$ must be corrected for the effects of reddening. The dereddened $c1$ index is usually denoted $c0$. The behaviour of these indices with T_{eff} is shown in figures 4.1,4.2 and 4.3, where we have plotted theoretical colours computed from Kurucz model–atmospheres against T_{eff} .

On figure 4.3 is also shown that the balmer jump is slightly sensitive to luminosity. We are thus led to look for methods which determine T_{eff} and surface gravity at the same time. The Strömgren colours are usually supplemented by Crawford's β index. One could think to construct a calibration using photometric indices of stars with fundamentally determined T_{eff} and $\log g$, however there are too few of such stars (Balona, 1984), one has therefore to use theoretical colours. To compute theoretical colours from a model–atmosphere is straightforward. However the calibration of theoretical colours is quite delicate. Several calibrations of theoretical colours grids based on Kurucz models has been attempted (Relyea & Kurucz, 1978, Moon & Dworetsky, 1985 hereafter MD, Lester *et al.*,1986 hereafter

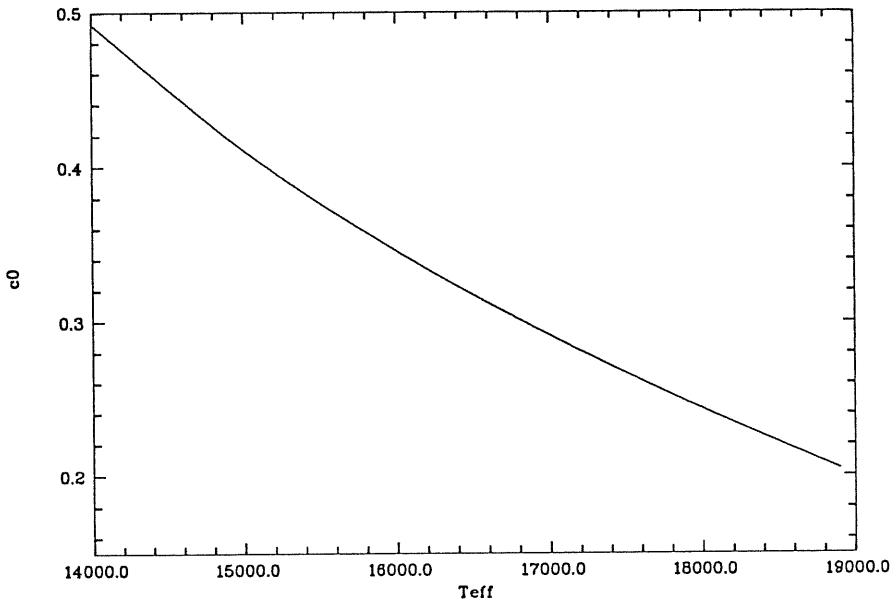

Fig. 4.1 The dependence of the c0 index on effective temperature. Theoretical colours for log g = 4.0

LGK). In all these papers several corrections were applied to computed indices in order to make them match the observed indices of one or more "standard" stars. The validity of the MD and LGK grids has been investigated by Castelli (1991) and Napiwotzki *et al.*(1993). Both groups find that the MD grid is superior. A calibrated colour grid is a powerful tool to determine T_{eff} and log g . Moon (1985) has developed a computer program which uses polynomial fits to the grid of MD to determine T_{eff} and log g from $c0$ and β. Castelli (1991) provided improved fits and also an extension of the original MD grid to higher T_{eff} 's, up to T_{eff} =20000. In the original program of Moon (1985), the hot–stars

were treated with the analytic formulas of Balona (1984), Castelli (1991) showed that the use of an extended MD grid considerably improved the agreement with flux–temperatures. Napiwotzki *et al.*(1993) showed that the effective temperatures derived from the Balona (1984) formulae are in poor agreement with fundamental effective temperatures, they also advocate the use of an extension of the MD grid. Instead of using polynomial fits to the grid like Moon (1985) and Castelli (1991) Napiwotzki *et al.*(1993) use an "iterative procedure searching for the matching point", though they do not detail what this procedure actually is. These authors provide a useful calibration of effective temperature as a quadratic function of [u-b], they also give calibrations of T_{eff} against $(b-y)_0$ and $(B-V)_0$ for A and F–type stars, but these do not concern us here. A very interesting test performed by Napiwotzki *et al.*(1993) on the MD and LGK grids was to check the gravity determined from Strömgren photometry against gravities determined from fitting Balmer line profiles observed at medium resolution. They found that for the MD grid there are differences of up to 0.2 dex with a marked trend in temperature, the lower the temperature the higher the ratio g_{MD}/g_H. A similar trend is found for the LGK grid but differences as large as 0.4 dex are found.

The Strömgren colours are very useful, they are very widely used and there is a considerable data–base of stars measured in this system. However other narrow–band systems may be used in the same fashion. In his seminal paper on blue halo stars, Newell (1973) made use of his own narrow–band photometric system (Newell *et al.*, 1969) which he calibrated against theoretical colours and line strengths. His system was pretty much like using Strömgren's u,v and y and an H_γ index rather than Crawford's β.

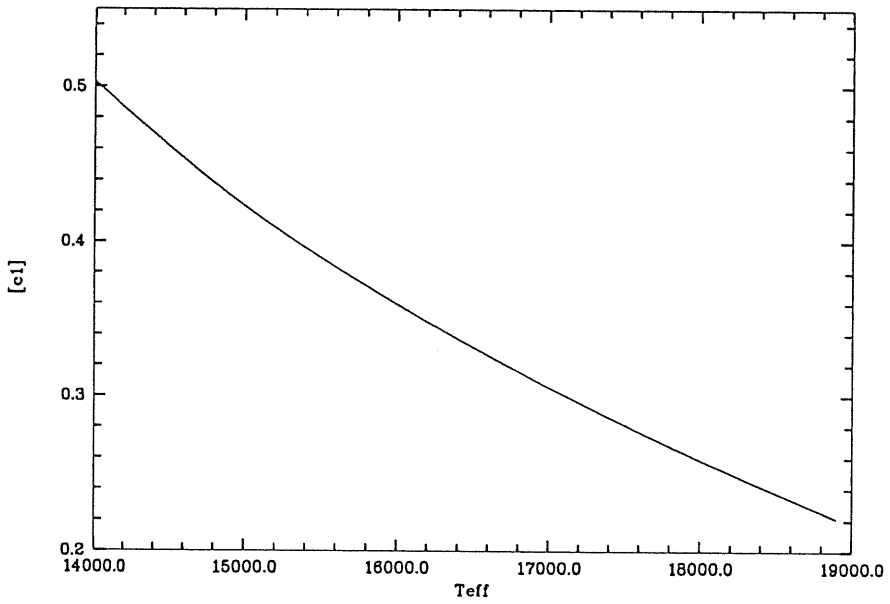

Fig. 4.2 The dependence of the [c1] index on effective temperature. Theoretical colours for log g = 4.0 .

4.3.4 Methods using the line spectrum

The Balmer line profiles are very sensitive to gravity for B–type stars. This fact is illustrated in figure 4.4 , were three theoretical profiles of H_β taken from the Kurucz grid are shown. Thus if medium to low resolution spectra of Balmer lines are available they may be used for gravity determination. Since the gravity sensitive parts of the profile are the far wings they may be used to determine surface gravity even in pathological cases when the Balmer lines are contaminated by an emission (as in Be stars, Mazzali *et al.*, 1993).

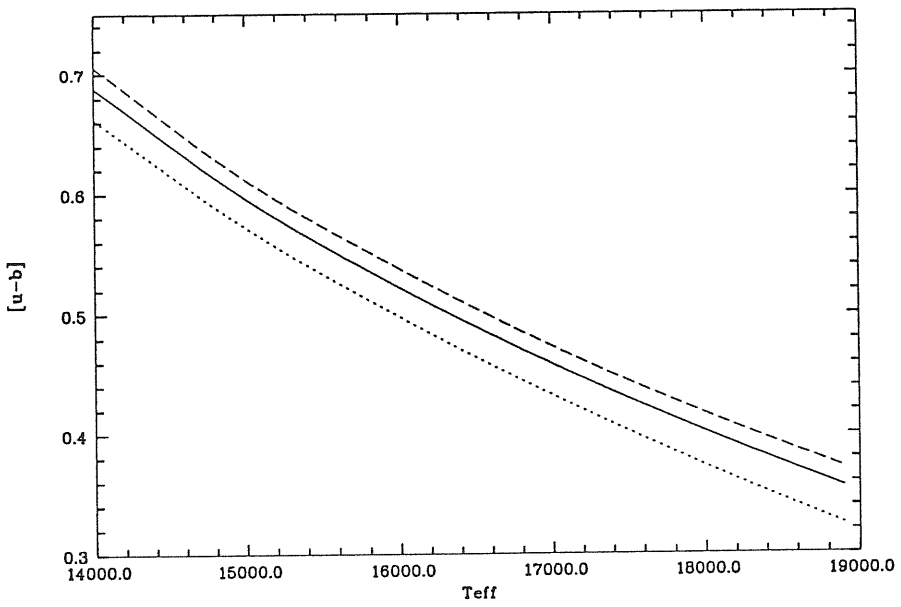

Fig. 4.3 The dependence of the [u-b] index on effective temperature. Theoretical colours for log g = 4.5 (dash), log g = 4.0 (line) and log g = 3.5 (dots)

.

Ionization equilibria provide both temperature and gravity diagnostic. Neutral species are insensitive to pressure, so the requirement that lines from the neutral species yield the same abundance as the lines from the singly ionized species is a constraint on gravity. On the other hand the requirement that the lines of two ionized species (e.g Si II/Si III) yield the same abundance is a constraint on temperature.

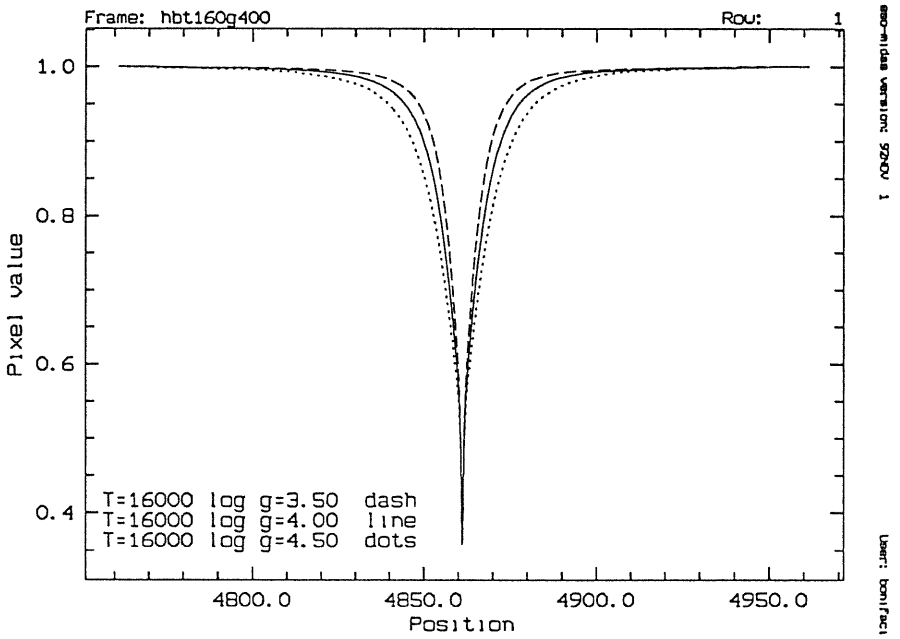

Fig. 4.4 The dependence of the profile of H_β on surface gravity. Theoretical profiles for T_{eff} =16000 K .

If high resolution far UV spectra are available one may use the Si II lines of UV multiplet 13.04, which are sensitive to temperature, but relatively insensitive to gravity (Singh and Castelli, 1990).

4.4 Effective temperature and gravity for G–type stars

4.4.1 The Paschen continuum

The slope of the Paschen continuum, which is nearly insensitive to effective temperature for B–type stars, is a very powerful temperature indicator for G–type stars. Figure 4.5 illustrates this fact by plotting the $(B-V)_0$ colour from metal–poor model atmospheres against effective temperature. On the same plot one sees that there is, however a marked effect of metallicity, thus (B-V) by itself is useless as a temperature indicator, unless we know the metallicity of the star. The ultraviolet excess provides such a measure. This was originally defined as $\delta(\mathrm{U-B}) := (\mathrm{U-B})_{\mathrm{Hyades}} - (\mathrm{U-B})_*$ and depended also upon effective temperature. Sandage (1969) noticed that for a constant metallicity $\delta(\mathrm{U-B})$ has a maximum for (B-V)=+0.6. He thus suggested that $\delta(\mathrm{U-B})$ be normalized at the value of a star of the same metallicity with (B-V)=+0.6. This normalized index is usually denoted as $\delta(U-B)_{0.6}$. It may be computed by interpolating in table 1A of Sandage (1969). Using this index Carney *et al.*(1987) define a calibration which makes use of the temperature sensitivity of the (B-V) colour taking into account also the effects of varying metallicity. The relation is

$$\theta_{\mathrm{eff}} = 0.540(\mathrm{B-V}) + \delta(\mathrm{U-B})_{0.6} + 0.537$$

where $\theta_{\mathrm{eff}} = 5040/\mathrm{T_{eff}}$. The colours must be corrected for the effect of reddening.

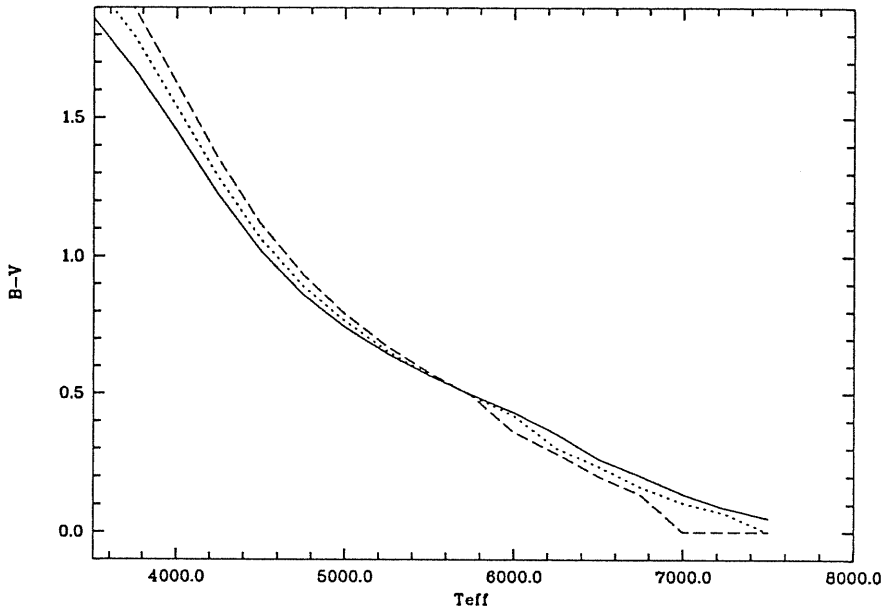

Fig. 4.5 The dependence of (B-V) on effective temperature. Theoretical colours from Kurucz models with [M/H]=-3.5 . log g =0.5 dash ; log = 1.0 dots ; log g = 1.5 solid line

4.4.2 The Balmer lines

For G–type stars the Balmer line profiles are quite sensitive temperature indicators. This fact is illustrated in figure 4.6 which shows profiles of H_δ taken from the Kurucz grid for T_{eff} = 5000 K, 5250 K and 5500 K and log g = 1. The changes are quite striking both in the core and in the wings. A statement is often made that for G–type stars the Balmer line profiles are independent of gravity (e.g. Carbon & Gingerich, 1969, quoted by Beers *et al.*1985). This statement is not strictly true, in fact figure 4.7 shows the profiles of H_δ for T_{eff} = 5000 K and

log g = 0.0, 1.0 and 2.0 respectively. There are significant effects on the profiles, it should be noted, though, that a change of 1 dex in gravity is very large and would alter significantly all the ionization equilibria. Insofar as we can pinpoint gravity to better than 1 dex the effect of gravity on Balmer line profiles may be neglected. The other thing worth noting in figure 4.7 is that stars with a lower gravity show stronger wings, quite contrary to what happens for B–type stars.

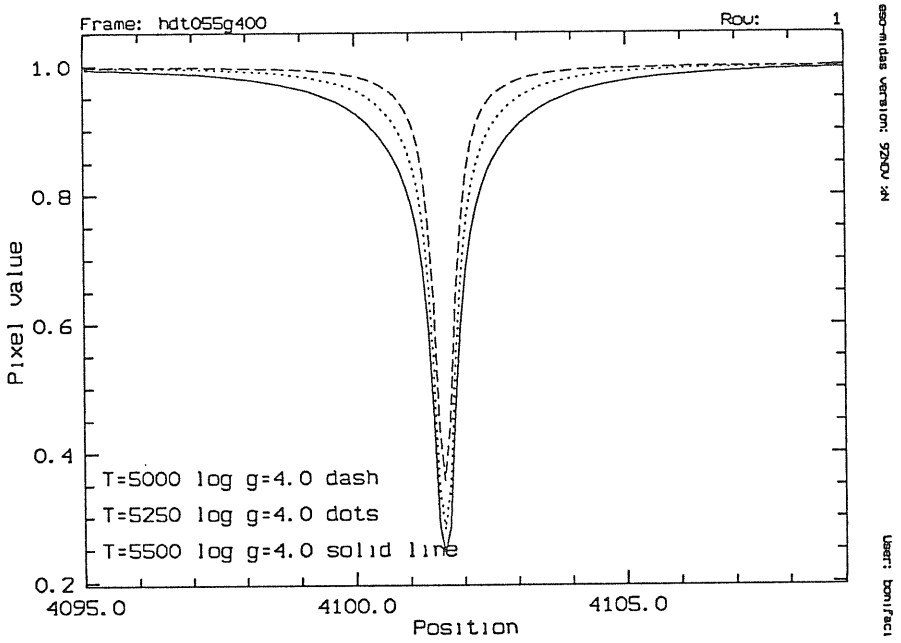

Fig. 4.6 The dependence of the profile of H_δ on effective temperature. Theoretical profiles for log g = 1.0 .

To exploit this sensitivity one may use fits of Balmer line profiles in order to fix the effective temperatures. An alternative approach is to use only the equivalent widths of Balmer lines. Measuring the equivalent width of lines with extended wings such as the Balmer lines is ambiguous because the result depends sensibly on just where we decide to truncate the wings and place the continuum. A better approach is to define a line index: for each line one defines two bands which define the continuum, one on the blue and one on the red side of the line, and one band for the line. a linear interpolation between the average values of the red and blue sidebands gives a pseudo–continuum, then the equivalent width of the line band with respect to this pseudo–continuum may be readily computed. The advantage of line indices is to be observationally well defined, the only delicate point is that the radial velocity of the star must be accurately determined, so that the bands be precisely placed. Beers *et al.*(1985) defined such indices for H_γ, H_δ, the Ca II K line and the G band. They noted also that there are slight systematic changes between the H_δ and H_γ index. These are due to the different contribution which metallic lines make to the two indices. This effect depends both on metallicity an temperature. Beers *et al.*(1985) mention also the curvature of the continuum to be a possible problem, numerical experiments we made with synthetic spectra indicate that this is most likely a second–order effect. Beers *et al.*(1985) define a new line index H', which is a linear combination of the H_γ and H_δ index, being substantially an average the statistical error on H' is better that on the single indices, however its systematic behaviour resembles closely that of the H_δ index. Molaro & Castelli (1990) used the H' index of a set of "standard" stars from Beers *et al.*(1985) to derive a calibration between this index and effective temperature. Although there is some scatter they found a least square fit of a 3rd

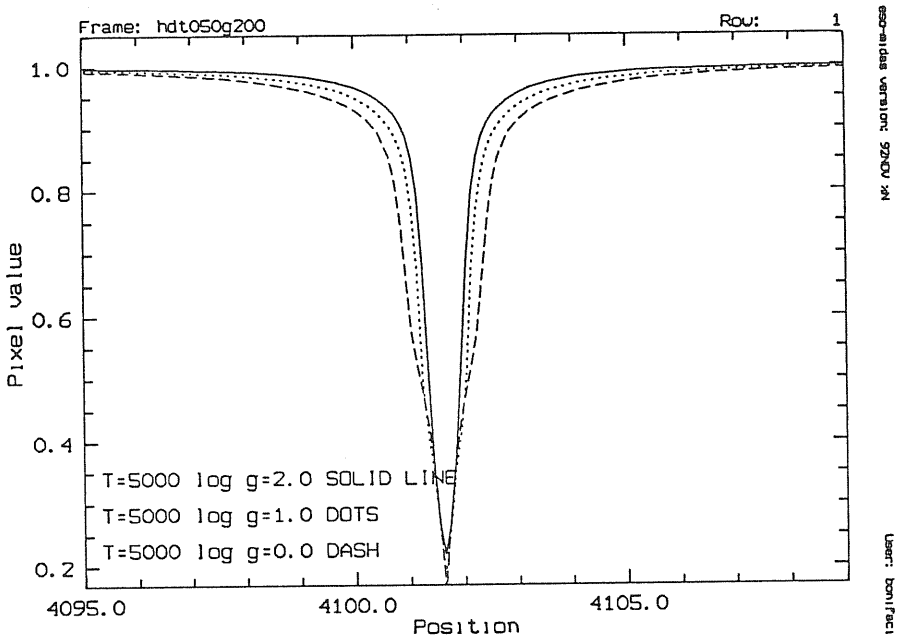

Fig. 4.7 The dependence of the profile of H_δ on surface gravity. Theoretical profiles for T_{eff} = 5000 K .

degree polynomial gives a convincing relationship between these two quantities (see figure 6 of Molaro & Castelli, 1990).

For gravity it is not easy to find a good diagnostic, when available ionization equilibria between neutral and singly ionized species are probably the best choice. In some cases, though, one does not observe both kinds of lines. This is the case, for instance, of CS 22876-32, studied by Molaro & Castelli (1990). In that case Molaro & Castelli (1990) used the $(U-B)_0$ index, which is reasonably sensitive to gravity in the temperature range 5500 K to 6500 K, relevant for CS 22876-32. For cooler stars, however this index loses its sensitivity.

Chapter 5

A computed spectrum for ι Herculis

5.1 Introduction

Compared to other scientists the astronomer is in a rather awkward position: he cannot use experimental methods, but merely observe what happens in the universe. In order to make some sense out of these observations he has to build some sort of model and compare the model's predictions to observations. If the model is non–parametric it either succeeds or fails to predict observations and in the latter case it is rejected. However more often the model is parametric and the parameters are physical quantities whose values we wish to determine. This is done through some sort of fitting procedure of the model to the data. In many cases this is the only way the astronomer has to "measure" some physical quantities. This procedure is very different from the concept of measure, for instance, in quantum mechanics and it is so because in astronomy we cannot act on the physical system we want to "measure". We see that the procedure does not provide any check of the adequacy of the model and, in fact, in ill-conditioned cases, we may well be able to fit an incorrect model to the observational data by choosing a suitable value of the fitting parameters.

Such is the case for spectral synthesis techniques applied to abundance determinations. It is often possible to fit computed to observed line profiles by choosing a suitable abundance, even if the gf value used in the computation is wrong. One may use certain internal checks of consistency like requiring that different lines of different ions of the same element yield the same abundance, however these may fail if the atomic data is affected by systematic errors. We may thus formulate the following principle which should apply to any parametric model used in astronomy: *the process of testing and assessing the degree of reliability must be*

logically separate from that of comparing the model to the observations in order to determine the values of physical quantities.

For synthetic spectra this means an evaluation of the completeness and reliability of the line list used for the computations, as well as a test of the correctness of the basic input physics. Such a test may be achieved by introducing the concept of "standard star". We select a star which we define "normal", is bright enough to be observed with high S/N, and whose atmospheric parameters (T_{eff} ,g, abundances...) are known independently of our model. Ideally we should then require that our computed spectrum reproduces the observed spectrum with no free parameters, and reject our computations as inadequate if it does not. In practice such a strict criterion would lead to the rejection of all synthetic spectrum codes and line lists ! There is of course the problem that the input parameters have in their turn been determined through some sort of fitting procedure to some other model and are therefore subject to errors both accidental and systematic. One has to allow some freedom in the choice of the parameters though requiring that the adjustments be "small" in some ill-defined sense. This sounds rather sloppy and, it is ! It is the nature of astronomy to be more sloppy than physics. Moreover some kind of not fully consistent test is likely to be better than no test at all. Lastly, it is our only chance to do something about testing our models.

Because we have selected to use the SYNTHE code (Kurucz& Averett, 1981) together with Kurucz's line lists in the study of the UV spectrum of F86 which I was doing under the supervision of Prof. M. Hack and Dr. F. Castelli and which is described in the next chapter, we felt the need to do some kind of testing of this code. We decided to test our synthetic spectra on a standard star of spectral type close to that of F86 and with a comparably low projected rotational velocity. The choice fell on ι Her because it had often been used as a comparison standard

(Heber, 1983 ; Cugier& Hardrop, 1988 a,b ; Sadakane *et al.*, 1983; Takada–Hidai *et al.*, 1986). Furthermore its abundances had been determined from the visible spectrum by Peters& Aller (1970) and preliminary results existed of an abundance analysis including both the UV and visible region (Peters& Polidan, 1985).

In the rest of this chapter I shall summarize the results of this comparison work between observed and computed spectra in the UV region 122.8 nm – 195.0 nm which has been published on Astronomy& Astrophysics Supplement Series (Castelli& Bonifacio, 1990). I shall also mention some results from optical data which I collected at Observatoire de Haute–Provence and is, so far, unpublished.

5.2 The UV Data

For the UV region we used the Copernicus Atlas (Upson and Rogerson, 1980) and two IUE high resolution spectra SWP3243 and SWP5720, taken from the IUE archive. The Copernicus Atlas consists of two spectra: a second order spectrum covering the range 99.93 nm to 142.22 nm which has a nominal resolving power of 0.0050 nm and a first order spectrum covering the range from 122.8 nm to 146.77 nm, whose nominal resolving power is 0.0101 nm. These spectra are normalized to the continuum and smoothed with a low–pass filter. The data has been supplied on magnetic tape by National Space Science Data Center at GSFC.

The log of the IUE observations is provided in table 5.1. Image SWP5720 has been reprocessed at VILSPA with the IUESIPS2 software. We normalized these spectra to the continuum with the code NORMA (Bonifacio, 1989), which fits a spline through a set of interactively chosen points, independently on each order. This procedure is, of course, subjective, yet the placement of the continuum was *a posteriori* adjusted against the continuum predicted by the synthetic spectra. We

Table 5.1

Log of IUE observations

IMAGE	Program id	aperture	T_{exp} (s)	obs. date yr	day
SWP3243	DGDSL	SMALL	52	78	311
SWP5720	DGDSL	SMALL	79	79	186

felt that often computations are more realistic than a subjective continuum. In most cases this comparison showed a good agreement, although in some cases we preferred to renormalize some orders in order to get a better agreement between observations and computations.

We compared the different spectra in order to get information on the wavelength scales, continuum placement and spectral resolution. From this comparison we deduced that the reprocessed SWP5720 image has a higher resolution than the SWP3243 image, and is, in fact, comparable to the second order Copernicus spectrum. Image SWP3243, on the other hand, has a resolution comparable to that of the first order Copernicus spectrum.

In order to compare a computed spectrum with an observed spectrum one has to take into account the effects of stellar rotation and of finite instrumental resolution. We computed the effects of rotation as described in Gray (1976, chapter 17) adopting $v \sin i = 11$ kms^{-1} (Hoffleit, 1982). We decided to model the instrumental broadening with a gaussian profile of different FWHM for the different images. For IUE spectra we found that it was necessary to adopt different instrumental broadenings for the different spectral ranges. Table 5.5 lists the finally adopted

broadening velocities. These were obtained by iteratively changing the instrumental broadening until an optimal match was obtained between computed and observed spectra. One may note that our estimated resolution for image SWP5720 is higher than that given by Imhoff (1984) for data processed with IUESIPS2.

Table 5.2

IMAGE NUMBER	GRATING	ORDER	FILTER	λ_c (nm)	R (nominal)	t_{exp} (seconds)	DATE
A32	5	II	OG5150	658.0	60000	900	12/6/1989
A60	1	I	NONE	427.5	40000	601	14/6/1989
A98	6	Echelle	interf.	655.5	96000	900	15/6/1989
C133	5	II	OG515	669.2	60000	300	21/2/1992
C263	5	II	OG515	587.5	60000	205	22/2/1992
C542	3	I	NONE	400.0	6500	1292	26/2/1992
D196	5	II	OG515	587.5	60000	1446	4/4/1993
D198	5	II	OG515	587.5	60000	2805	4/4/1993

In order to compare observed and computed spectra one has to match the wavelength scales and origins. The observed spectrum will be shifted with respect to the computed spectrum (which assumes vacuum laboratory wavelengths, below 200 nm) by an amount which depends on the stellar radial velocity and on the earth's motion. If the wavelength scales are the same a unique shift would suffice to superimpose the observed and computed spectra. This is the case for the Copernicus Atlas, for which which the wavelengths had already been reduced to this scale. For the IUE spectra this is not enough, different shifts were necessary for different orders and, sometimes, for different ranges of the same order. For image SWP5720 the shifts are in the range [0.005,0.0113] nm . For image SWP3243 the range is [.0025,.0125] nm.

Table 5.3
T_{eff} and log g for ι Her from the literature

T_{eff} (K)	log g	method	models	Sources
			LTE Unblk.	
17380	4 (prefixed)	Bj	SA	WKH
18000	4 (prefixed)	Bj, UV+Vis. flux	SA	PA
19000-18000	4 (prefixed)	H_gammah_delta (G), (He/H)=0.15	M1	PA
20000	4 (prefixed)	Si II/Si III,S II/S III	SA	PA
18000	3.5	Vis. Flux	M1	KS
18500	3.5	H_γ, H_δ (KG), (He/H)=0.15	M1	KS
20000-21000	> 4	Si II/Si III,S II/S III	M1	KS
			NLTE Unblk.	
18000	3.6	He I 402.6,438.7,443.8,447.1,501.5,587.6 nm,NLTE profiles	M2	AM
			LTE Blk.	
17000-17250	4 (prefixed)	Si II/Si III,S II/S III	MM,AM	PA
16800	4 (prefixed)	Bj,UV+Vis. flux and $H_\alpha, H_\beta, H_\gamma, H_\delta$ (ESW) (H/He)=0.11	AM	PA
17500	4	Vis. Flux reduced to the Oke-Schild(1970) system	VM	L
16700	3.9	Vis. Flux reduced to the Hayes (1970) system	VM	L
17460	4 (prefixed)	Vis. Flux	K	MM
17000	3.55	H_γ, H_δ, HeI402.6, 438.7, 447.1, 471.3nm	M2,K	BBKT
17500 ± 1500	3.75 ± 0.15	UV+Vis.Flux	K	PP
17700	4	$c_0$index, H_γ	KWH	
17135	3.66	$[c_1] - \beta$indices$[c_1] - T_{eff}$calib. of Lester et al.(1986) $\log g - \beta$calib.ofSchmidt(1979)	K	BM
16728	3.5	$c_0 - T_{eff} - \log g$ calib. of Balona (1984)	K	BM
17180 ± 1110	3.43 ± 0.02	$c_0 - \beta$ indices	K	CB
18000	4 (prefixed)	from the angular diameter,Bj, $(B\text{-}V)_0$	K	UDPD
			without models	
17814	4 (prefixed)	Flux temperature	/	UDPD
17180	3.43	Strömgren photometry ; LGK grid	ATLAS 9	CB
17640	3.71	Strömgren photometr ; MD grid	ATLAS 9	C
17640	3.71	β & Si II UV mult.13.04 ; MD grid	ATLAS 9	SC

Sources in Table 5.3

Models:
AM: Adams and Morton (1968), M1: Mihalas (1965), M2: Mihalas (1972), MM: Mihalas and Morton (1965), K: Kurucz (1979), SA: Strom and Avrett (1965), VM: Van Citters and Morton (1970)
Theories for H profiles:
G: Griem (1964), KG: Kepple and Griem (1968), ESW: Edmonds, Schluter and Wells (1967)
Sources:
AM: Auer and Mihalas (1973):the data are from KS and Peters (1969,unpublished)
BBKT:Baschek et al. (1982): The data are from Kodaira and Scholz (1970) and private communications. The Teff scale of Mihalas's (1972) models was reduced to that of Kurucz's (1979) models.
BM: Barnett and McKeith(1988): c_1 and β were taken from Philip and Egret (1980)
C: Castelli (1991) c_1 and β taken from Hauck& Mermillod (1980)
CB: Castelli and Bonifacio (1990) as above
KS: Kodaira and Scholz (1970): The observed visual energy distribution was normalized to that of Vega, which was normalized to that predicted by a blanketed model with Teff=9600 K, log g=4.0. The lines were measured on spectrograms with a dispersion from 1.0 to 6.5 A/mm.
L: Leckrone (1971): The observed energy distribution was from WKH. The lines were from PA and Peters(1969,unpublished).
MM: Morossi and Malagnini (1985): The visual observed energy distribution was from Breger's (1976) Catalogue, where the flux was normalized to the absolute calibration of Vega of Hayes and Latham (1975). MM used only Kubiak's (1973) observations.
PA: Peters and Aller (1970): The visual observed energy distribution was the same as that of WKH. They also used UV measuraments at 111.5, 131.4, 137.6, 210.0, and 280.0 nm. Lines were measured on spectrograms with dispersions of 2.02 and 8 A/mm.
PP: Peters and Polidan (1985): For the continuum, UV data from the Voyager (90.0-170.0 nm) and from TD1 (Jamar et al.,1976) were used, while visible data from Breger(1976) were adopted. For the UV line spectrum the Copernicus Atlas of Upson and Rogerson (1980) was used.
SC: Singh and Castelli (1991) β from Hauck& Mermillod (1980)
UDPD:Underhill et al. (1979): The data are the absolute UV fluxes measured by the S2/68 experiment on the TD1 satellite (Jamar et al.,1976) and the absolute fluxes of Johnson and Mitchell (1975) given in 13 bands.
WH: Wolff and Heasley (1985). c_{11}.288 was taken from the compilation by Philip et al.(1976), H_γ was observed by WH.
WKH: Wolff, Kuhi, and Hayes (1968): The observed energy distribution from 320.0 to 643.6 nm was normalized to the absolute calibration of Vega by Hayes (1967).

5.3 The optical data

I observed several optical spectra of ι Her in the years 1989–1993 during observational runs at Observatoire de Haute–Provence at the 1.52 m telescope equipped with the Aurelie spectrograph. The reader is referred to chapter 4 of my Magister thesis (Bonifacio, 1991) for a description of the instrument and of the data handling techniques. A brief account of data reduction procedures is also given in the next chapter.

The main targets were the CII lines used by Barnett and McKeith (1988) to determine the C abundance, to be compared with the UV results, the He I lines at 667.8 nm and 587.5 nm, for a comparison with F86, and Balmer line profiles, for gravity determination. The detailed observation's log is given in table 5.2.

5.4 The model atmosphere

To determine the abundances we used the spectral synthesis code SYNTHE (Kurucz& Avrett, 1981), which requires as input a model–atmosphere. The model atmosphere was computed with version 8 of the ATLAS code (Kurucz, 1970), which was the latest available to us at the time of writing the paper which appeared on A.& A. Supplement.

The parameters T_{eff} and g were fixed by comparing the observed c_0 and β indices taken from the Hauck & Mermilliod (1980) catalogue with the computed indices. We believed that it was better to use a grid of theoretical colours consistent with the model–atmospheres which we were using. We therefore modified the code TEFFLOGG of Moon (1985) in order to use the synthetic colour grid of Lester *et al.*(1986, hereafter LGK), rather than that of Moon& Dworetsky (1985, hereafter MD). However the thorough comparison of the two grids later performed by Castelli (1991), showed the superiority of the MD grid for B–type stars. This result is also supported by the results of Napiwotzki *et al.*(1992). As discussed by Castelli (1991) the problem with of using the LGK grid for the determination of T_{eff} is likely due to the use by LGK of η UMa as a zero point for B-type stars. This star is an extremely fast rotator and its colours might be anomalous. In the case of ι Her the use of c_0 index from the two grids (assuming a gravity $\log g = 4.$, yields a difference in T_{eff} of about 460 K, the temperature determined

Table 5.4

Sources of atomic data for some elements observed in ϵ Her. The symbol (K) indicates data adopted from Kurucz's(1988a) files. In the other cases the log gf of Kurucz's files have been replaced with data from other sources. The last column lists the replaced sources. The symbol c indicates that the values of γ_r and γ_S have been computed in SYNTHE. $\sum A$ indicates that γ_r is the sum of the transition probabilities A_{ij}. Ar indicates γ_r from Artru and Lanz(1987).

		Sources			Replaced Sources
ion	Mult. or λ	log gf	γ_r	γ_S	
B II	1	BRO (K)	$\sum A$	G	
C I	2,5-9,34,37	NS2	$\sum A$	G	SW,BRS,NBS1,MS
	3,4	NS2	$\sum A$	c	BRS
C II	1	NS1	$\sum A$	SS	SIN
	10	NS1	$\sum A$	c	Guess
	11	LD (K)	$\sum A$	c	
C III	9	FT (K)	$\sum A$	SS	
C IV	1	WAR (K)	$\sum A$	SS	
N I	4,5,9,10,11	DBG (K)	$\sum A$	G	
	12,13	NBS1 (K)	$\sum A$	G	
N II	129.979-130.0 nm	KP (K)	c	c	
O I	2	NBS1 (K)	$\sum A$	G	
Mg II	123.99,124.0 nm	WM	$\sum A$	G	KP
	148.289 nm	KP (K)	c	c	
	173.4-175.3 nm	KP (K)	c	c	
Al II	2,10	WM	$\sum A$	c	KP
	4	WM	$\sum A$	G	KP
	5, 135.02 nm	NBS2 (K)	$\sum A$	c	
	6(a)	KP (K)	$\sum A$	c	
Al III 1	WM	$\sum A$	c	KP	
	160.6-161.2 nm	WM	$\sum A$	c	KP
	137.9-138.4 nm	WM	$\sum A$	c	KP
	135.3 nm	KP (K)	c	c	
	193.6 nm	KPOBD	$\sum A$	c	KP
Si II	1,3	CS (K)	$\sum A$	SS	
	2	NBS2 (K)	$\sum A$	G	
	4	CS (K)	$\sum A$	G	
	7	LA	c	c	KP
	8	BBCB (K)	$\sum A$	c	
	8.01,9.02	LA	c	c	KP
	10	LA	c	c	Guess
	10.01	LA	c	c	Guess
	11.01	LA	c	c	KP
	10.02,11,12,12.01	Guess(K)	c	c	
	12.02,13,13.01	Guess(K)	c	c	
	13.02	LA	c	c	KP
	13.03	Guess(K)	c	c	
	13.04	LA	Ar	c	KP
	13.05	LA	c	c	Guess
	15.04	LA	Ar	SS	Guess
	18.04,18.05	LA	c	c	Guess
	18.06	LA	Ar	c	Guess
	23,27	LA	c	c	Guess
	28	LA	Ar	c	Guess
	29	LA	Ar	c	KP

from the MD grid being higher ($T_{LGK} \approx 17104$; $T_{MD} \approx 17458$). The value of log g determined from the MD grid is 0.28 dex higher than that determined from the LGK grid ($(\log g)_{LGK} = 3.43$; $(\log g)_{MD} = 3.71$) . Because we observed at Observatoire de Haute–Provence several Balmer lines we checked the gravity using the profiles of H_δ, H_ϵ and H_8. The spectrum we have covers about 43 nm centered around 400 nm . This spectral coverage allows to select the continuum in an straightforward way. We selected a number of points in regions which are predicted to be line–free by our computed spectrum and connected these points with a spline. Shortwards of about 390 nm this is not possible because the wings of successive lines of the Balmer series blend with each other so that the residual intensity is always below unity. Hence H_δ and H_ϵ should be regarded better gravity indicators than the higher lines in the series, which may be affected by problems due to the placement of the continuum. As can be seen from figures 5.1-5.3 the model with log g = 3.70 predicts wings which are slightly too narrow for all three lines. The model with log g = 3.80, instead predicts satisfactorily the line wings. The model with log g = 3.90 predicts line wings which are too strong. From this analysis we conclude that log g for ι Her is between 3.70 and 3.90, our finally adopted value is 3.80. We also note that all the profiles are slightly asymmetric, the blue wing agrees well with the theoretical profile computed with log g= 3.80, while the red wing would better agree with a slightly lower gravity. This value of log g is consistent both with that of Peters & Polidan (1985), and with that of Grigsby (1991). The former authors determine a gravity of log g = 3.75 from both the continuum energy distribution and fits to H_γ and H_δ, unfortunately they did not publish their line profiles so no comparison is possible. Grigsby (1991) shows an excellent fit of an H_γ profile, computed using a model with T_{eff} = 17500 K and log g= 3.75, in this case I do not have any observations of H_γ, so again no

Table 5.4

(continued)

		Sources			Replaced Sources
ion	Mult. or λ	log gf	γ_r	γ_S	
Si III	1(b)	KP (K)	c	c	
	4	WM	$\sum A$	SS	BBCB
	9,10,20,35,38,39	NBS2 (K)	$\sum A$	c	
	36	LS	$\sum A$	c	BBCB
	37	KP (K)	c	c	
P II	1	NBS2 (K)	$\sum A$	c	
	2	WM	$\sum A$	c	SMTH
P III	1	WM	$\sum A$	c	LKI
	7	CMB		c	c
S I	2,5,6,8	NBS2 (K)	$\sum A$	G	
	3,9,10,12	NBS2 (K)	$\sum A$	c	
	11	NBS2 (K)	c	c	
S II	1	NBS2 (K)	$\sum A$	c	
Cu III	11,12,13,14,15,16,	KP /	c	c	
	17,18,19,21,22,24,	KP /	c	c	
	25,26,27,28,30,31,	KP /	c	c	
	32	KP /	c	c	
Zn III	all the lines within the range	KP (K)	c	c	
Ga II	1	WM	c	c	WA
Ga III	1	FF /	c	c	
Ge II	4	WM	c	c	MIG

(a) log gf from WM are available, but the differences are very small.
(b) log gf from CHY is also available.

Sources of log gf
BBCB: Berry et al.,1971; BRO: Bromander,1971; BRS: Brooks et al.,1977;
CHY: Cowan et al.,1982; CMB: Curtis et al.,1971; CS: Curtis and Smith,1974;
DBG: Dumont et al.,1974; FF: Froese Fischer,1977;
FT: Friedrich and Treffitz,1969; K: Kurucz,1988a;
KP: Kurucz and Peytremann, 1975; KPOBD: Kernahan et al.,1979;
LA: Lanz and Artru,1985; LD: Laughlin and Dalgrano,1973;
LKI: Livingston et al.,1975; LS: Livingston et al,1976;
MIG: Migdalek,1976; MS: Morton and Smith,1973; NBS1: Wiese et al.,1966;
NBS2: Wiese et al.,1969; NS1: Nussbaumer and Storey,1981;
NS2: Nussbaumer and Storey,1984; SIN: Sinanoglu,1973; SMTH: Smith,1978;
SW: Stuck and Wende,1974; WA: Warner,1968a; WAR: Warner,1968b;
WM: Wiese and Martin,1980.

Sources for the Stark damping constants γ_r, γ_S
G: Griem,1974; SS: Sahal-Brechot and Segre,1971.

Table 5.5

wavelength shifts adopted for the different images

Image	Orders	λ range nm	VB kms^{-1}	FWHM nm	
				observed	nominal
SWP5720	112-86	122.8-161.1	17	.0070-.0091	.0083-.0120
(IUESIPS2)	85-74	161.1-187.8	21	.0113-.0132	.0120-.0172
	73-71	187.8-195.0	25	.0157-.0163	.0172-.0183
SWP3243	94-74	146.7-187.8	25	.0122-.0157	.0117-.0178
(IUESIPS1)	73-71	187.8-195.0	30	.0188-.0195	.0178-.0185
Copernicus	II	122.8-142.2	17	.0070-.0081	0.05
	I	142.2-146.7	25	.0119-.0122	0.101

comparison is possible. Napiwotzki *et al.*(1992) used H_γ and H_β to determine a gravity of $\log g = 3.82$. The fits they show are quite convincing.

The computed spectrum described in the 1990 paper used as input a model with T_{eff} =17180 K ,log g = 3.43, an assumed microturbulent velocity of 2 kms^{-1} for the ODF's and solar abundances, which was generated with version 8 of the ATLAS code. Today, in the light of the optical data and a better understanding of the validity of different theoretical colours grids, we prefer a model with parameters T_{eff} = 17640 log g= 3.80 ξ = 0.00. We computed an ATLAS 9 model with these parameters, and, with this new model, a synthetic spectrum for the whole region 122.8 nm to 195.0 nm which is plotted, together with the observations in appendix B, in a fashion similar to that of the 1990 paper. The new computed spectrum does not change the line identification, in fact I have only

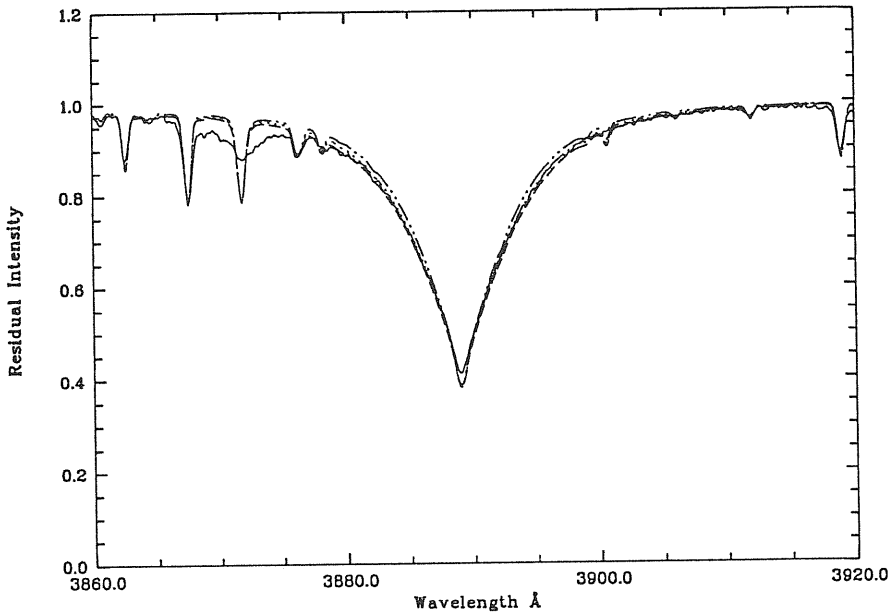

Fig. 5.1 The observed profile of H_8 in ι Her compared with computed profiles for T_{eff} = 17640 and log g = 3.70 (dash – dotted line), log g = 3.80 (dotted line) and log g = 3.90 (dashed line).

labelled the lines whose theoretical residual intensity at line center is less than or equal to 0.800, weaker lines can be identified using appendix A of the 1990 paper. The abundances turn out to be only slightly different.

To have a consistency check of our the model we compared the theoretical with the observed flux. We used the visual magnitudes of Kubiak (1973) as listed in the Breger (1976) catalogue, but renormalized at 556 nm. For the UV we used the TD1 fluxes (Jamar *et al.*, 1976). We used the V magnitude (V=3.80 ; Hauck& Mermilliod, 1980) and the Hayes& Latham (1975) calibration of Vega to convert

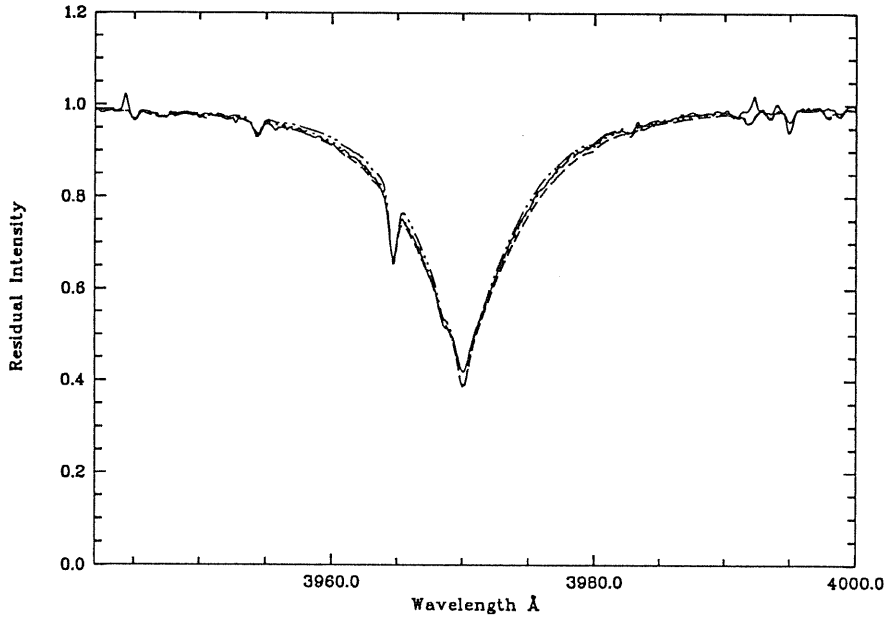

Fig. 5.2 The observed profile of H_ϵ in ι Her compared with computed profiles for T_{eff} = 17640 and log g = 3.70 (dash – dotted line), log g = 3.80 (dotted line) and log g = 3.90 (dashed line).

these to magnitudes normalized at 556 nm. We corrected the observed fluxes for the effect of reddening by assuming E(B-V)=0.02 (Underhill *et al.*, 1979) and the Mathis (1990) extinction curve.

The computed flux fits rather well the visible data falls slightly below the observations in the far UV, though still within the error bars of the observations, as can be seen in figure 5.10. There is little difference between the flux computed from the presently adopted model and that computed from the model adopted in the 1990 paper as can be seen in figure 5.11

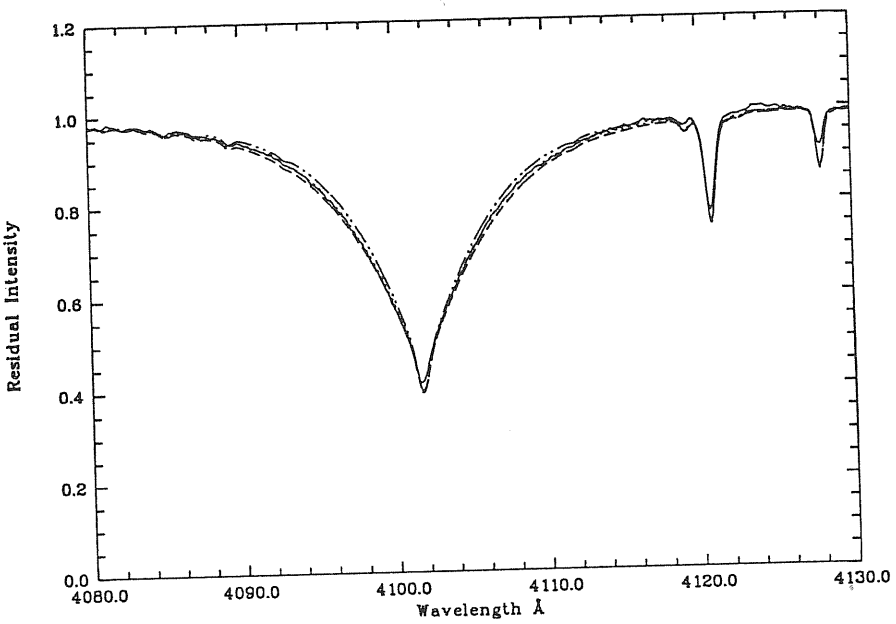

Fig. 5.3 The observed profile of H_δ in ι Her compared with computed profiles for T_{eff} = 17640 and log g = 3.70 (dash – dotted line), log g = 3.80 (dotted line) and log g = 3.90 (dashed line).

5.5 The input atomic data

The atomic line list used for the computations is that provided by R.L. Kurucz on magnetic tape. At the time of writing the 1991 paper it contained about 76000 lines in the region 122.8–195.0 nm. Several changes were made, substituting some of the Kurucz & Peytreman (1975, hereafter KP) and guessed gf values with data taken from critical compilations, where possible.

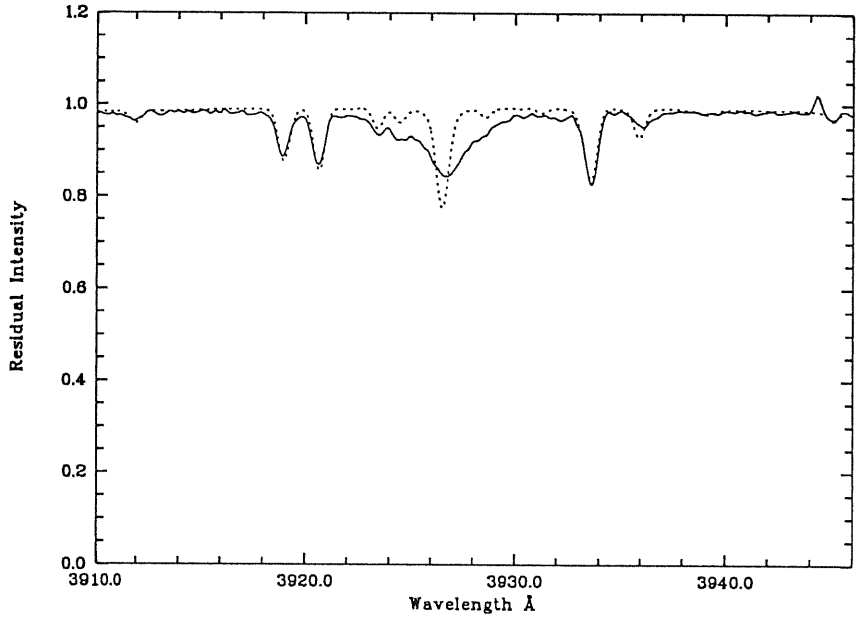

Fig. 5.4 The observed spectrum of ι Her in the region around the He I $2^1P - 8^1D$ transition compared with our computed spectrum (dots). The profile of this line is poorly reproduced, because the Stark profile for diffuse He I lines is not taken into account in the computation. The two lines on the blue side are C II 391.8968 nm and C II 392.0681 nm ; the line on the red side is the Ca II K line.

In the far UV we used the critical compilation of Lanz & Artru (1985) for the Si II lines. The changes were significant only for multiplets 9.02 and 13.02.

We used the compilation of Wiese& Martin (1980) for PII, PIII, Ga and GeII. For CI and CII we used the computed gf values of Nussbaumer& Storey (1984) and Nussbaumer& Storey (1981). The values for CI are in good agreement with

Table 5.6
Unidentified features and missing lines in the adopted line lists.

unidentified lines with our line lists	Missing lines	Sources
122.987		
123.235		
123.335	123.3354 Si II	AR
123.482		
123.592	123.5920 Si II	UR,AR
123.675		
123.775		
123.800		
123.865		
124.090		
124.225		
124.247		
124.380		
124.535		
124.642		
124.955		
125.020		
125.035		
125.737		
125.995		
126.9025 (a)		
127.030		
127.432	127.4300 Si II	ABL,AR
127.505	127.5038 N II	UR
127.5275		
127.5675	127.5662 Si II	ABL,AR
127.6225	127.6201 N II	UR
.....	127.6800 N II	UR
127.8100	127.8094 P II	UR
127.8450		
128.3175		
128.450		
128.590		
130.5-130.6 (b)	130.529 Si II	AR

Table 5.6
(continued)
Unidentified features and missing lines in the adopted line lists.

unidentified lines with our line lists	Missing lines	Sources
130.9-131.0 (c)		
131.125	131.1265 Si II	AR
131.152		
131.825		
131.880		
132.6200		
132.8175 (a)		
132.8550	132.852 S III	UR
132.8650		
133.2625		
134.3600		
134.5075		
134.5325		
134.6400		
134.6725		
135.0925		
135.1075		
135.1425		
135.5550	135.5605 O I(1) ?? (e)	
135.85	135.8524 O I(1) ?? (e)	
.....	135.9751 Si III(68)	MOO2
136.0350	136.0360 Si III(68)	MOO2
.....	136.1719 Si III(68)	MOO2
136.3000		
136.3400 (a)		

the experimental values of Goldbach& Nollez (1987) and Goldbach *et al.*(1989)

Table 5.6
(continued)
Unidentified features and missing lines in the adopted line lists.

unidentified lines with our line lists	Missing lines	Sources
137.2100		
.....	137.271 P III	UR
137.290	137.2947 Si II	ABL
137.325	137.3246 Si II	ABL
138.335		
138.785	138.7845 Si II	ABL
138.815	138.8150 Si II	ABL
.....	140.342 Cr III	UR
.....	140.690 Cr III	UR
140.8575	140.8541 Si II	ABL
140.885	140.8855 Si II	ABL
141.130		
.....	142.904 Cr III	UR
142.970		
142.995		
143.3650	143.3690 Si III(66)	UR
.....	143.385 Ti III	UR
143.4200	143.4218 Si II	ABL
143.6700	143.6724 Si III(66)	UR
143.6950		
143.7150	143.717 Cr III	UR
143.7500		
143.8200	143.8228 Si III(66)	UR
143.8650	143.8702 Si III(66)	UR
143.940	143.9391 Si III(66)	UR
"	144.0908 Si III(66)	MOO2

Table 5.6
(continued)
Unidentified features and missing lines in the adopted line lists.

unidentified lines with our line lists	Missing lines	Sources
144.1775	144.1732 Si III(3.05)	UR
144.7200	144.7196 Si III(3.05)	UR
144.7650		
.....	145.195 Cr III	UR
145.2400		
145.2575		
145.460	145.4616 Co II	UR
.....	145.5950 Cr III	UR
145.7350	145.7253 Si III(60) UR	
.....	146.387 Cr III	UR
146.4100		
146.4275		
...	End of the Copernicus data	
146.643		
146.7225		
146.810		
147.265		
.....	147.297 S I(4)	MOO1
147.3525		
147.365		
147.560		
147.710		
.....	148.165 S I(4)	MOO1
148.265		

with the exception of multiplet 4 at 132.9 nm and the weak lines of multiplet 6 at 127.9056 nm and 127.9498 nm. The adopted gf value for these weak lines

Table 5.6
(continued)
Unidentified features and missing lines in the adopted line lists.

unidentified lines with our line lists	Missing lines	Sources
148.475		
.....	148.561 S I(4)	MOO1
148.65-148.865(d)		
149.105		
150.000		
.....	150.2228 P III	ABL
150.265		
150.475	150.4663 P III	ABL
150.68		
150.715		
150.730		
151.00		
151.05		
151.692		
151.76		
151.775		
151.895		
151.915		
151.995		
152.85		
152.89		
153.1075		
153.400		
153.4225		
153.537		
153.6075		

Table 5.6
(continued)
Unidentified features and missing lines in the adopted line lists.

unidentified lines with our line lists	Missing lines	Sources
153.737		
154.575		
154.6-154.67		
154.7300		
154.8325	C IV interstellar ??	
155.310		
155.5175		
156.180		
156.510		
156.5575		
156.590		
156.700		
156.730		
156.775		
156.84		
157.105		
157.140		
157.215		
157.2475		
157.575		
157.605		
157.6725		
157.7475		
157.975		

has a negligible effect on the computed spectrum. For CII this theoretical data replaced guessed values. We used the transition probabilities A_{ij} from the papers

Table 5.6
(continued)
Unidentified features and missing lines in the adopted line lists.

unidentified lines with our line lists	Missing lines	Sources
158.1975		
158.355		
158.415		
158.545		
158.780		
159.29		
159.435		
159.465		
.....	159.5755 Si I	ABL
.....	159.7962 Si I	ABL
159.830		
160.020		
160.335		
160.660		
160.750		
160.945		
161.482		
162.230		
162.285		
162.340		
162.670		
163.045		
164.160		
.....	164.4809 Al II	ABL
165.245		
166.210		
166.2625		
166.715		
.....	167.3315 Si III(58)	MOO2

Table 5.6

Unidentified features and missing lines in the adopted line lists.

unidentified lines with our line lists	Missing lines	Sources
167.575		
167.705		
167.765		
168.9325		
169.115		
169.290		
170.060		
170.150		
.....	170.4525 Si II	ABL
171.8575		
172.895		
174.6275		
174.890		

of Nussbaumer& Storey to compute the radiative damping constants γ_r for each line.

Several gf values for Si III were also replaced. We did not change the values in Kurucz's lists for the NI lines of multiplets 4,5,9,10 and 11, which are from Dumont *et al.*(1974), since they are in good agreement with the experimental values of Goldbach *et al.*(1986) and Goldbach& Nollez (1988).

For some lines, which were absent from Kurucz's lists we were able to find gf values in the literature. For PIII multiplet 7 we used the gf values from Curtis *et al.*(1971). For Ga II multiplet 1 we used the gf values of Froese–Fischer

Table 5.6

Unidentified features and missing lines in the adopted line lists.

unidentified lines with our line lists	Missing lines	Sources
175.230		
175.5575		
175.605		
175.690		
176.215		
177.745		
177.920		
178.165		
179.595		
179.640		
179.690		
179.80		

(1977). For all the Cu III lines listed in Moore's multiplet tables we used the gf values from Kurucz& Peytremann (1975), which were omitted in the new Kurucz's lists. All the changes performed for the 1990 paper are listed in table 5.4, which is essentially table III of that paper. The lists currently distributed by Kurucz contain gf values from the more recent literature for several of these lines.

For the lines of the iron–group elements the data–base contains radiative, Stark and Van der Waals damping constants.

$$\gamma_r = \sum_{i<l} A_{li} + \sum_{j<u} A_{uj}$$

Table 5.6
(continued)
Unidentified features and missing lines in the adopted line lists.

unidentified lines with our line lists	Missing lines	Sources
180.685		
181.7375		
.....	183.6739 N I	MOO1
185.730		
185.835		
190.12		

A_{li} are the probabilities for spontaneous emission from the lower level l to level i, while A_{uj} are from the upper level u to level j, in units of s^{-1}.

$$\gamma_S/N_e = 38.8V^{\frac{1}{3}}C_4^{\frac{2}{3}} = 15385C_4^{\frac{2}{3}} \quad (\text{for} \quad T = 10000K)$$

$$\gamma_{VW}/N_H = 17V^{\frac{3}{5}}C_6^{\frac{2}{5}} = 84762C_6^{\frac{2}{5}} \quad (\text{for} \quad T = 10000K)$$

These were computed as described by Kurucz (1981). The formulas for the Stark and the Van der Waals damping constants are those given by Aller (1963). For the elements other than those of the iron group the damping constants are taken from the literature, when available, or set to zero. When the SYNTHE code finds a zero damping constant it computes the classical radiative damping constant

$$\gamma_r = \frac{2.223 \times 10^{15}}{\lambda^2}$$

Notes to table 5.6

(a) Double line, of which the other line is identified

(b) Region of the autoionized Si II (13.04) line at 130.559 nm

(c) Region of the autoionized Si II (13.04) lines at 130.9453 and 130.9725 nm

(d) numerous lines are unidentified in this range

(e) The O I lines of UV multiplet 1 are not missing in the line lists. They are not predicted, because their log gf is too low. Artru et al. (1989) have tentatively identified the feature at 135.56 nm as O I(1).

Sources of the missing lines:

ABL:Artru et al. (1989), AR:Artru(1986), MOO1:Moore (1950)
MOO2:Moore (1965), UP: Upson and Rogerson (1980)

where λ is expressed in Å. For C_4 and C_6 the approximate formulas of Kurucz& Avrett (1981) are used.

For the purpose of computing the Voigt profiles the Stark broadening parameter is assumed to be temperature independent, while for Van der Waals broadening it is given by

$$\Gamma_{VW} = \frac{\gamma_{VW}}{N_H}(N_H + 0.42N_{He})(T \times 10^{-4})^{0.3}$$

The computed spectrum was rotationally broadened with $v \sin i = 11$ kms^{-1} and further broadened with a gaussian profile to take into account both instrumental and macroturbulent velocity broadening. The broadening velocities are given in table 5.5. A zero microturbulent velocity was assumed in the computations, since it gave the best agreement between observations and computations for

Table 5.7

Abundances $\log \epsilon = \log(N/N_{tot})$ for ι Her. The values from this paper are compared with those from Peters and Polidan(1985) (PP), and with the solar ones (Anders and Grevesse,1989), reduced to the same scale.

Ion	$\log \epsilon$ used in the computations	$\log \epsilon$ *PP*	$\log \epsilon$ Sun
B II	-10.00	.....	-9.44
C I	-3.75	.....	-3.48
C II	-3.75	-3.62 ± 0.46	
C III	-3.75	-3.13	
N I	-5.00	.....	-3.99
N II	-5.00	-4.15 ± 0.39	
O I	-3.11	-3.05 ± 0.15	-3.11
O II	.....	-3.37 ± 0.44	
Mg II	-4.46	-4.70 ± 0.09	-4.46
Al II	-5.75	.....	-5.57
Al III	-5.75	-5.62 ± 0.24	
Si II	-4.49	-5.00 ± 0.47	-4.49
Si III	-4.49	-4.63 ± 0.47	
Si IV	-4.49	-4.65 ± 0.06	
P II	-7.50	-5.67 ± 0.55	-6.59
P III	-7.50	-7.02 ± 0.60	
S I	-4.83	.....	-4.83
S II	-4.83	-4.87 ± 0.35	
Ti III	-7.05	-6.67 ± 0.55	-7.05
V III	-8.04	-7.74 ± 0.83	-8.04
Cr III	-6.37	-6.63 ± 0.63	-6.37
Mn III	-6.65	-6.49 ± 0.40	-6.65
Fe II	-4.37	-5.22 ± 0.41	-4.37
Fe III	-4.37	-4.54 ± 0.31	
Co II	-7.12	.....	-7.12
Co III	-7.12	.....	
Ni II	-5.79	.....	-5.79
Ni III	-5.79	.....	
Cu III	-7.83	.....	-7.83
Zn III	-7.44	.....	-7.44
Ga II	-8.00	.....	-9.16
Ga III	-8.00	.....	
Ge II	-8.63	.....	-8.63

Table 5.8
Equivalent widths of lines in the visible spectrum and derived abundances.

Ion	λ (nm)	EW (pm)	log ϵ	log gf	Source log gf
C II	391.8968	6.55	-3.74	-0.512	MC
	392.0681	7.92	-3.80	-0.212	MC
	426.7001	8.30	-4.00	0.609	BRO
	426.7261	9.10	-4.05	0.769	BRO
	657.8052	12.90	-3.14	0.118	MC
	658.2882	10.90	-3.16	-0.182	MC
N II	399.4997	3.78	-4.24	0.276	NBS
	404.1310	1.31	-4.48	0.853	NBS
O II	407.2155	1.98	-3.39	0.530	NBS
	411.9275	1.10	-3.57	0.480	NBS
Al II	390.0675	1.65	-5.81	-1.270	NBS
Al III	414.9913	1.74	-5.27	0.620	KP
Si II	385.3665	3.73	-4.68	-1.517	BBCB
	385.6018	8.10	-4.63	-0.557	BBCB
	386.2595	7.06	-4.62	-0.817	BBCB
	403.5278	1.17	-4.44	-1.300	BBCB
	412.8054	5.54	-5.11	0.316	KP
	419.0707	1.56	-4.55	0.000	GUESS
Si III	380.6526	2.85	-4.00	0.527	BBCB
S II	392.3445	2.95	-4.77	0.440	NBS
	399.3499	3.08	-4.09	-0.815	MWRB
	403.2768	1.32	-4.63	-0.233	MWRB
	413.2984	0.58	-5.17	-1.130	GUESS
	415.3068	3.83	-4.54	0.395	MWRB
	416.2665	3.36	-5.09	0.830	MWRB
	417.4265	2.75	-4.73	0.760	GUESS
	418.9681	0.96	-5.08	-0.040	NBS
Ca II	393.3663	11.4	-5.11	0.134	BWL
Fe III	416.4731	1.61	-4.05	0.923	K

large sections of the spectrum. A zero microturbulent velocity was adopted also by Peters& Aller (1970) and Peters& Polidan (1985).

5.6 Line identification

The number of lines in the UV spectrum of a B-type star is enormous, a conventional identification list in the form of a table would be difficult to manage and to understand. We therefore decided to adopt a different approach: we computed

a synthetic spectrum for the whole range under study, and produced a number of plots on which observed and synthetic spectra are superimposed. We used the plotting package described in Kurucz & Avrett (1981). At the top of each plot there are labels which identify the lines used in the computations. If the computed feature reproduces well the observed feature one may identify the observed line with that identified by the label.

We wish to point out that the theoretical spectrum predicts that all lines are blended and that there is no region which may be defined as essentially "line–free" continuum, contrary to what happens in the visible. There is a considerable number of observed features for which there is no theoretical counter–part, we refer to these as "missing lines"; they could be either lines which have not been included in the computations (due, for instance, to the lack of atomic data) or lines which have been included, but with a wrong gf value. The reverse case case happens also, there are some theoretical features for which the corresponding observed feature is too weak; again the problem most probably lies in the atomic data. In spite of this the overall agreement between observations and computations is quite good. There seem to be less "missing lines" toward longer wavelengths, however this is probably the effect of the decreased resolving power of the instrument.

We compared our plots with the identifications provided by Upson & Rogerson and with those of Artru *et al.*(1989) for the normal B stars π Ceti and ν Capricorni. This allowed us to find some lines which were missing from Kurucz's lists. Many more lines, however, are not present in the above–mentioned identification lists, but our computations, using the Kurucz data, match closely the observations. They are, mainly lines of the iron-peak elements for which we used the Kurucz (1988a,b) data. We give, in table 5.6 a list of unidentified features and in column 2 we give some lines which are missing from the Kurucz data–base, which may be

taken as tentative identifications. Several Si lines of the singly and double ionized spectra appear to be missing, in particular the six new Si II lines identified by Artru (1986) and the Si III lines of multiplets 3.05,58, 66 and 73. We could not include any of the lines, listed in column 2 of table 5.6, in our computations since we lack the necessary atomic data.

An identification list for the UV spectrum of ι Her is provided by Ramella *et al.*(1987), who used an automatic procedure and found results in conflict with those of Upson & Rogerson (1980). Our spectral synthesis allows to remove the disagreement: both the lines identified by Ramella *et al.*(1987) and Upson & Rogerson contribute to the observed features. Ramella *et al.* considered only the lines stronger than a given threshold, therefore missing some of the lines identified by Upson & Rogerson. On their side Upson & Rogerson identified some lines which are predicted to be only minor contributors to blends, since the did not make any intensity estimate.

5.7 The abundances

As stated in the introduction in order to test our model we should fix all the parameters, hence also the abundances. We adopted this approach for all of the iron group elements, which show virtually no unblended lines but have many lines which are major contributors to blends. We selected those lines for which the computed spectrum matches well the observed spectrum when solar abundances are adopted in the computations. This is consistent with the results of Heber (1983) who found a solar Fe abundance from 11 UV Fe III lines. Such lines are, therefore, assumed to have reliable atomic data and should be used for abundance determinations for B-type stars. For elements B through S and Ga the situation is less

clear. These elements show several strong resonance lines of the first and second spectra, which, although blended, are by far the major contributors to spectral features. For some of these lines the computations with solar abundances give an unsatisfactory match to the observations. In some cases the atomic data appear to be quite accurate, judging from the agreement of theoretical end experimental values and the number of prominent lines to be discarded for abundance analysis would be uncomfortably large. Moreover the presence of chemically peculiar stars on the upper main–sequence warns us that, due to atmospheric, or environmental, effects, a Pop I star may show abundances which differ from the solar values. We therefore decided to allow ourselves the freedom of adjusting the abundances in order to get a better agreement between observations and computations.

For each element we selected a number of lines and then computed theoretical profiles with solar abundances as a starting point. We then changed the abundance of the given element by steps of 0.25 dex in an iterative fashion, until a match which was satisfactory to visual inspection was reached. This kind of approach relies on a subjective estimate and may be criticized on these grounds. However we were not able to find a non-subjective goodness–of–fit estimator that proves robust when applied to spectra. The conventional maximum–likelihood estimators such as χ^2 proved to be too sensible to noise in the data, on the one hand, and to inadequate input data ("missing lines") in the models, on the other, to be of any practical use in this context. This is a well known problem, it has been dicussed, for instance, by Voels *et al.*(1989), who reach the conclusion that the human eye is probably superior to a χ^2 test to decide on the agreement between observed and computed spectra. A semi–quantitative approach has been used by Grigsby *et al.*(1992), which still relies on subjective estimates of the goodness–of–fit.

It is, perhaps, not surprising to find out that different lines of the same element yield different abundances. In general we adopted as final abundance either the value which fits the largest number of lines (the mode) or that indicated by the "most reliable" lines. In this case " most reliable " usually means that the atomic data is judged to be very accurate, due to a good agreement between experimental values, with small internal errors, and theoretical values, or is quoted as reliable is some critical compilation. In some cases "reliable" simply means that a given line has been used in the literature for abundance determinations yielding results which are consistent with other lines both in the UV and in the optical. In table 5.7 we list the adopted abundances and also, for comparison those of Peters & Polidan (1985) and the solar values from Anders & Grevesse 1989). The abundances are referred to the total number of atoms, as usual. There is a substantial agreement between our values and those of Peters & Polidan (1985) who give rather large error limits. An exception is P II, for which our abundance is over one dex below the value of Peters & Polidan (1985). It is worth to note that our C and N abundances deduced from the neutral lines are lower than those deduced from the lines of the singly ionized atoms. Si II and Si III lines, on the other hand, yield the same abundances, contrary to the results of Wolf and Reitermann (1989) who found that the Si abundance from the Si II lines is about 0.8 dex lower than the abundance deduced from the Si III lines. They used a Kurucz model–atmosphere with $T_{eff} = 17500$ $\log g = 3.55$ and a zero microturbulent velocity.

There are several sources of uncertainty which affect the adopted abundances: the position of the continuum, the value of the macroscopic broadening velocity and the noise in the observed data, as far as the observational data is concerned; the structure of the model–atmosphere, the atomic data used and the incompleteness of the line list, as far as the theoretical data is concerned. There is a marked

difference between observations and computations on the red wing of Ly-α. Either the computed spectrum predicts a too weak Ly-α red wing or the continuum on the Copernicus spectra was placed too high. As a consequence the abundances derived from lines up to 126.0 nm may be systematically overestimated.

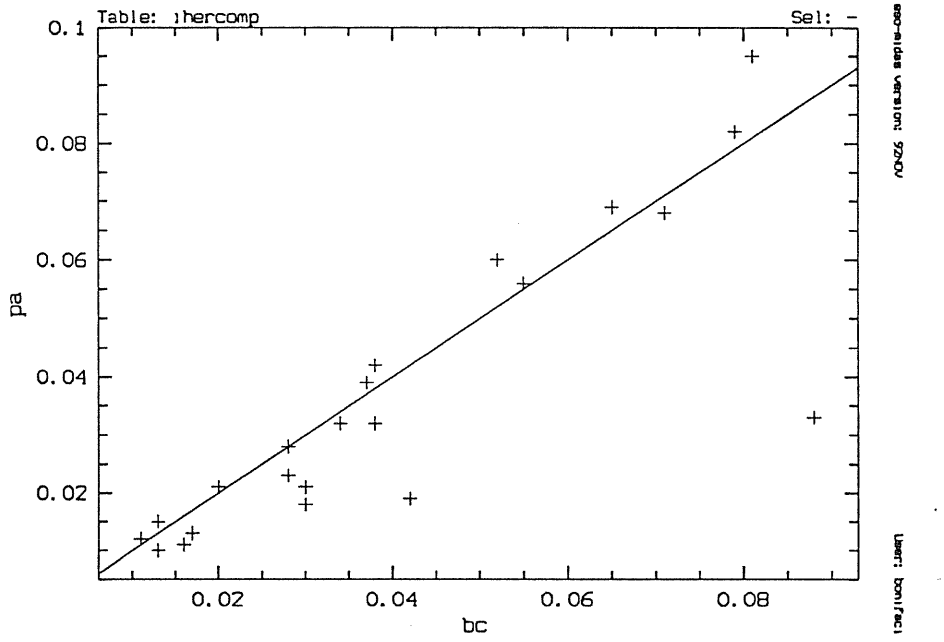

Fig. 5.5 Comparison between our measured equivalent widths (on the x–axis, expressed in pm) and those of Peters& Aller (on the y–axis,expressed in pm).

For the optical spectra, in addition to the synthetic spectrum approach we measured equivalent widths, which are reported in table 5.8. Figure 5.5 shows a comparison between our measured equivalent widths and those of Peters & Aller (1970), the agreement is quite good, in spite of the fact that our lowest resolution

spectrum (image c542) has a $\Delta\lambda$ which is some 24 times larger than that of the 2.02 Å/mm photographic spectra used by Peters & Aller (1970). We used only the unblended lines, or those lines for which blending features are predicted to be minor contributors to the observed feature by our computed spectra, to determine the abundances using version 9 of the WIDTH code. Results are described in the next section.

5.8 Remarks on the individual ions

5.8.1 Helium

There is no He lines in the ultraviolet, however we observed all the He I lines in the region 377.5 nm to 420.0 nm at medium resolution (16.5 Å/mm) and He I 587.5 nm and 667.8 nm at high resolution (2.6 Å/mm). Our computations are not capable of reproducing well any of the observed profiles. This is due to the fact that the code presently does not treat realistically Stark broadening for any of these lines. Work is in progress to use the theory of Barnard *et al.*(1974) to treat He I 447.1 nm. In the case of 587.5 nm and 667.8 nm it is certainly not legitimate to use LTE, as was demonstrated by Auer& Mihalas (1972).

For comparison we show the profile of 587.5 observed with Aurelie together with the theoretical profile of Auer& Mihalas for T_{eff} =20000 and log g= 4.0, the theoretical profile has been broadened with a gaussian profile of FWHM 10 kms^{-1}(figure 5.6). The agreement is quite good, the wavelength scale is that of the observed spectrum, the theoretical spectrum has been shifted to match the observed wavelengths by -0.06 nm. For this same line Auer& Mihalas (1972) show

Fig. 5.6

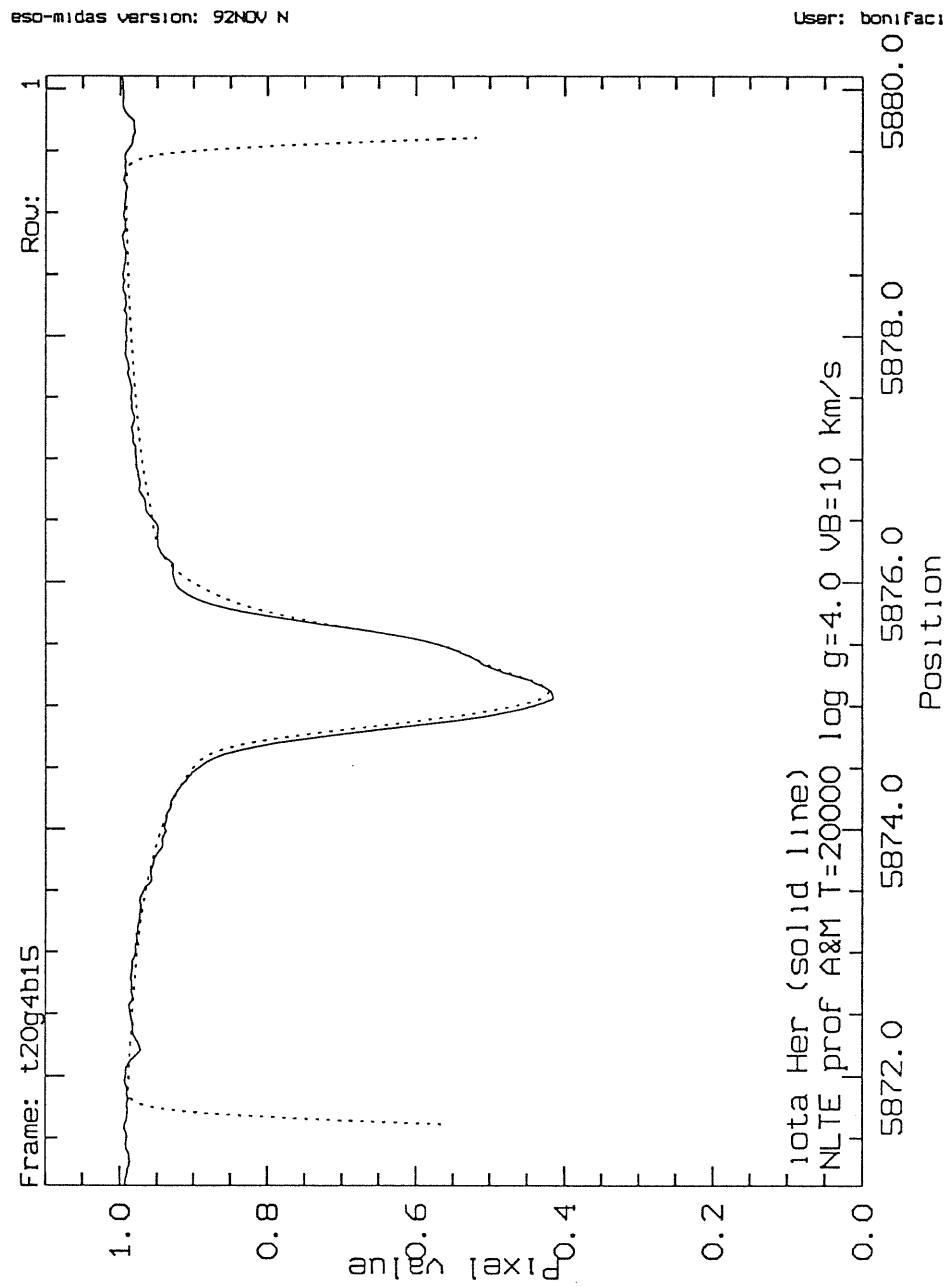
eso-midas version: 92NOV N
User: bonifaci
Row: 1
Frame: t20g4b15
iota Her (solid line)
NLTE prof A&M T=20000 log g=4.0 VB=10 Km/s
Position
Pixel value
5872.0
5874.0
5876.0
5878.0
5880.0
0.0
0.2
0.4
0.6
0.8
1.0

a comparison between the profile of ι Her observed by Peters& Aller (unpublished, quoted by Auer& Mihalas as quoted by Leckrone in his thesis (1969)) and an interpolated profile for the parameters T_{eff} =18000 log g= 3.6 and broadened with $v \sin i$ 5 kms^{-1}. In their plot the core of the line is very poorly reproduced, contrary to what happens by adopting a higher temperature as we do. The comparison of temperature scales of blanketed and unblanketed models is by no means straightforward. In figure 5.7 we show a comparison between the observed profile of He I 667.8 nm and the NLTE profiles from Auer & Mihalas (1972) with T_{eff} = 17500 log g= 4.0 and T_{eff} = 20000 log g=4.0 , both profiles have been broadened with a gaussian with FWHM of 10 $kms^{-1}$and shifted by -0.08 nm to match the observed wavelengths. As can be seen the lower temperature profile fits better the core, while the one with the higher temperature fits better the wings. It would be useful to perform new NLTE line formation computations for these lines using our LTE models as input. We plan to do this in the future using the PANDORA code to solve the equations of statistical equilibrium and the SYNTHE code for spectral synthesis*.

Gravity seems to have little effect on He I 667.8 nm, in figure 5.8 we show the comparison between the observed profile and the profiles from Auer & Mihalas with T_{eff} = 20000 and log g= 3.00 and log g= 4.00. There is a slight effect only on the line wings. If the NLTE effects could be treated satisfactorily it is likely that this line could be successfully used for abundance determination. A definitive statement on the He abundance in ι Her will have to wait until we specifically

---

* SYNTHE is already geared to perform NLTE line formation computations for some lines, but it needs as input the b factors for the populations of each level of the model atom employed. Such b factors may be computed by solving the equations of statistical equilibrium, this is done by the PANDORA code.

Fig. 5.7

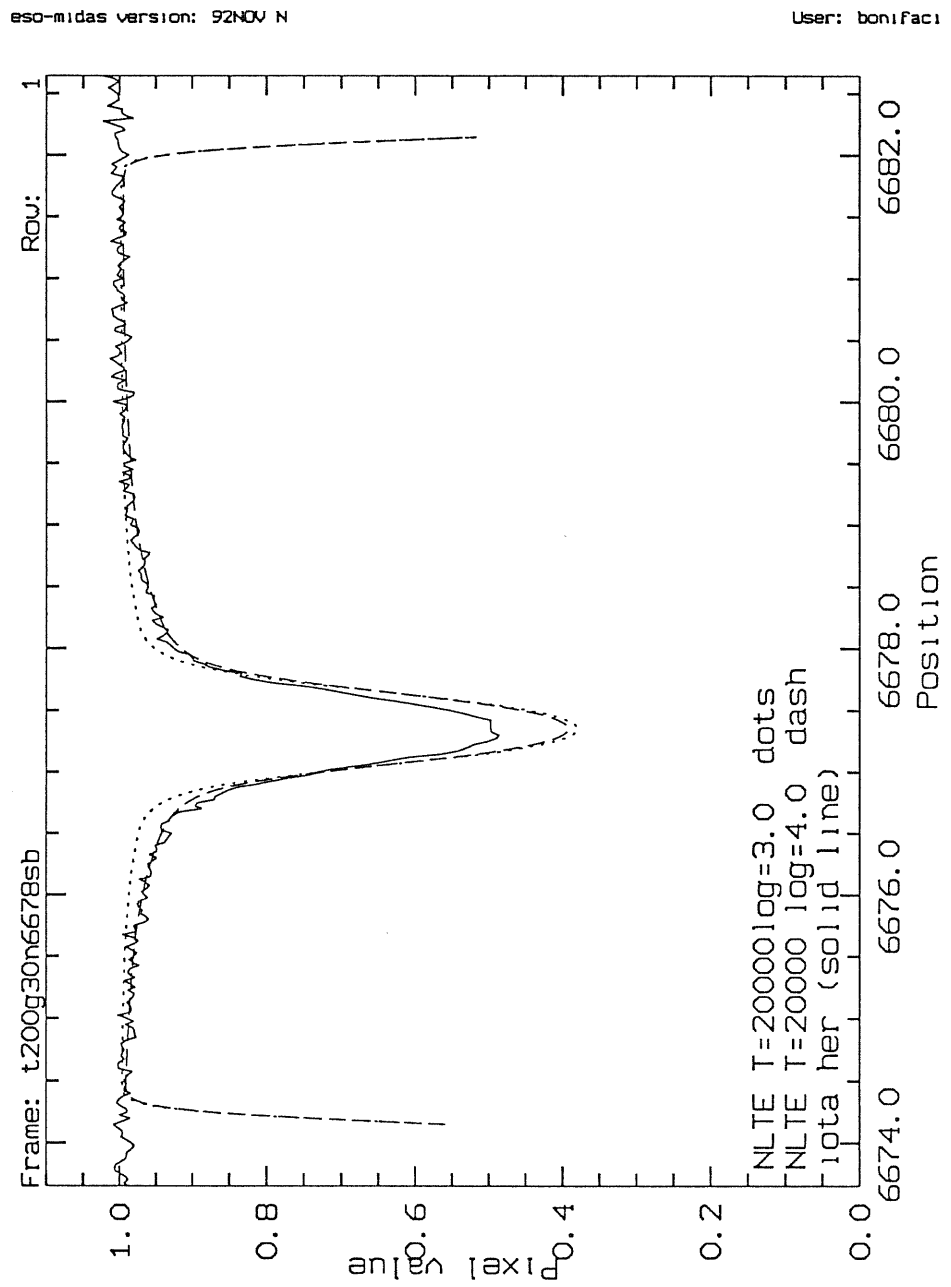
eso-midas version: 92NOV N
User: bonifaci
Frame: t200g30n6678sb
Row: 1
Pixel Value
Position
1.0
0.8
0.6
0.4
0.2
0.0
6674.0
6676.0
6678.0
6680.0
6682.0
NLTE T=20000log=3.0 dots
NLTE T=20000 log=4.0 dash
Iota her (solid line)

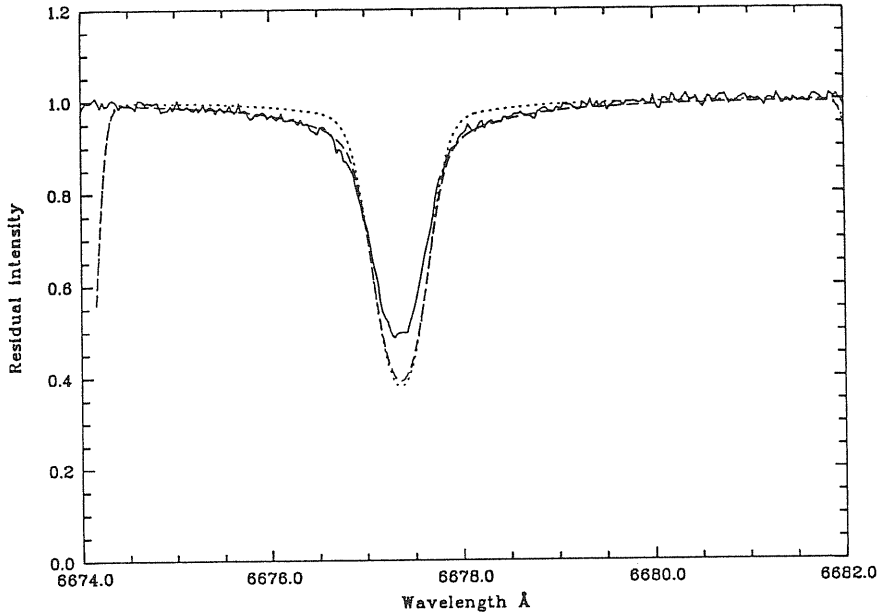

Fig. 5.8 Comparison between the observed He I $2^1P - 3^1D$ transition in ι Her and theoretical NLTE profiles from Auer& Mihalas (1973). The dotted line corresponds to $T_{eff} = 20000$ and $\log g = 3.0$, the dashed line corresponds to $T_{eff} = 20000$ and $\log g = 4.0$.

modify the spectrum synthesis code to treat the Stark broadening of the blue–violet He I lines, which are little affected by NLTE effects.

5.8.2 Boron

There is a single detectable Boron line in our spectra: the B II resonance line at 136.246 nm. This line is heavily blended. Different line lists have been used in the literature to compute this feature, our spectrum computed with Kurucz's line list predicts the Following components: Fe II 136.2267 nm (0.081), Ni II 136.2354 nm (0.790), Si III 136.2361 nm (0.257), Fe III 136.2361 nm (0.190), B II 136.2461 nm (0.033), V II 136.2508 nm (0.466), Zn III 136.2520 nm (0.696), Fe II 136.2535 nm (0.695). The numbers in brackets indicate the predicted residual intensity at line center of each line prior to convolution with rotational and instrumental profiles.

To check the influence of the minor components on the computed feature we performed four computations each time omitting one of the following lines: V III, Zn III, Fe II 136.2535 nm and Fe III 136.2361 nm. The effect is negligible, when compared to the the observational data. We concluded that the different line lists adopted in the literature are equally valid for the purpose of computing this feature.

We derived a Boron abundance $\log(N(\mathrm{B})/\mathrm{N_{tot}} = -10.0$. The B abundance in the sun, as determined from the B I lines at 249.6772 nm and 249.7723 nm, is $\log(N(\mathrm{B})/\mathrm{N_{tot}} = -9.40 \pm 0.3$(Kohl *et al.*,1977 ; Anders & Grevesse, 1989). The boron abundance determined from the B II resonance line in early type stars ranges from -10.52 to -9.40 dex (Leckrone, 1981). For ι Her Heber (1983) used our same IUE spectra, a blanketed model of $\mathrm{T_{eff}} = 18000$ K and $\log g$=3.5 and the line list of Boesgard & Heacox (1978) to compute synthetic profiles. He found $\log(N(\mathrm{B})/\mathrm{N_{tot}} = -10.3$. Our result is consistent with that of Heber (1983) and with the typical values of B abundance found in normal B–type stars.

5.8.3 Carbon

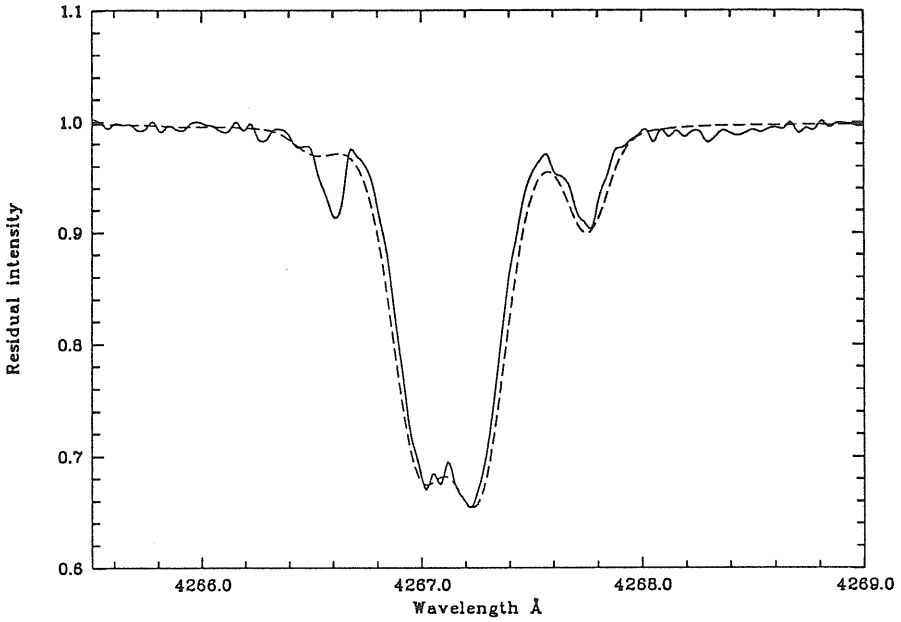

Fig. 5.9 The observed C II doublet at 426.7 nm of ι Her compared with our computed profile (dashed line), assuming solar abundances.

In the 1990 paper we used the C II lines of multiplets 1,10 and 11 to derive an abundance of -3.75, which is 0.25 dex lower than the solar value. The abundance determined from the C I lines, on the other hand, decreases from -3.75 to -4.75 as the multiplet numbers decrease from 9 to 2. The C I lines of multiplets higher than 9 are consistent with an abundance of -3.75, however all of them are either heavily blended or very weak. The use of the new model does not alter this conclusion.

The C III line of UV multiplet 9 at 124.7383 nm is consistent with a C abundance of -3.75, but is equally well reproduced by a computation using solar abundance.

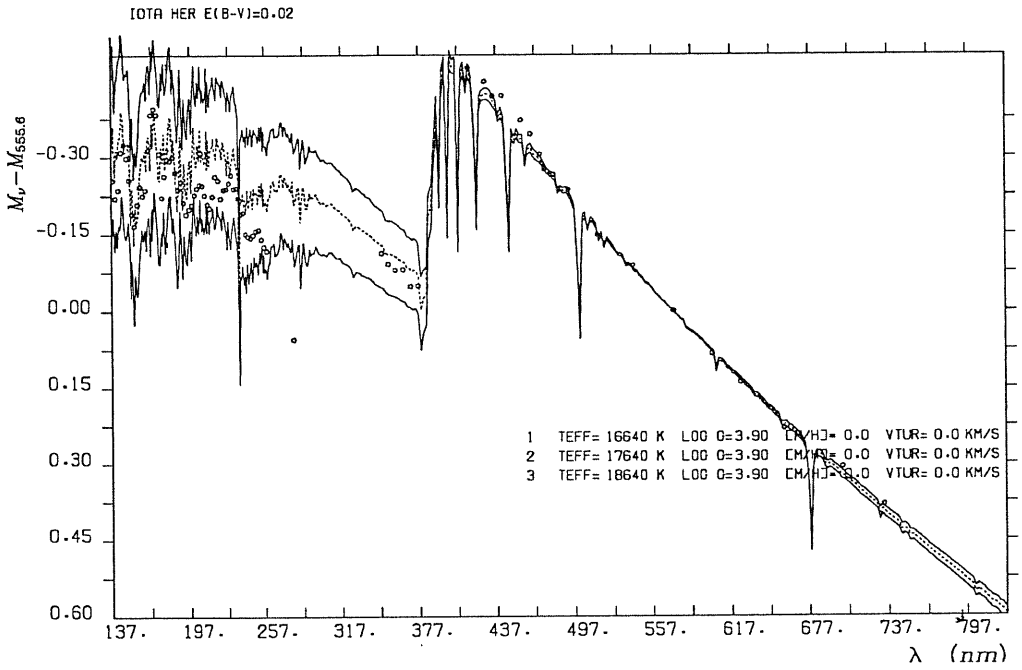

Fig. 5.10 The observed flux of ι Her , expressed in magnitudes normalized at 555.6 nm (visible data from Kubiak (1973), UV data from Jamar *et al.*,1976), compared with theoretical fluxes computed for log g = 3.90 and T_{eff} =16640 K, T_{eff} =17640 K and T_{eff} = 18640 K.

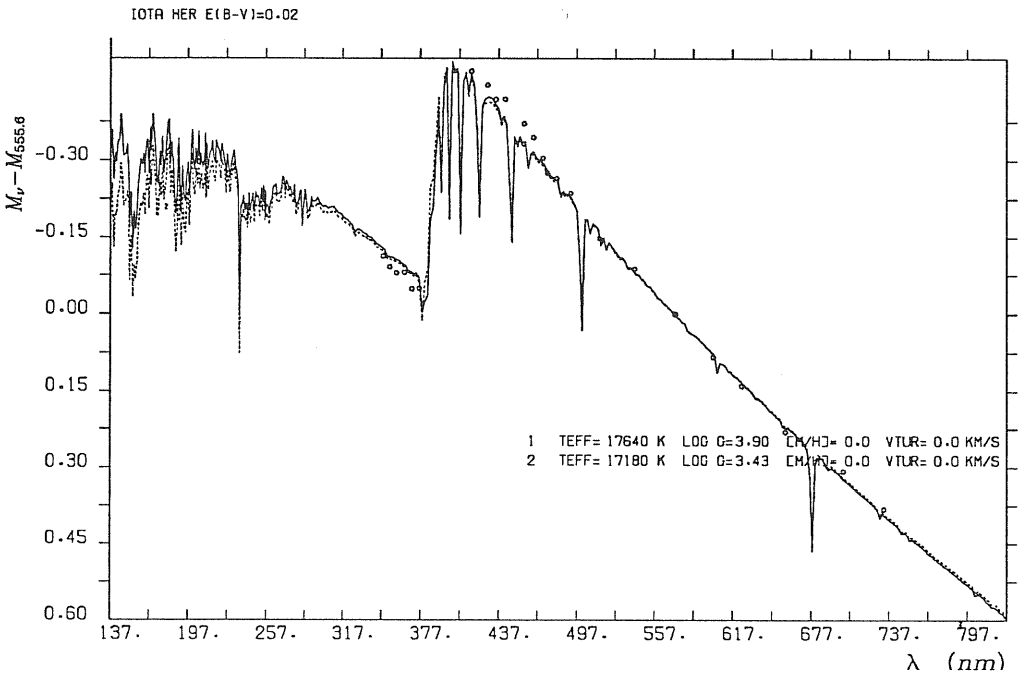

Fig. 5.11 The observed flux of ι Her , expressed in magnitudes normalized at 555.6 nm (visible data from Kubiak (1973), UV data from Jamar *et al.*,1976), compared with theoretical fluxes computed for log g = 3.90 and T_{eff} =17640 K and log g = 3.43 KT_{eff} = 17180 K (the model parametrs adopted in the 1990 paper).

Grigsby (1991) computed a non–LTE, line-blanketed synthetic spectrum of ι Her. He modelled C II lines of multiplet 1 and 11 and the C III line of UV multiplet 9. For the C II lines he finds that a spectrum computed with a C abundance of -3.78 fits the observations better than one computed with a solar C abundance. Both his computed spectra, however, predict slightly stronger lines than are observed. The same is true for the C III line, however in this case the spectrum computed

with solar abundance predicts a line far too strong, particularly in the wings. This is somewhat at odds with our LTE computations, since we find that the line is not particularly sensitive to the effect of abundance. Even the best–fitting computed spectrum of Grigsby seems to have wings which are slightly stronger than the observed ones. The model parameters used by Grigsby are $T_{eff} = 17500$ and $\log g = 3.75$ The temperature is reasonably near to the one adopted in our paper, the gravity is slightly lower and should have a non–negligible effect on the lines of the ionized species. In any case it is not straightforward to compare the temperature scales defined by the two different kinds of models.

From the analysis of the visible spectrum Peters& Aller derive a mean C abundance of -3.31, therefore slightly over the solar value. From the C II doublet at 426.7 nm, which is resolved in their spectra, they find an abundance of -3.55 for the weaker and -3.38 for the stronger component. This is consistent with our observation of this feature, which is well reproduced by a computation with a solar C abundance (figure 5.9). This doublet, though frequently used to determine C abundances, usually yields abundances which are a few dex lower than other lines. Lennon (1983) computed LTE and non–LTE equivalent widths for this doublet, as well as for the doublet 657.8 nm, 658.2 nm and found that theoretical widths are systematically larger than observed widths, he therefore recommended that the 426.7 nm doublet should not be used for abundance determinations.

We measured the equivalent widths of C II 391.8968 and C II 392.0681 and used the WIDTH code and a model atmosphere with $\log g = 3.80$, $T_{eff} = 17640$ K and zero microturbulent velocity and find an average abundance of -3.77, in good agreement with that determined from the UV. For the C II lines of multiplet 2, which lie on the red wing of H_α we determine a much higher abundance: -3.15. We doubt that this result is due to an error in the placement of the continuum,

since our synthetic spectrum fits well the observed wings of H_α. Our equivalent widths are in good agreement with those of Peters & Aller (1970) and Barnett & Mc Keith (1988), if anything our equivalent widths are slightly smaller than those of the above–mentioned authors. Yet Barnett& Mc Keith derive a C abundance which is essentially solar, while Peters& Aller derive an overabundance of about .5 dex, in substantial agreement with our result. The difference in the gf values adopted by us and by Barnett& Mc Keith on the one hand and Peters& Aller on the other, has little influence on the derived abundance. We checked this by using our equivalent widths and model and the log gf values from the other two papers, the changes in the derived abundances are less than .1 dex on the individual lines. The difference lies mainly in the different microturbulent velocity, in fact, by using our model and atomic data, but a microturbulence of 5 kms^{-1} as do Barnett& Mc Keith (1988), we derive an abundance which is solar, or only slightly above solar, in accordance with Barnett& Mc Keith (1988). Instead Peters & Aller (1970) adopt a zero microturbulent velocity, as we do, and derive a significant carbon overabundance from these two lines. In their discussion Peters& Aller state that an increase in microturbulent velocity from $0kms^{-1}$ to 4 kms^{-1} would decrease abundances of the order of .1 dex. This is certainly not true for C II multiplet 2 where the change is of the order of .3–.5 dex. That this multiplet yields results in disagreement with those derived from other multiplets unless a higher microturbulence is adopted is a clear indication that these lines are affected by NLTE. Further theoretical work on these lines is highly desirable.

5.8.4 Nitrogen

The neutral lines of multiplets 4,9 and 13 indicate a Nitrogen abundance of -5.00, i.e. 1.01 dex lower than the solar value. The lines of multiplets 5 and 12, instead, indicate an abundance of -4.5. The lines of multiplet 5 at 124.3 nm lie on the red wing of Ly_α, where the continuum is difficult to define. The lines of multiplet 10 at 141.9 nm are consistent with a solar N abundance.

We could not use the strong lines at 127.5027 nm, 127.6202 nm and 127.6791 nm, identified as N II by Upson & Rogerson, for the abundance analysis because the gf values are not known. However our computed spectrum predicts N II lines at 129.9788 nm, 129.9814 nm and 130.0035 nm, which agree well with the observed features if a nitrogen abundance of -5.00 is used.

The analysis of Peters & Aller (1970) yields a nitrogen abundance which is about 0.1 dex above the solar value. Peters & Polidan (1985), instead, give a value which is 0.16 dex *below* the solar value. Both these papers used N II lines in the visible range. All of the lines used by Peters & Aller are very weak, the strongest being N II 399.4997 nm, with a equivalent widthof 4.2 pm . For this feature We measure an equivalent widthof 3.78 pm which yields an abundance of -4.24 with our new model, this agrees with the result of Peters & Polidan (1985). We also measure an equivalent width of 1.31 pm for the N II line at 404.1310 nm and this yields an abundance of -4.48, in substantial agreement with the other, stronger line. So there is some inconsistency between the UV results, based primarily on neutral Nitrogen and the results from lines in the blue–visible region, which are based on N II lines. This could be due to an incorrectly chosen temperature, however to force the ionization equilibrium between N I (in the UV) and N II (in the visible) would require a temperature in excess of 19000 K. An alternative explanation is that we are confronted with NLTE effects.

5.8.5 Oxygen

The only observable oxygen lines in the IUE short-wavelength range are those of O I multiplet 2 at 130.2, 130.4 and 130.6 nm. The two lines at the longest wavelengths are well reproduced by computations assuming solar abundance. The line at 130.2 is stronger than the computed feature. Since this is a resonance line, and the radial velocity of ι Her is low (-20 kms^{-1} ,Lesh, 1968), there could be a contribution from an interstellar component (Underhill & Doazan, 1982). There are two unidentified features which correspond to the wavelengths of the lines of O I multiplet 1 (135.5605 nm and 135.8524 nm), these are semiforbidden lines and could be of interstellar origin. The feature at 135.5 nm in π Cet and ν Cap has been tentatively identified as O I by Artru *et al.*(1989). However the log gf values both from Wiese *et al.*(1966) and from Cowan *et al.*(1982) are so small that the observed feature may not be reproduced with a solar oxygen abundance.

Our result for the abundance is consistent both with that of Peters & Aller (1970) (-3.12 from many O II lines in the blue and visual regions), Peters & Polidan (1985) (-3.05 , from the O I lines at 130.4 nm and 130.2 nm and -3.37 from 49 O II lines in the visible) as well as with that of Kane *et al.*(1980) (-3.34 from O II lines in the visible).

We wish to remark that all O II lines in the visible are very weak. The largest equivalent width measured by Peters & Aller is 2.9 pm for the line at 464.9 nm. We measured the equivalent widths of two weak O II lines at 407.2155 nm and 411.9215 nm. With our new model these yield an Oxygen abundance of -3.39 and -3.57 respectively, which is consistent with the above–mentioned results. We conclude that the oxygen abundance in ι Her is solar.

5.8.6 Magnesium

We used the Mg II lines at 173.4852 nm, 173.7613 nm, 173.7628 nm and 175.3474 nm to determine an Mg abundance of -4.46. Peters and Polidan (1985) determine a Magnesium abundance which is some .26 dex below the solar value. Unfortunately we do not have any observation of visible Mg lines. Peters and Aller (1970) find a solar Mg abundance.

5.8.7 Aluminium

The lines of Al II and Al III in the UV yield abundances which range from solar (-5.57) to -6.00. In the 1990 paper we adopted an abundance of -5.75 to compute the spectrum. With the new model we prefer a slightly higher abundance, i.e. essentially solar. We also measured the equivalent widths of Al II 390.0675 nm and Al III 414.9913 nm; they yield an abundance of -5.81 and -5.27 respectively, the average is -5.54 i.e. solar.

5.8.8 Silicon

There is some ambiguity in the Silicon abundance. In the UV, Si III lines of multiplets 1,9,10,20,36,38 and 39 indicate a solar abundance. On the other hand the Si III lines of multiplet 4 would be better reproduced assuming an abundance some 0.25 dex below the solar value. In the 1990 paper we also pointed out a discrepancy between the profiles of these lines observed with Copernicus and IUE; the IUE profiles show deeper cores. This could be due to an overestimate of the background in the IUE data. At these short wavelengths the Copernicus data ought to be superior. The lines of multiplet 4 have been shown by Singh & Castelli (1991) to be quite insensitive to temperature and gravity, and therefore are well

suited to be used for abundance determination. For the Si II lines in the UV the situation is intricate as well. Si II lines of multiplets 2,3 and 4 would be better reproduced by assuming an abundance of -4.75 dex. Several Si II lines indicate a solar abundance (multiplets 1,2,8,10.01,13.02,13.05), while multiplets 7, 10 and 11.01 indicate an abundance which is some 0.5 dex above the solar value. Si II lines of multiplet 13.04 are very sensitive to temperature (Singh & Castelli, 1991) and are therefore not recommended to determine the Si abundance.

The Si IV lines at 139.3755 nm and 140.2770 nm show extended wings, which make the placement of the continuum problematic. The wings of the lines seem to be satisfactorily reproduced by computations which assume a solar Si abundance, while the cores of the computed lines are always too weak.

In the visible we measured the equivalent widths of 6 Si II lines and the average abundance is -4.67 ± 0.21 (the quoted error is simply the standard deviation from the mean). Using our model and the equivalent widths of Peters & Aller (1970), for the four Si II lines which we have in common we get an average abundance of -4.76 ± 0.24, in close agreement with the result obtained using our equivalent widths. We also measured the equivalent width of the Si III line at 380.6526 nm and found a value in close agreement with that published by Peters & Aller (1970). This line, however, yields the extraordinarily high abundance of -4.00. From the same line, but with a different model and log gf value Peters & Aller (1970) deduced an abundance of -5.01 . There is probably some problem with the gf value for this line. From Berry *et al.*(1971) one finds log gf = 0.527, it would require log gf $\approx$ 1.200 to get, from the equivalent width of this line, the same abundance as the average of the Si II lines.

We conclude that the Si abundance is solar, but have to place a rather high uncertainty of 0.5 dex on this value, in view of the large scatter of the values derived from the different lines.

5.8.9 Phosphorous

There are relatively few P lines in the UV spectrum of ι Her we were interested in assessing the reliability of the gf values to be used in the analysis of F86. We adopted an abundance which is a factor of 10 lower than the solar value, based mainly on P II lines. However there is a large scatter in the abundance determined from individual lines. For P II we used the experimental gf values of Miller *et al.*(1971); we also used the theoretical f values of Hibbert (1988). In the UV our synthetic spectra computed with the log gf values derived from the f_l values of Hibbert, and solar P abundance predict lines which are far too strong, thus suggesting the P abundance to be much lower than the solar value. We want to point out the following facts: for P II 145.2900 there is a good agreement between IUE image S5720 and a theoretical profile computed with the Miller *et al.*(1971) log gf and a P abundance 10 times lower than the solar value. The use of the log gf from Hibbert (1988) would require an even lower P abundance. However in the Copernicus second order spectrum there is no detectable line. For the lines of multiplet 1 the situation is similar, the use of the log gf from Hibbert (1988) would imply a P underabundance of a factor 100.

All that can be said is that there probably are problems with the gf values of phosphorous. In view of this any P abundance ought to be considered a rough estimate.

5.8.10 Sulfur

The Sulfur abundance is solar, although some of the S I lines in the UV indicate an abundance which is slightly lower. The strong S II lines of UV multiplet 1, on the contrary, would better agree with computations which assume an S overabundance by a factor of 6 or 7. Since these are resonance lines they may be affected by an unresolved interstellar component. We measured the equivalent widths of 8 S II lines in the visible and deduced an S abundance of -4.76 ± 0.34, which is consistent with the solar value (-4.83). We used the equivalent widths of Peters & Aller (1970), for the four S II lines which we had in common, and our model and determined an S abundance of -4.85, in close agreement with the result determined from our equivalent widths. Peters & Polidan (1985), also derived a solar abundance from the visible S II lines, but an underabundance by a factor of two from 5 S III lines.

5.8.11 Gallium

Two Ga III lines are clearly detectable at 149.5045 nm and 153.446 nm. These are well reproduced by our computations if we assume a Ga overabundance of a factor of 10 or so. This value is also consistent with the Ga II line at 141.444 nm observed with Copernicus, however the IUE spectra show a much weaker line. Our result is at odds with that of Takada-Hidai *et al.*(1986) who derived, from the equivalent widths of Ga II 141.444 nm and Ga III 149.5045 nm an *underabundance* by a factor of 1.25 to 3 with respect to their adopted solar value, which is some .1 dex below the value given by Anders & Grevesse (1989). The above group adopted a Kurucz model with T_{eff} = 17800 K log g= 3.8 and a microturbulent velocity of 2 kms^{-1}.

5.9 Conclusions

The analysis of ι Her has been useful to test the capabilities of the Kurucz codes and data. It is quite reassuring to find that the model which best reproduces the observed colours and fluxes is also well suited to be used as input for a synthetic spectrum calculation, both in the UV and in the visible.

However there are some problems. In the first place in the UV there still is a large number of "missing lines", in spite of the considerable growth and improvement of the Kurucz data base in the recent years. In the second place the scatter in the abundances determined from individual lines is always quite large and ranges from 0.3 to over 1.0 dex. Particularly striking is the smooth decrease in the C abundance determined from C I lines, with decreasing multiplet number. It is likely that these inconsistencies are rooted in the shortcomings of the models and of the atomic data available, rather than due to stellar peculiarities or problems with the observational data.

The comparison between our LTE analysis and that of Grigsby (1991), which is NLTE, legitimates the use of LTE methods for the analysis of dwarf stars in this temperature range. NLTE effects are certainly important for some lines, noticeably He I 587.5 nm and He I 667.8 nm, on the other hand the C II doublet at 426.7 nm seems quite satisfactorily reproduced by our LTE computations. On the other hand we have shown that there are good reasons to suspect NLTE effects for the C II doublet 657.8 nm , 658.2 nm .

The conclusion one may draw from the above discussion is that estimated errors in the abundances lower than 0.3 dex ought to be frowned upon.

The usefulness of the published atlas is mainly as a comparison standard to help line identification in stars of similar spectral type. It also may be used as

a way of selecting spectral features suitable for abundance analysis. We plan to extend this work in the future to the long–wavelength range of IUE, making use of coadded spectra.

Chapter 6

The Halo blue star Feige 86

6.1 Introduction

In the thesis I submitted for the degree of *Magister Philosophiae* (Bonifacio 1991), I thoroughly reviewed the existing literature on F86, nor has any other relevant paper appeared in press since. I shall here only briefly recall the main characteristics of this star.

It is a relatively bright ($m_V = 10.055$; Neckel and Chini, 1980), high galactic latitude (l=47.89° b=79.42°) blue ((B-V)=-0.13 ; *ibid.*) star, with a high proper motion ($\mu_\alpha = -0.034''$; $\mu_\delta = -0.103''$; Luyten, 1959) and a low radial velocity ($v_r = -23$ kms^{-1} ; Berger, 1963). In order to transform this data into space velocities relative to the galactic center the distance of the star must be known. To estimate its absolute magnitude we must fix to which population the star belongs: if we assume the star is on the main sequence, we find a spectral type of B3, by using the table of Fitzgerald (1970) relating the spectral type to the (B-V) colour. Next, using the table of Underhill& Doazan (1982, p.23) to estimate M_V from the spectral type we find $M_V = -1.3$ (adopting the calibration of Lesh, 1979). Thus the distance modulus would be 11.355 and the space velocity vector (U, V, W) (in kms^{-1}) would be (-336,-897,55) , where U is pointing away from the galactic center , V is along the direction of galactic rotation and W is towards the North Galactic Pole. Such a velocity vector is quite unlike that of any MS Pop I star and unheard of even for a B runaway star. Note that the star would have a large retrograde motion !

Alternatively, if we assume that the star is a Pop II HB star, its absolute magnitude would be $M_V \approx +2.0$ because this is the typical absolute magnitude of blue HB stars in globular clusters such as M92 and M3 (Sandage, 1970). Its

velocity vector (in kms^{-1}) would then be (-71,-199,-5). Such a velocity is typical of extreme Pop II.

We may thus conclude that, on kinematical grounds, F86 is expected to be a halo HB star. This makes it only a mildly interesting object to study. What makes it exceptional is its spectrum: at low dispersion in the visible it shows He lines all very weak. In fact in the SAO catalogue the star is assigned a spectral type of A2. At classification dispersion the most prominent lines in B type spectra are the He I lines, weak He I line characterize early A and late O, early B stars. However late O and early B stars also show He II lines (noticeably He II 468.6), which are absent from the spectrum of F86. It is thus not surprising that the star was classified as early A-type. However this spectral type is inconsistent with its (B-V) colour. B stars with weak He lines form a class of chemically peculiar (hereafter CP) Pop I stars. It is therefore interesting to study a Pop II star which shows this characteristic. In fact a HB star has a totally different mass and luminosity than a MS star of the same spectral type, in spite of the fact that it has roughly the same surface gravity and effective temperature. That the weak He line phenomenon should show up in both kinds of star is a clear indication that it must depend only on the "atmospheric" parameters T_{eff} ,g and not on the "global" parameters M,L . A further spectral peculiarity of F86 is evident only on medium or high dispersion spectra: many weak, narrow absorption lines, which are absent from normal B-type spectra are present in the whole visible region from 390 nm to 670 nm. These lines have been identified as PII by Sargent& Searle (1967 ; hereafter SS) and our optical data and synthetic spectrum calculations have confirmed the identifications.

The most straightforward explanation for the presence of these strong PII lines is that in the atmosphere of F86 the P abundance is enhanced above the

solar value, which is difficult to understand for a Pop II star. Pop I CP stars whith a P overabundance are known in the literature. One such example is the Pop I Bp star 3Cen A (Jugaku & Sargent, 1963, Stalio & Hack, 1975). Often the spectrum of F86 has been claimed to be similar to that of (SS, Baschek& Sargent 1976, Hartoog, 1979). The fine abundance analysis performed by Baschek& Sargent (1976; hereafter BS) on the basis of high dispersion optical spectra confirm the P overabundance and the whole abundance pattern resembles that of He-weak Pop I stars rather than that of Pop II stars. Thus F86 appears to be an extraordinary object. The results of BS have been often quoted (Michaud, 1980; Bonsack& Wolff, 1982 ; Glaspey *et al.*, 1989) to give support to the diffusion theory (Michaud, 1970; see also Bonifacio, 1991 pp. 12–16 and references therein). The claim is that only diffusion theory gives an explanation for the similarity of atmospheric abundances in stars of such different M,L and age. I wish to give here four remarks which ought to be kept in mind when trying to interpret the abundances of F86. Here and elsewhere we shall call "intrinsic" the abundances which characterize the star's interior[1] , which may or may not differ from the abundances of the gas from which the star was formed, and "atmospheric" the abundances which characterize the atmosphere only.

1. If F86 is a typical Pop II star the intrinsic P abundance was less than solar when diffusion began to operate. That the present P abundance should be comparable with that of 3Cen A, whose intrinsic P abundance is solar, implies that one of the following is true: either diffusion has been more effective in F86 than in 3Cen A or there exists a maximum P abundance which may be supported in a B star atmosphere and both have reached such limiting

[1] obviously excluding the core, whose chemical composition is changing in time due to nuclear reactions.

abundance. There exists a third, though very unlikely, possibility: that P abundance is some complex function of time such that, given that diffusion has been operating for different lengths of time in F86 and 3Cen A, the two present P abundances have *by chance* the same value albeit the different initial values.

2. The star CL1083 in NGC 6752, analyzed by Glaspey *et al.*(1989) has atmospheric parameters similar to those of F86. It is certainly a Pop II star and does show chemical peculiarities such as He underabundance and Fe overabundance (over, here, means with respect to the intrinsic abundance), however does not show P overabundance. No PII lines have been detected. This suggests that there exists some parameter other than T_{eff} , g and slow rotation which governs the chemical peculiarities.
3. If F86 is indeed a Pop II star it would be interesting to asses whether it is a rare weird or a rather common object. The presence of a considerable number of HB stars with chemical peculiarities (as would be expected if diffusion is the cause of the peculiarities) may seriously affect the study of metallicity in different populations.
4. It would be interesting to derive, from the study of F86 spectroscopic criteria to separate HB stars, albeit with peculiar spectra, from MS Bp stars, and then test them on a non–kinematically selected sample.

I began to study F86 in 1986, under the supervision of Prof. M. Hack and Dr. F. Castelli as the topic of my "Tesi di Laurea" which I discussed in October 1988. Initially the goal was to perform an abundance analysis from the IUE high–resolution spectra of F86 one of which (SWP4616) had been described by Hack (1980). For a B–type star many more lines of many more elements are observable in the UV spectrum than in the visible spectrum. It was hoped that

the UV analysis would have enlarged and improved that of BS owing to the larger number of lines analysed. However the complexity of the UV spectrum of F86 very soon frustrated these high hopes. The analysis was performed through spectral synthesis techniques, these require 1) a model–atmosphere for the star 2) a set of reliable atomic data to predict the spectral lines. These two points needed a lot of time and effort to be sorted out and resulted in the definition of some of the methods described in chapter 4 for the determination of T_{eff} and g on the one hand and on the publication of the UV spectral atlas of ι Her on the other (Castelli and Bonifacio, 1990; see chapter 5).

At an early stage we also realized that the analysis would have also greatly benefited from the availability of optical spectra. I therefore undertook a number of observational runs at Observatoire de Haute–Provence with the 1.52 m telescope equipped with the AURELIE spectrograph (Gillet, 1989). In the following paragraphs I shall describe the data and the results of the analysis of F86 based on UV and optical spectra.

6.2 The Data

6.2.1 Colour indices

Since we did not perform any photometric observations we searched the SIMBAD data base for UBV, uvby and H_β photometry. The colour indices given in table 6.1 were used to compute the colour excess E(B-V), given in table 6.2, and to derive the first estimates of the atmospheric parameters as discussed in section 6.4.

Table 6.1

Photometric data for F86

Strömgren photometry[1]				
Reference	(b-y)	m1	c1	β
Hauck& Mermillod (1990)	-0.062	0.104	0.320	2.696
Stetson (1991)	-0.060	0.111	0.293	2.700
Johnson photometry				
Reference	V	$(B-V)$	$(U-B)$	
Klemola (1962)	10.11	-0.15	-0.64	
Westerlund (1964)	10.13	-0.20	-0.62	
Sargent & Searle (1967)	10.0	-0.15	-0.68	
Neckel & Chini (1980)	10.055	-0.135	-0.632	
Carney (1983)	10.06	-0.14	-0.645	

[1] The measurements prior to 1990 are all included in the Hauck & Mermillod catalogue.

6.2.2 Energy distributions – low resolution data

For the visual range we have used the spectrophotometric data given in the Breger (1976) catalogue. This is the energy distribution measured by Sargent& Searle (1968), in the range from 339.0 nm to 555.6 nm and converted by Breger to

the Hayes and Latham (1975) absolute calibration of Vega. We converted Breger's magnitudes, which are normalized at 500.0 nm to magnitudes normalized at 555.6 nm .

For the ultraviolet we searched the ULDA (Wamsteker *et al.*,1989) archive for low resolution spectra of F86. We found 11 spectra and we rejected all those taken with the small aperture owing to the centering problems which make the transmission always uncertain (Harris and Sonneborn, 1987). We also rejected all overexposed and underexposed images, since they cannot be photometrically accurate. We were then left with three images: LWR3303L, SWP3723L and SWP9522L. We corrected them for the change in sensitivity of the IUE cameras with subroutine TCHANG of Bohlin and Grillmair (1988).

The spectral energy distribution of F86, ranging from 117.0 nm to 516.2 nm is given also by Huenemoerder *et al.*(1984). However, we preferred not to use these data due to the lack of information on the normalization constant and the adopted calibration.

6.2.3 Optical line spectra–medium and high resolution data

All the visible spectra used in this work have been secured at Observatoire de Haute–Provence with the 1.52 m telescope and the AURELIE spectrograph (Gillet, 1989) during three observational runs from 1990 to 1992. The detailed observations log is given in table 6.3. Different grating/filter calibrations have been used with resolution ranging from 6000 to 31000. The main goal was the observation of the Balmer lines, in order to fix the gravity, and of those lines of HeI and PII for which BS give equivalent widths, in order to compare the results. In addition we observed the HeI line at 587.5 nm and the one at 667.8 nm; the latter was observed also by Hartoog (1979).

The reduction of the Aurelie data was done using the MIDAS software. The general procedure is described in Bonifacio (1991).

For each spectrum we took several calibration exposures, which were of four types: 1) offsets (zero seconds exposures in order to give the value of the electronic offset), 2) flat-fields (obtained with a tungsten lamp, to be used to remove the pixel to pixel variations in the response of the detector), 3) Th-Ar hollow cathode spectra (for wavelength calibration) and 4) dark exposures (long exposures with the spectrograph shutter closed, used to monitor dark current). We computed a mean offset (from at least five offset exposures) and a mean flat–field for each image. Whenever possible we obtained flat–fields with roughly the same number of counts as the stellar image. After having subtracted the mean offset from the stellar spectrum this was divided by the offset–subtracted mean flat–field. A wavelength calibration was derived by interactively identifying lines in the Th-Ar spectrum and fitting a second or third order polynomial to the dispersion relation. The typical R.M.S. on the fit was .1 to .2 pixels. Using the dispersion coefficients so obtained each image was rebinned at steps of constant wavelength. We took care to oversample the spectra. Typical step–size was $\frac{\Delta\lambda}{3}$ where $\Delta\lambda$ is the nominal resolving power of a given grating/filter combination; the corresponding nominal resolution is given in table 6.3. The spectra were normalized to the continuum, by fitting a spline through interactively chosen points. Whenever more than one image was available for a given spectral range, we coadded the spectra, after having checked that there was no sign of variability. Prior to coadding the spectra each image was filtered with a median filter to remove spiky noise. For the range from 377.4 nm to 420.8 nm we coadded images C691 and C692, as described in section 6.3. In a similar way we coadded images C847,C627 and C65 to cover the range from 407.2 nm to 451.0 nm, we shall refer to this coadded spectrum as LOW43.

We also coadded all the the five above–mentioned images to yield the H_δ shown in figure 6.10.

Our optical spectra cover most of the classical photographic region available to BS and SS, though we have a lower spectral resolution. In addition we were able to observe some regions in the red which were not accessible to IIaO emulsions.

We measured equivalent widths for most of the lines measured by BS. We used the interactive code BANDGEN, which fits a gaussian to the observed profiles using the Frazer& Suzuki (1966) algorithm, we assumed the equivalent width to be the area of the fitted gaussian. When a coadded spectrum was available we measured equivalent widths on the coadded spectrum. Lines in the overlapping region of two coadded spectra were measured independently on each coadded spectrum.

Our material is rather heterogeneous having a variety of resolutions provided by the different grating/filter combinations employed. This makes it impossible to make a detailed analysis of equivalent widths systematics.

Of our spectra only two have a considerable wavelength overlap: image M232 and the coadded spectrum LOW43. The former image has the reciprocal dispersion of 8 Å/mm while the latter 16.5 Å/mm. We were able to measure 11 lines on both spectra the mean difference between the two measurements is 1.3 pm with a standard deviation of 2.2 pm from the mean. A regression analysis yields the following relation:

$$EW_{LOW43} \approx 1.6\text{pm} + 0.959 EW_{M232}$$

This result gave us confidence that our set of equivalent widths is self–consistent, in spite of the heterogeneity of the observational material. We therefore decided, for the lines which could be measured on at least two spectra, to take a straight

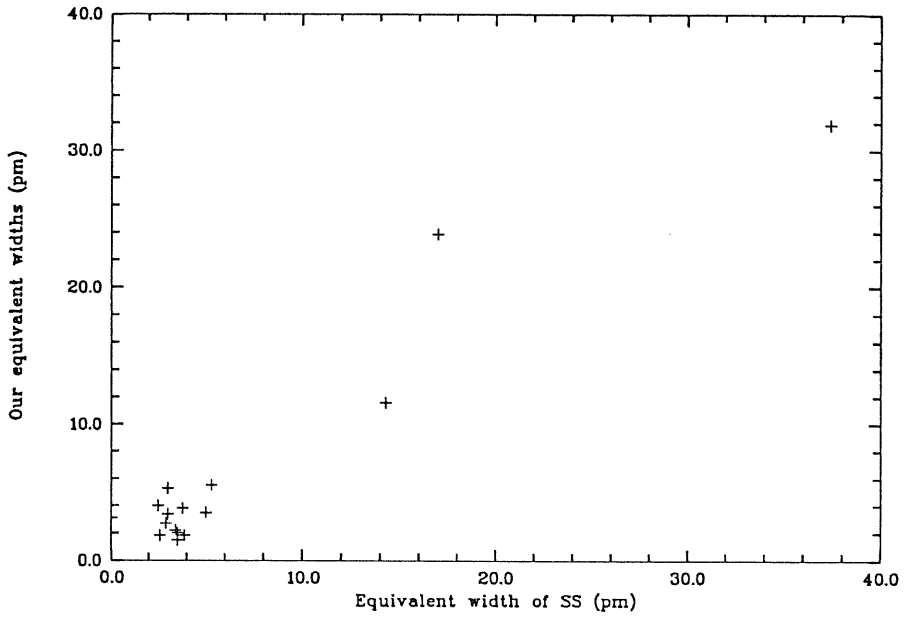

Fig.6.1 Comparison between our measured equivalent widths (on the vertical axis) and those of SS(on the horizontal axis).

average of the measurements. The rationale behind this choice being that, to some extent, the lower resolution is compensated by the higher S/N.

The measured equivalent widths are listed in table 6.4, an asterisk indicates that the line was observable on one spectrum only. We compared these equivalent widths with those of SS and BS, there are 22 lines common to the three papers. In figure 6.1 we plotted our equivalent widths against those of SS. In figure 6.2 we plotted our equivalent widths against those of BS, while figure 6.3 shows the equivalent widths of BS against those of SS.

Our equivalent widths compare quite well with those of SS. The worst discrepancies occur for the diffuse He lines, where the placement of the continuum is

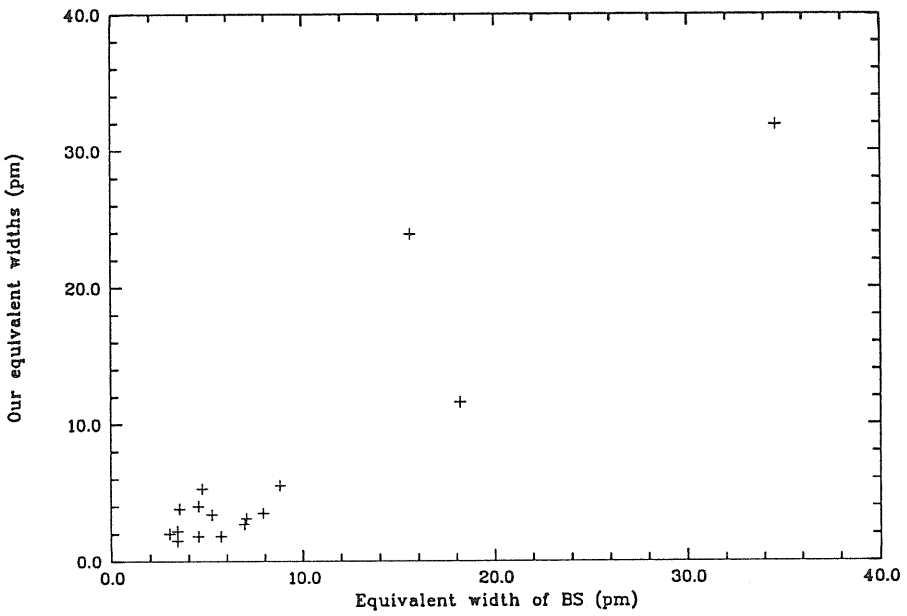

Fig.6.2 Comparison between our measured equivalent widths (on the vertical axis) and those of BS(on the horizontal axis).

crucial. Instead, if we look at figure 6.2 we see immediately that our equivalent widths are systematically smaller than those of BS, while the agreement on the strongest lines is quite good. The third plot shows clearly that the equivalent widths of BS are systematically *larger* than those of SS. This is somewhat surprising since one of the spectra used by BS is the very same used by SS, albeit re–digitized and re–calibrated. The regression analysis confirms the qualitative impression gained from the plots. We get the following fits:

$$EW \approx 0.16\text{pm} + 0.996 EW_{SS}$$

$$EW \approx -1.10\text{pm} + 0.901 EW_{BS}$$

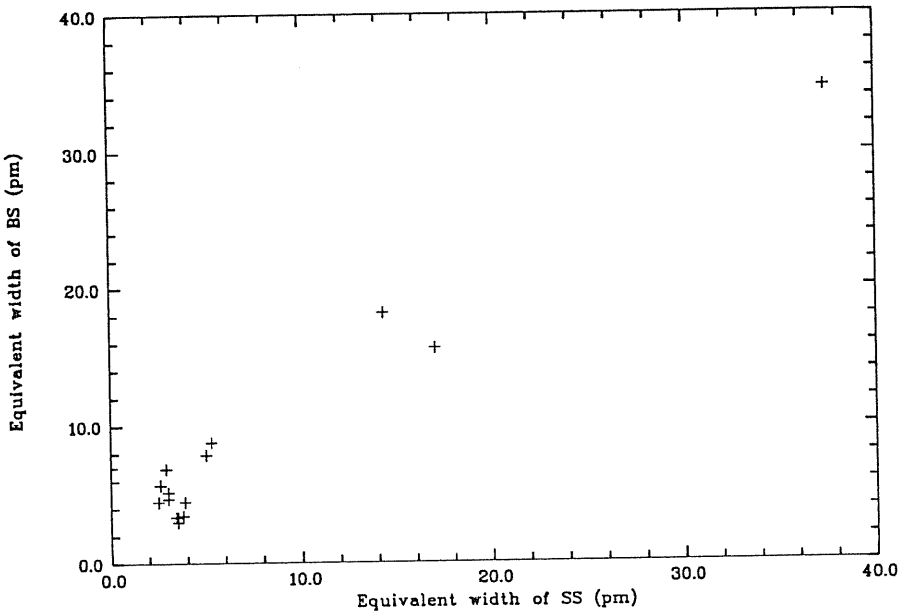

Fig.6.1 Comparison between the equivalent widths of BS (on the vertical axis) and those of SS(on the horizontal axis).

$$EW_{BS} \approx 1.69\text{pm} + 1.063 EW_{SS}$$

where EW without any subscript denotes the values listed in table 6.4.

Note that, while the regression coefficient of our equivalent widths with respect to those of SS is just as good as the one of the BS equivalent widths with respect to those of SS, the offset of our data is an order of magnitude smaller than that of the BS data. This is to say that our equivalent widths agree more closely with those of SS than those of BS do.

Since phosphorous is of special interest in F86 we also compared the equivalent widths of P lines alone. Again we find that the equivalent widths of BS are systematically larger than ours and Sargent& Searle's. There is no systematic

trend when comparing our equivalent widths with those of SS, in spite of the large scatter.

Our spectra cover H_α, H_γ, H_δ, H_ϵ, H_8, H_9 and H_10 regions. H_γ, H_δ and H_ϵ show a slight asymmetry, the blue wing being steeper than the red one. We also compared our profiles of H_γ and H_δ with those published by BS and SS. For H_γ the agreement is quite good, whereas for H_δ our profile agrees with that of SS but not with that of BS, in the latter the core is deeper and the wings are less extended. No asymmetry is apparent in the SS or BS profiles.

6.2.4 Ultraviolet high resolution spectra

We had at our disposal three IUE SWP and one LWR high resolution spectra. Images SWP20127 and LWR11155 where taken from the IUE archive, while SWP4616 and SWP15592 where observed by M. Hack and P.L. Selvelli, respectively, in the framework of a program aimed at the study of chemical peculiarities in early–type stars. Details on the images may be found in table 6.5. All four images were reprocessed at VILSPA with the IUESIPS2 software.

Ripple corrected images where read from magnetic tape with the IUEOAT software (Allocchio *et al.*, 1988). Each image was independently normalized with the interactive code NORMA (Bonifacio, 1989) in the same way as described in Castelli& Bonifacio (1990)

We superimposed the three SWP spectra available to us on each other and on synthetic spectra, to search for signs of spectral variability. From this analysis no variability can be firmly established; this conclusion is supported also by our visible spectra. We coadded the three SWP spectra, in order to increase the S/N ratio. For this purpose we wrote a MIDAS procedure. We computed cross–correlation functions for each order of the normalized spectra SWP20127 and SWP4616, with

SWP15592, which was used as a template. The maxima of these cross–correlation functions gave us the wavelength shift necessary to superimpose SWP20127 and SWP4616 on SWP15592. After shifting the spectra of the appropriate quantity they were coadded using exposure times as weighting factors. We did not perform any filtering in order to avoid loss of spectral resolution. When cosmic ray hits perturbed some spectral feature we coadded only the two spectra which were not affected. The only high resolution long–wavelength spectrum available, LWR11155, is slightly underexposed and has a rather high background. We estimated S/N $\approx$ 6 at the MgII lines around 280 nm ; since these are the strongest lines present in this range it is clear that this is really an upper limit to the S/N of this spectrum. No serious abundance analysis is feasible with data of this quality. After inspecting the whole spectrum we selected a few lines which are just strong enough that a qualitative analysis is possible. Therefore for the long wavelength range we limited the analysis to these lines.

6.3 Reddening

The effects of reddening may be important when observed colours and fluxes are compared with computed quantities, in order to determine the model–atmosphere parameters.

Table 6.2 lists the E(B-V) values quoted in the literature for F86, as well as those we deduced from the Johnson and the Strömgren photometry. Literature values range from 0.11 mag (Newell, 1973) to -0.04 mag (Hack, 1980). We investigated the reasons of the large value given by Newell (1973) and of the negative values given by Hack (1979, 1980). We came to the conclusion that the large value

Table 6.2

Reddening of F86

Found in the literature	
$E(B-V)$	Reference
0.06	Sargent & Searle (1967)
0.11	Newell (1973)
0.03	Baschek & Sargent (1976)
-0.03	Hack (1979)
-0.04	Hack (1980)
Computed using published UBV photometry	
$E(B-V)$	Reference for phot.
-0.02	Westerlund (1964)
0.05	Klemola (1962)
0.06	Neckel & Chini (1980)
0.06	Carney (1983)

Computed using published uvby photometry	
$E(B-V)$	Reference for phot.
0.01	Hauck & Mermillod (1990)
0.02	Stetson (1991)
Computed using ultraviolet colours	
$E(B-V)$	Reference for UV col.
-0.36	Thompson *et al.*(1978)
0.05	comp. from IUE spectra
Computed from polarization	
$E(B-V)$	Reference for polarim.
$\geq$ 0.01	Korhonen & Reiz (1986)

of Newell (1973) is due to the use of a non-standard procedure. In fact, he computed the narrow band colours in his own photometric system from the spectrum scan of Sargent& Searle (1968). Then this narrow band colour excess was empirically related to E(B-V). The other discrepant values from Hack (1978,1979),

were obtained by using the formula given by Thompson *et al.*(1978) to compute E(B-V) from UV colours. Hack computed the colours from low resolution IUE spectra, taken with the small aperture, therefore photometrically inaccurate. To check Hack's procedure we used the Thompson *et al.*formula with:

1. the broad band colours listed in the TD1 catalogue
2. the broad band colours computed from the absolutely calibrated IUE spectra SWP3723L and LWR3303L (for the colours at 156.5 nm, 196.5 nm and 236.5 we used rectangular bandpasses of width 33 nm, for the 274.0 nm colour we used a gaussian bandpass which was a least squares fit to the profile given graphically by Thompson *et al.*).

Table 6.3

Log of observations at Observatoire de Haute–Provence

IMAGE NUMBER	GRATING	ORDER	FILTER	λ_c (nm)	R (nominal)	t_{exp} (seconds)	DATE
J84	5	I	OG590	663.0	31000	5400	2/1/1990
J104	5	I	OG590	643.3	31000	4500	2/1/1990
J196	5	I	OG590	650.5	31000	11000	3/1/1990
J275	2	Blaze 5000	NONE	430.0	20000	3000	4/1/1990
M232*	2	Blaze 5000	NONE	451.0	20000	4868	9/5/1990
C65	3	Blaze 5000	NONE	430.0	6500	11697	21/2/1992
C627	3	Blaze 5000	NONE	430.0	6500	10800	28/2/1992
C847	3	Blaze 5000	NONE	430.0	6500	8987	2/3/1992
C691	3	Blaze 5000	NONE	400.0	6500	8987	29/2/1992
C692	3	Blaze 5000	NONE	400.0	6500	8988	29/2/1992
C120	5	II	OG515	669.2	60000	17631	22/2/1992
C249	5	II	OG515	587.5	60000	10033	23/2/1992
C250	5	II	OG515	587.5	60000	7104	23/2/1992

From the data in the TD1 catalogue we obtained E(B-V)=-0.36, while from the data computed from the IUE spectra we obtained E(B-V)=+0.05. The latter value is consistent with those we determined from both Johnson and Strömgren photometry, while the former is not. This is probably due to systematic errors in the fluxes at 274.0 nm listed in the catalogue; such errors have already been pointed out by Faraggiana and Malagnini (1984) by comparing TD1(S2/68) with OAO-2 colours. According to them $F_{274}(OAO-2) = F_{274}(S2/68) \times 10^{-\Delta_1}$ and Δ_1 takes values in the interval $[-0.17, 0.0]$. If we apply this correction to the value of F_{274} listed in the catalogue for F86, with $\Delta_1 = 0.17$ we find $F_{274} \approx 1.27 \times 10^{-12}$ergcm^{-2}s^{-1}Å^{-1} in close agreement with the value determined from the IUE spectra $F_{274}(IUE) \approx 1.30 \times 10^{-12}$ergcm^{-2}s^{-1}Å^{-1}.

We computed colour excesses by using the relations (4.6) to (4.9) of chapter 4 and the published photometric data given in table 6.1. The negative value obtained from the photometry of Westerlund (1964) is suspect. While V and U-B values given by Westerlund are in agreement with those of other observers, his B-V value is discrepant. This may be due to the fact that he converts his instrumental magnitudes to P,V magnitudes and then converts the P-V to B-V with the linear relation given by Kron and Mayall (1966), which is claimed to be accurate only to ± 0.03 mag by them. Another possible source of systematic error is that the standard stars used by Westerlund to convert from instrumental to P,V magnitudes are rather cool (the hottest is A3p), therefore the calibration has to be extrapolated for hotter stars.

If we omit the discrepant E(B-V) value of Newell, that obtained from Westerlund's photometry, as well as those obtained by Hack, the set of E(B-V) data is rather consistent and suggests that F86 is slightly reddened with an E(B-V) value between 0.01 and 0.06. We give more weight to the value of 0.06 because it results

from the photometry of Neckel and Chini (1980) who established F86 as a primary standard, hence their colours should have a higher intrinsic accuracy. The computed flux reddened with this value of E(B-V) also gives the best fit to the slope of the Paschen continuum (Bonifacio&Castelli, 1992). Further evidence for the non zero reddening of F86 comes from the polarization measurement of Korhonen and Reiz (1986). If we use the relation given in Allen (1976) $2.2P \leq 0.19E(\mathrm{B}-\mathrm{V})$, we find $E(\mathrm{B}-\mathrm{V}) \geq 0.01$. These values of polarization and reddening are perfectly consistent with the star's galactic location.

6.4 The atmospheric parameters of F86

6.4.1 Effective temperature and gravity

In order to derive abundances we have to fix an atmospheric model for F86 , and therefore the values of effective temperature, surface gravity and microturbulent velocity. Stellar parameters can be obtained by comparing observed and computed quantities, such as colours, fluxes and line profiles. Table 6.6 reports the different values of log g and T_{eff} found in the literature for F86, together with an indication of the methods employed to determine them. There is a considerable scatter both in the values of T_{eff} and log g derived with different methods.Surface gravity ranges from log g = 3.8 to log g =4.5. Effective temperature ranges from 14250 K (Huenemoerder *et al.*, 1984) to 19600 (Hartoog, 1979).

To get a first estimate of the stellar parameters we compared the c and β indices from the Hauck& Mermilliod (1990) catalogue, dereddened with the U-VBYBETA code of Moon (1985), with those of the grid of Moon& Dworetsky

(1985). We used the TEFFLOGG program of Moon (1985) as modified by Castelli (1991). We obtained T_{eff} = 16970 K ± 200 K and log g =4.1 ± 0.03. The errors are the r.m.s of the fit.

To test these values we adopted different criteria: for the temperature we considered both the Q–T_{eff} calibration and the energy flux distribution; for the gravity we looked at the profiles of the Balmer lines.

The reddening–free parameter of Johnson photometry, Q, may be related to effective temperature. Using the UBV photometry of Neckel and Chini (1980) we find Q = -0.535 which yields T_{eff} =16900 K on applying the calibration of Schild *et al.* (1971).

We compared the UV and visible observed fluxes with fluxes computed with version 9 of the ATLAS code(Kurucz, 1979). The visible and UV fluxes have been corrected for the effect of reddening assuming E(B-V)=0.06, R_V = 3.1 and using the average extinction curve of Mathis (1990). Computed fluxes were derived from models computed with zero microturbulent velocity and solar abundances for all the elements except for helium, for which an abundance of $N(He)/N_{tot}$ = 0.006 (BS) was adopted, i.e. an underabundance of 1.17 dex with respect to the solar value. Consistently we used ODF's computed with the same abundances and microturbulent velocity. The calculation to transform from the abundance scale used by Baschek and Sargent to the abundance scale used by ATLAS is shown in Appendix A. We compared the flux computed with low helium abundance and zero microturbulent velocity with the fluxes computed from model atmospheres with the same T_{eff} and g but solar He abundance and a microturbulent velocity of 2 km/s. The differences appeared to be negligible, of the order of a few thousandths of a magnitude.

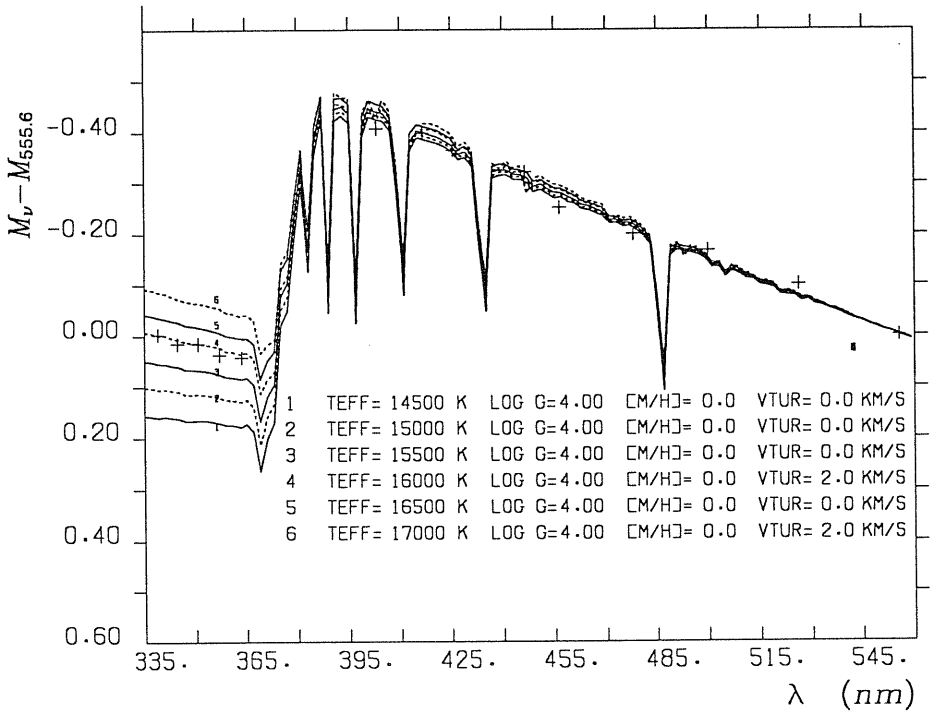

Fig. 6.4 The visual flux of F86 from the Breger catalogue (magnitudes are normalized at 555.6 nm) compared with computed fluxes. The observed flux has been corrected for the effect of reddening assuming $E(B-V) = 0.06$ mag.

Figure 6.4 shows that the visible spectrum scan is rather well reproduced by the model with log g = 4.0 and T_{eff} = 16000 K (see also Bonifacio&Castelli; 1992) after having dereddened the flux for E(B-V)=0.06.

Figures 6.5,6.6 and 6.7 show the comparison of the low resolution IUE spectra described in section 6.2.2 with the fluxes computed from models with log g = 4.0 and the different values of T_{eff} 14500,15000,15500,16000,16500 and 17000 K). A temperature between 16000 K and 17000 K gives the best agreement for both

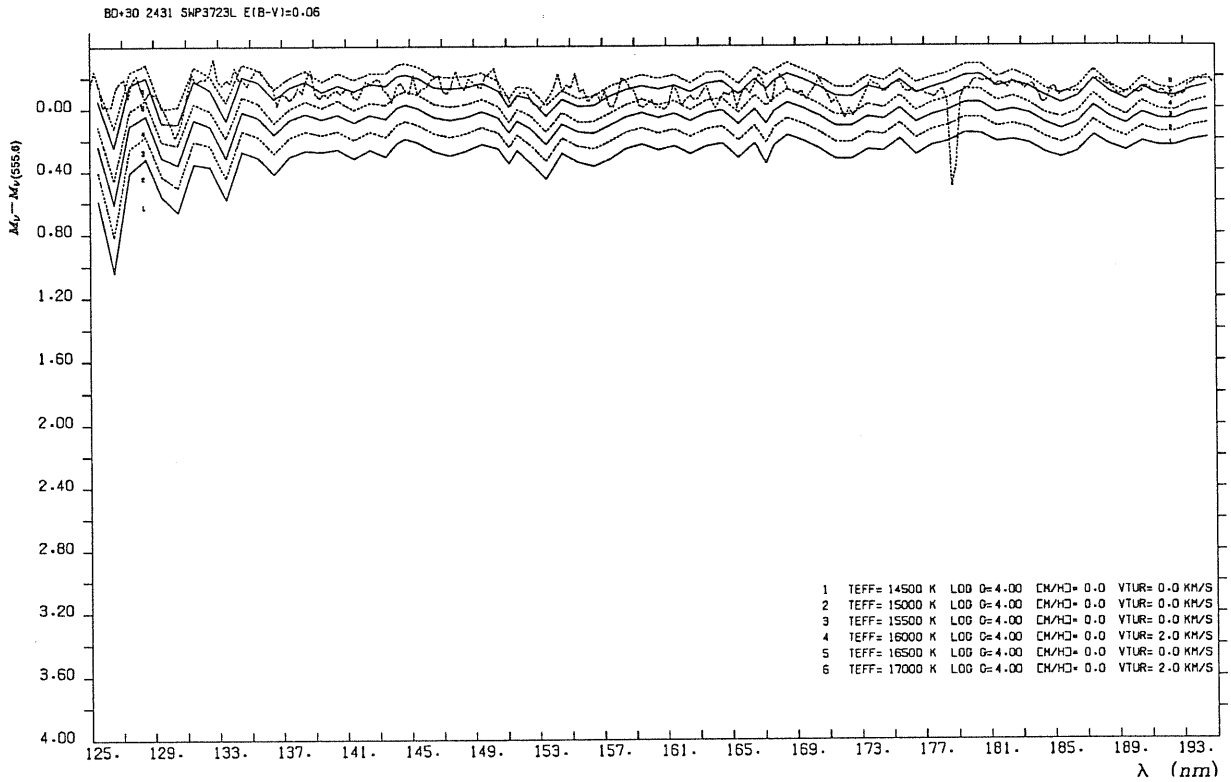

Fig.6.5 The IUE low resolution spectrum SWP3723L compared with theoretical fluxes. The observed flux has been dereddened assuming $E(B-V) = 0.06$.

the 120 nm – 200 nm range. The fit is not so good in the 200 nm – 330 nm range which would require a higher temperature to be satisfactorily fitted. There is therefore an inconsistency between the effective temperature derived from the visual and the UV regions. This temperature difference could be due to the error on the calibration of the IUE fluxes, which is estimated to be of the order of 10 % (Bohlin *et al.*1980). Such an error induces an error in the estimate of the temperature of roughly 1000 K, for B–type stars.

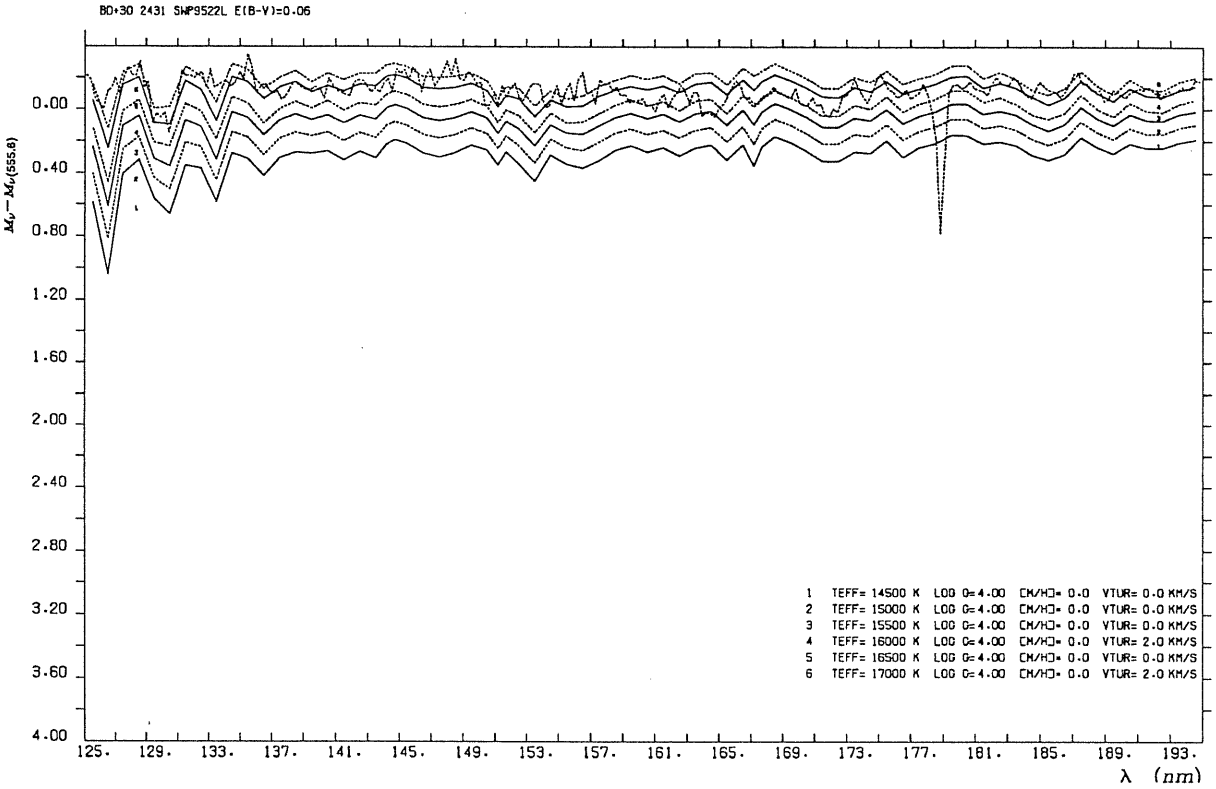

Fig.6.6 The IUE low resolution spectrum SWP9522L compared with theoretical fluxes. The observed flux has been dereddened assuming $E(B-V) = 0.06$.

We wish to point out the result of Singh and Castelli (1991), who showed that the SiII lines of UV mult. 13.04 are a good temperature indicator for B type stars and used them to estimate an effective temperature of 15500 K for F86.

From our analysis and the result of Singh and Castelli (1991) we may conclude that the temperature of F86 is between 15500 K and 17000 K. This result is to be compared with that of BS $T_{eff} = 17500K \pm 1500K$.

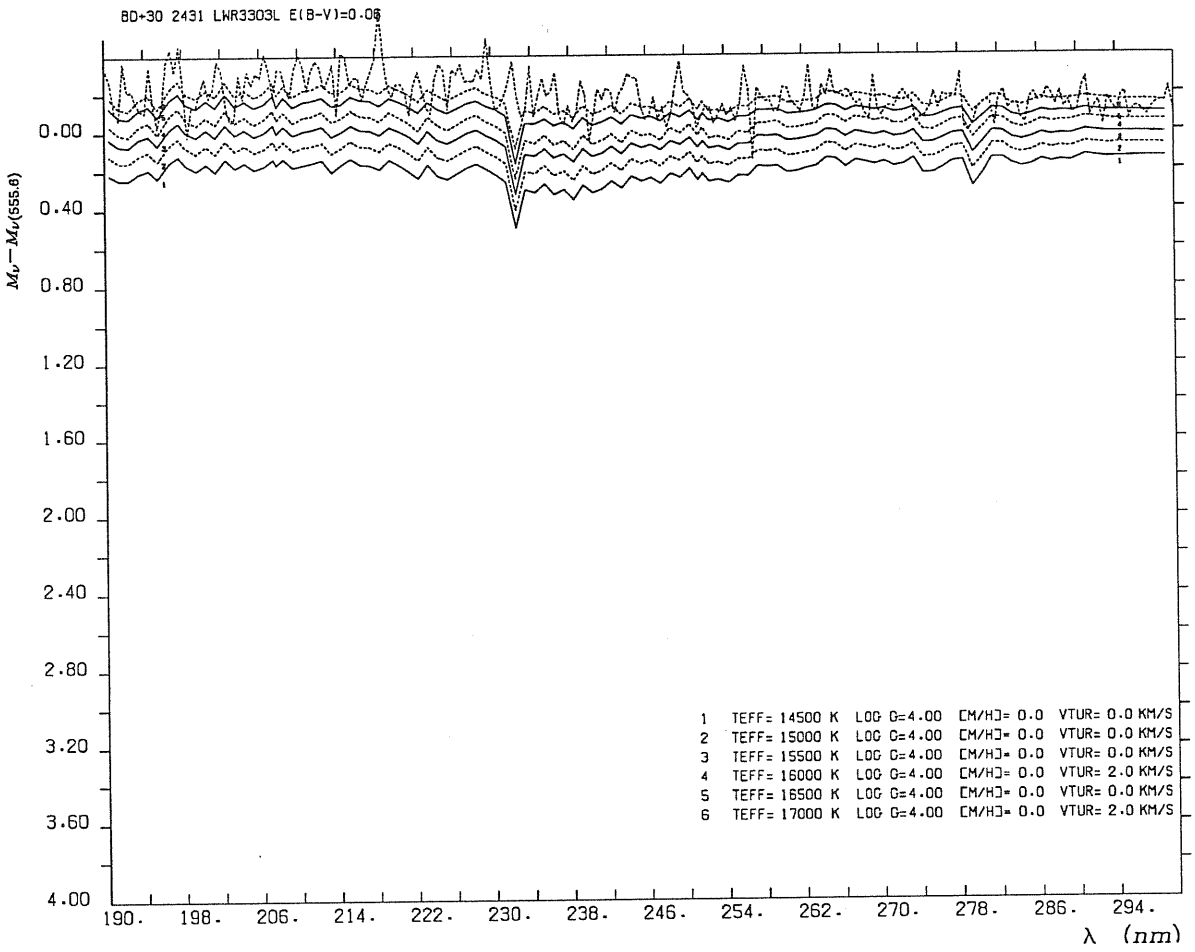

Fig.6.7 The IUE low resolution spectrum LWR3303L compared with theoretical fluxes. The observed flux has been dereddened assuming $E(B-V) = 0.06$.

We believe that low weight should be given to the UV flux as a temperature indicator for F86. Both because of the calibration uncertainties of IUE and because of the large number of unidentified lines present in the high resolution UV

Fig.6.8

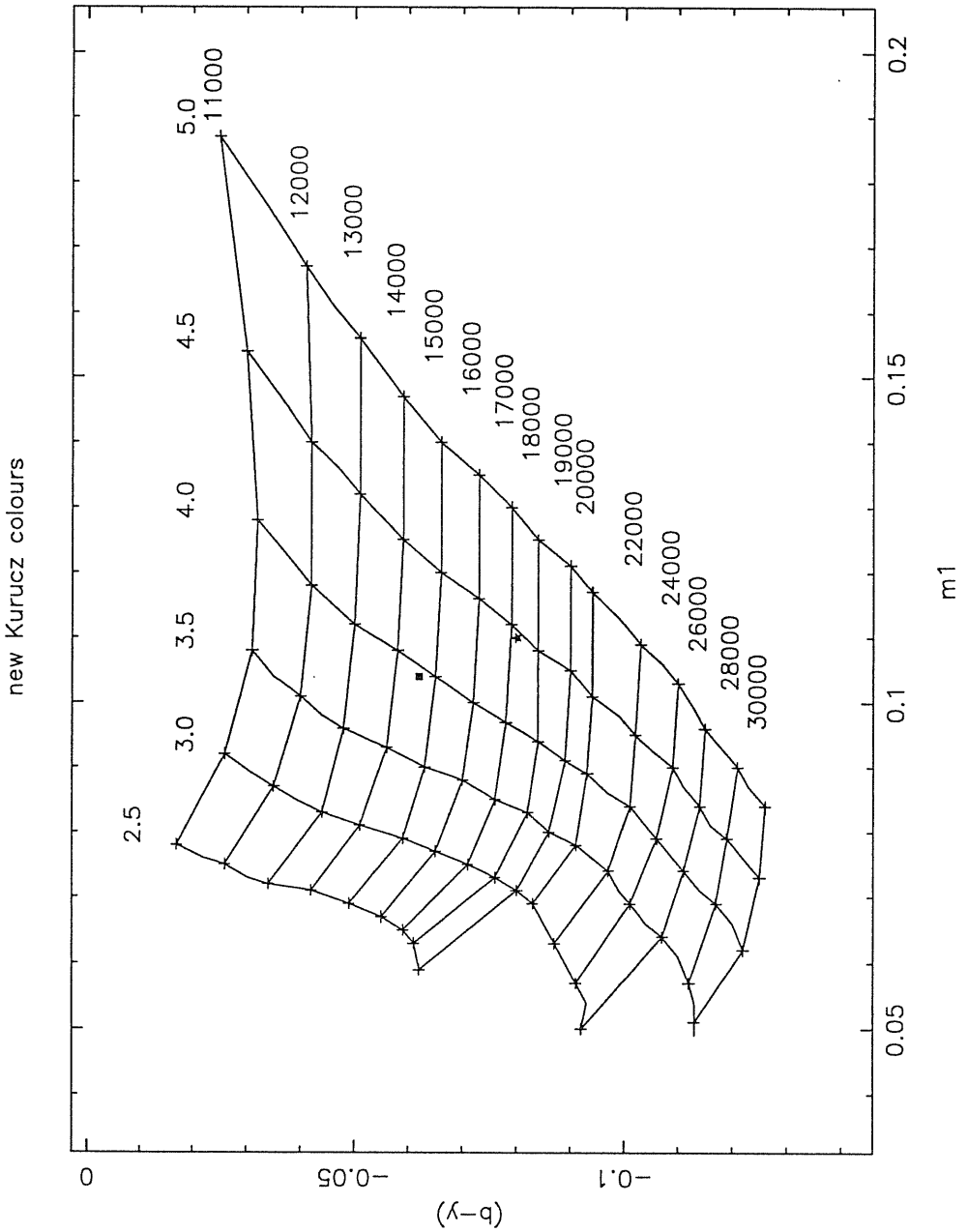
new Kurucz colours
(b−y)
m1
0
−0.05
−0.1
0.2
0.15
0.1
0.05
5.0
4.5
4.0
3.5
3.0
2.5
11000
12000
13000
14000
15000
16000
17000
18000
19000
20000
22000
24000
26000
28000
30000

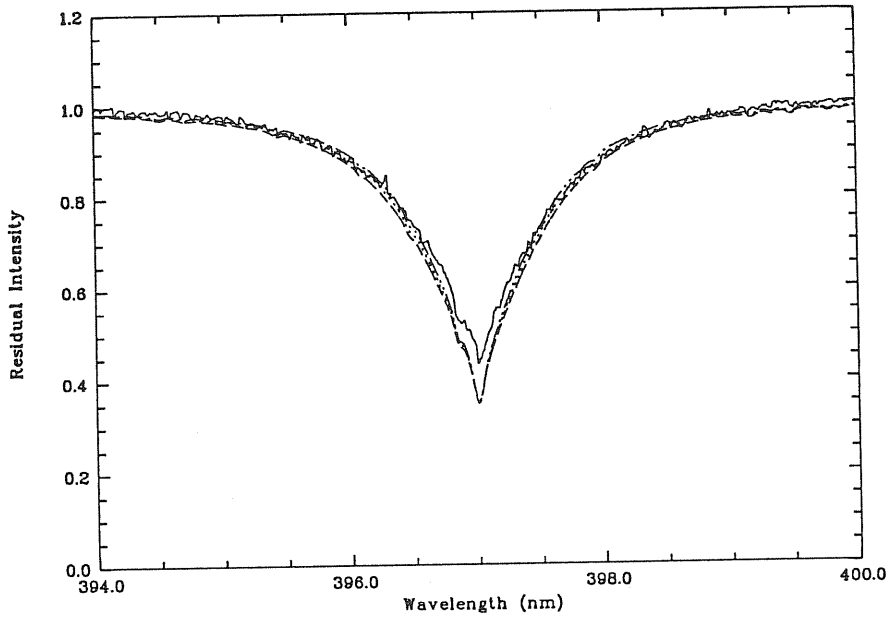

Fig 6.9 The observed profile of H_ϵ in F86 compared with theoretical profiles computed with T_{eff} = 16000 K and log g = 4.0 (dash–dotted line), 4.1 (dotted line) and 4.2 (dashed line).

spectrum. These are a source of extra blanketing which is not included in our models. Hence our models will overestimate T_{eff} . Caution should also be used when interpreting the colour indices of F86. It is well known that Ap stars have anomalous colours, and the hotter ones (especially the Si and He–weak ones) are too blue for their T_{eff} (Deutsch, 1947; Leckrone, 1973; Schneider, 1992). In this respect it is useful to consider F86 as peculiar, not so much for the weak P lines in the visible spectrum as for the forest of unidentified lines in the UV. The fact that the far UV and visible fluxes may not be fitted by the same computed flux must be regarded as a peculiarity of F86. Huenemoerder *et al.* (1984) noted that F86 has

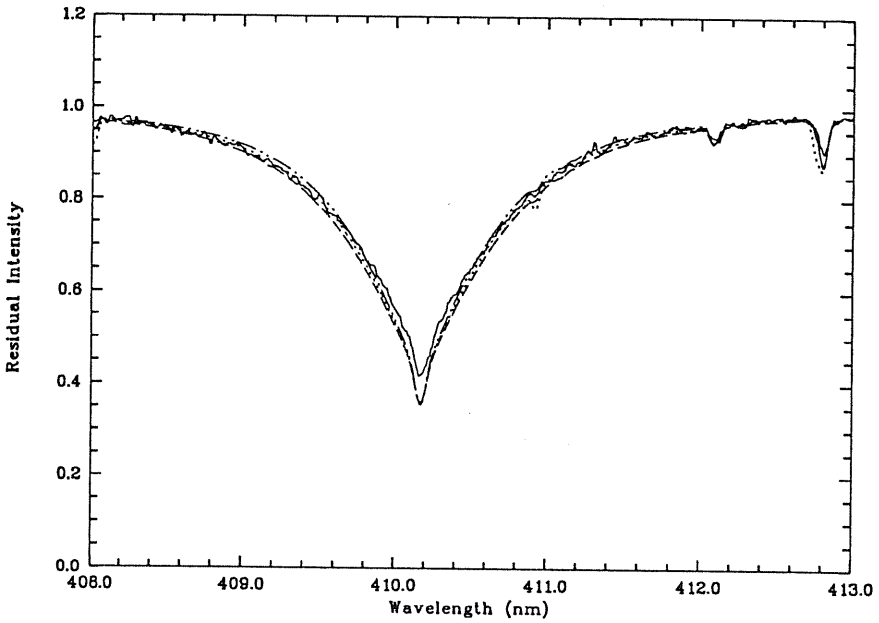

Fig 6.10 The observed profile of H_δ in F86 compared with theoretical profiles computed with T_{eff} = 16000 K and log g = 4.0 (dash–dotted line), 4.1 (dotted line) and 4.2 (dashed line).

a smaller Balmer jump than Pop I stars of the same temperature. However their temperatures, deduced from different colour-colour plots, show differences of up to 2000 K and have an average value of $T_{eff} \approx=$ 15000 K, thus lower than our value. We investigated their temperature determinations both to understand the scatter in T_{eff} and the disagreement from the temperatures determined from the Strömgren photometry. In figure 6.8 we show an $(m1, b-y)_0$ plot of the kind employed by Huenemoerder *et al.* (1984). The star represents (m1,b-y) value given in the Hauck and Mermilliod (1980) catalogue; Huenemoerder *et al.* assume $E(B-V) = 0.0$. The filled square on the same plot represents the (m1,b-y)

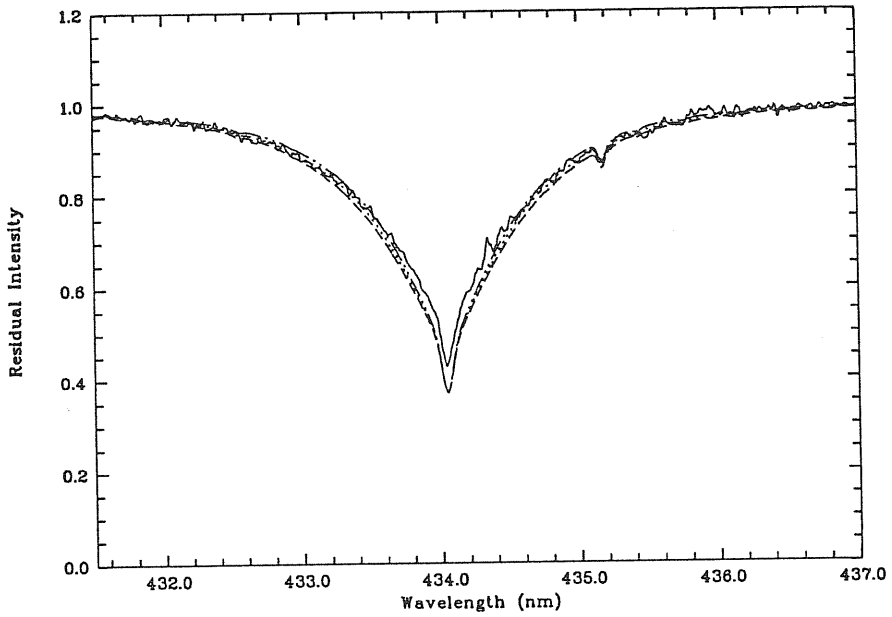

Fig 6.11 The observed profile of H_γ in F86 compared with theoretical profiles computed with T_{eff} = 16000 K and log g = 4.0 (dash–dotted line), 4.1 (dotted line) and 4.2 (dashed line).

value obtained after correcting for reddening assuming $E(B-V) = 0.03$ as used by Baschek and Sargent (1976). It is clear how a small colour excess will have a large effect on the temperature determination, from this particular colour-colour plot.

Another argument which supports the peculiarity of the continuum energy distribution of F86 is the fact that Stetson (1991), using purely photometric criteria, classifies it as a normal B star and it lies, in his ([c1],β) diagram, just *below* the ZAMS, well separated from the HB stars, while Sargent and Searle (1967) and

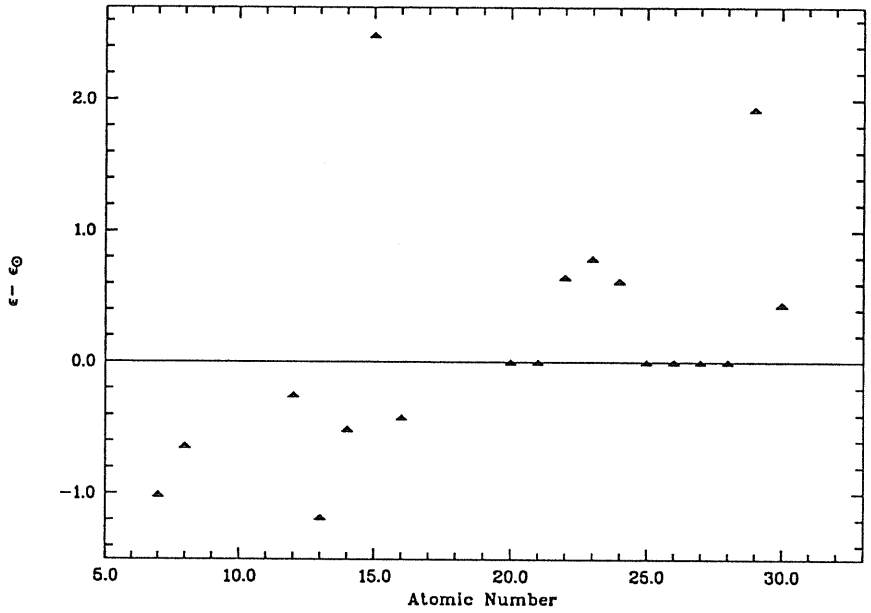

Fig.6.12 The relative abundances (with respect to solar) of F86 versus atomic number

Hartoog (1979) showed that the kinematic reasons to believe F86 to be a Pop II HB star are quite strong.

For the purpose of the abundance analysis we decided to adopt T_{eff} = 16000 K. Thus giving low weight to the temperatures determined from the UV flux and from the colour indices, as discussed above. However in view of the uncertainties discussed above we decided to attach a formal error of ±1000 K to this number.

After having fixed the temperature we looked at the Balmer line profiles to fix the gravity. We used the SYNTHE code to compute profiles of H $_\alpha$, H $_\gamma$, H $_\delta$ and H $_\epsilon$ from models with T_{eff} = 16000 K, N_{he}/N_{tot} = 0.006 , zero microturbulent velocity and gravities of log g = 4.0 , 4.1 and 4.2 . The results are shown in figures

6.9,6.10 and 6.11. Visual inspection shows that log g = 4.1 gives the best match in the wings. The cores are subject to non-LTE effects and are clearly independent of gravity. This value of log g is in close agreement with the result obtained from the β index and the Moon& Dworetsky (1985) grid.

We can use the adopted temperature and gravity do derive a spectral type using the calibrations of Straizys and Kurilene (1981), assuming that F86 may be treated for this purpose as if it were a MS star. We find a spectral type of B5 V.

6.4.2 Microturbulence

BS stated that "the few lines observed in F86 do not permit a determination of the microturbulence", they therefore determined abundances for two values of microturbulent velocity: 0 kms^{-1} and 5 kms^{-1}. Singh and Castelli (1991), in their analysis of the profiles of the SiII lines of UV mult. 13.04, found a good agreement assuming a zero microturbulent velocity. We investigated the effect of microturbulence on SiII 412.8054, SiII 413.0894. These two Si II lines are rather well reproduced by our synthetic spectrum computed assuming the Si abundance deduced from the UV (see section 6.5) and a $0kms^{-1}$ microturbulent velocity. On the contrary the lines computed with a microturbulent velocity of $2kms^{-1}$ and $5kms^{-1}$ are much stronger than the observed lines. In the following analysis we therefore adopt $\xi = 0kms^{-1}$. This is consistent with the results of Adelman (1984) who, analysing 6 late B stars found values of ξ always less than 2.2 kms^{-1}; if we omit 134 Tau from his sample all the other values are less than 1 kms^{-1}.

6.5 Abundance Analysis

The UV spectrum of F86 appears to be overwhelmingly rich of lines. This results clearly from the comparison with ι Her, which has a similar spectral type and projected rotational velocity. There are many features in F86 which have no counter–part in ι Her and viceversa. We computed synthetic spectra for the whole IUE range, as well as for the optical ranges available to us. For each species we selected the lines listed in table 6.7 to fix the abundance, proceeding as in Castelli&Bonifacio (1990). The adopted abundances are given in table 6.8 where $\epsilon_X = \log\frac{(N(X)}{N_{tot}}$. They give the overall best agreement with the observed spectra; however remarkable discrepancies still exist.

Some lines coming from the ground level often appear to be either shifted or show a multiple structure with a slightly red–shifted component. This could be due to the presence of interstellar components. We attempted to identify interstellar lines with the aid of the atlas of SN 1987a (Blades *et al.*,1988). Some interstellar lines are probably present as sharp components, slightly redshifted with respect to the photospheric lines; however they are all irremediably blended with the latter. Most of the lines which are very strong in the atlas of SN 1987a appear to be rather weak in the spectrum of F86. This seems to point to a low column density of gas in the direction of F86. This is at odds with our adopted value of E(B-V). Using the relation of Bohlin *et al.*(1978) one finds $N(H) = 3.5 \times 10^{20}$, which is comparable with the column density in the direction of SN 1987, one would therefore expect lines of comparable strength in both spectra.

Bonifacio *et al.*(1991) suggested the presence of circumstellar material responsible for some of the peculiarities observed, the most evident being the CI and SiII resonance lines. We still believe this possibility to be rather appealing, although

we could not find any conclusive evidence of the existence of such material. Several of the unidentified features could be formed in such circumstellar material and doppler shifted with respect to the corresponding photospheric line, if any.

Another, possibly concomitant, explanation for many observed features could be that F86 shows a photospheric overabundance of several heavy species which were not included in the calculations, owing to the lack of gf values of the corresponding lines. Such heavy species, however do not show up in the optical spectrum, which is characterized by weak lines, most of which are PII.

6.5.1 Remarks on individual ions

Helium

We have data for six diffuse and one sharp He I lines. We measured the equivalent widths of all of them although the gaussian–fitting routine we used is inadequate for lines with complex profiles such as these. We did not use this data to determine abundances, since the theoretical equivalent width is strongly affected by the Stark broadening theory used and the version of the spectrum synthesis code which we are using does not treat Stark broadening realistically for He I lines, as pointed out in the previous chapter. A marked He deficiency is never the less evident from the spectrum and the He abundance of -2.21 given by BS does not contradict our observations. We therefore adopted this abundance to compute the model–atmosphere and the synthetic spectra. Work is in progress to modify the code in order to be able to compute realistic He I profiles. We plan to address the problem of He abundance in F86 as soon as the code is in good shape for it.

The presence of ^{3}He in the atmosphere of F86 we still consider an open issue. The data presented by Hartoog (1979) is of poor quality, as is the material so far

available to us. We believe no firm detection of ^{3}He from the shift of the He I $2^1P - 3^1D$ transition (λ 667.8 nm) can be made unless one has :

1) fixed the Ne abundance; the Ne I line which is blended with He I may become important if the He line is weak, as in F86, and/or if Ne is enhanced. So far we have no information on Ne abundance;
2) a spectrum synthesis code which treats realistically Stark broadening and pressure shifts of the lines of both isotopes. Work is in progress in this direction;
3) treated realistically departures from LTE which are of major importance for this line (Auer& Mihalas, 1972).

It is of some interest to consider the singlet to triplet ratio in F86. Sargent& Searle (1968), in studying sdB stars showed that in these stars the singlet to triplet ratio is lower than in Pop I MS stars. Baschek & Norris (1969) explained this as a combined effect of the high gravity of the sdB stars ($\log g \approx 5.0$) and the low He abundance. In F86 the gravity is the same as in a MS star, however the He abundance is particularly low; it is therefore legitimate to ask whether there is a singlet/triplet anomaly.

Consider first the ratio EW(438.8)/EW(447.1), the behaviour of this ratio with spectral type for MS stars was first investigated by Struve (1928). In F86 the ratio is ≈ 0.45 if we use the equivalent widths of BS or SS, it is instead ≈ 0.62 if we use our own equivalent widths. The former value is what is expected for a MS star of $T_{eff} \approx 12500$ K (extrapolating from the NLTE equivalent widths of Auer& Mihalas,1972), the latter is expected for stars of T_{eff} around 16000 K. In any case it is important to stress that a singlet/triplet anomaly of the type described by Sargent& Searle (1968) and Baschek& Norris (1970) for B subdwarfs

is not present. In sdB stars this ratio has the low value of 0.25 (Baschek&Norris, 1970).

When we compare λ 438.7 with λ 447.1 we are comparing transitions between levels with different lower and upper principal quantum numbers. In fact λ 438.7 corresponds to 2^1P-5^1D transition, while λ 447.1 corresponds to 2^3S-4^3D . This makes the analysis of this ratio a little intricate, as discussed by Baschek& Norris (1970). It is therefore preferable to compare λ438.7 with λ 402.6 ($2^3P - 5^3D$). The behaviour of this ratio with spectral type for MS stars is shown in Fig. 7 of Leckrone (1971). The theoretical values of Leckrone (1971) were computed assuming LTE. The subsequent NLTE computations of Auer& Mihalas (1972) showed that NLTE effects on the blue–violet lines of He I affect the singlet to triplet ratio by no more than 10% . Therefore the computations of Leckrone may still be used as a useful reference. If we take our equivalent widths we find EW(438.7)/EW(402.6)$\approx$ 0.5, which is expected for a spectral type around B4 ($T_{eff} \approx$ 17000K). If we use the equivalent widths of SS we find this ratio to be $\approx$ 0.66, which is much too high for any B (or O, for that matter) star. On the contrary the BS equivalent widths yield a ratio of about 0.37, which is much *lower* than that predicted for any MS star. It therefore appears that by using the BS equivalent widths for λ 438.7 nm and λ 402.6 nm,1 a singlet/triplet anomaly of the type observed in B subdwarfs exists.

To cast new light on this rather puzzling situation, consider next the ratio EW(667.8)/EW(587.5) . This ratio is strongly affected by NLTE effects (Auer& Mihalas ; 1972). Unfortunately no data exists for these lines from either SS orBS. If we use our equivalent widths we find a ratio of 0.56 which is what is expected for a MS star of effective temperature around 15000 K (Fig. 3 of Auer& Mihalas; 1972). Does F86 show a singlet/triplet anomaly, of the type displayed by B subdwarf

stars ? Our data do not suggest it; the EW(438.7)/EW(402.6) computed from the BS data does. We give a qualitative argument to support the view that a singlet/triplet anomaly should **not** be present. While it is true, as pointed out by Baschek& Norris (1970) that a low He abundance does enforce a singlet/triplet anomaly, one also has to bear in mind two results of Auer& Mihalas (1972):

1) NLTE effects strengthen singlets with respect to triplets in the blue–violet range;[2]
2) Departures from LTE are largest when the He lines are weaker.

Therefore one can expect that in He–weak star deviations from LTE are important even for the blue violet lines, which are otherwise very little affected.

One may therefore envisage these two effects operating in different directions: low He abundance tends to produce a low singlet/triplet ratio, NLTE effects tend to produce a high singlet/triplet ratio. The net result may well be that the singlet/triplet ratio in He–weak star such as F86 is the same as that in a MS star of the same T_{eff} . We plan in the future to make a detailed investigation of the behaviour of the singlet/triplet ratio with T_{eff} ,log g, He abundance and microturbulence, taking also NLTE effects into account.

Boron

The BII resonance line at 136.2416 nm suggests a marked boron deficiency of about 1.7 dex. This line is, in fact, a minor contributor to a blend of several lines, so that our derived abundance should be regarded as an upper limit. No other boron lines are observable in our spectra.

---

[2] It is true that the NLTE effects on the singlet/triplet *ratio* in this range are found to be of the order of 10%, however the investigation of Auer& Mihalas did not explore what happens at very low He abundances.

Carbon

Carbon is certainly strongly deficient. This may be inferred, qualitatively from the fact that no C lines, and in particular the CII doublet at 426.7 nm, are detectable both in our 8 Å/mm and in our 16.5 Å/mm spectra. Baschek and Sargent give an upper limit of ϵ_C=-5.21 based on the non-detectability of the above–mentioned CII doublet. This qualitative impression is confirmed when we look at the C lines in the UV, especially if we compare the spectrum of F86 with that of ι Her, which is only slightly C–deficient with respect to the sun (Castelli& Bonifacio, 1990). The lines of CI,CII and CIII listed in table 6.7 are consistent with ϵ_C=-5.00, in close agreement with the upper limit of Baschek& Sargent. However several lines which are well reproduced in the computed spectrum of ι Her are very poorly reproduced by our synthetic spectrum of F86. This is the case of the CI lines of multiplet 7 and the CII lines of multiplets 10 and 11 .

As noted by Bonifacio *et al.*(1991) many of the CI show a complex structure and some seem to be slightly shifted in wavelength, suggesting an interstellar origin.

Nitrogen

We adopt a Nitrogen abundance which is 1.5 dex lower than solar by looking at the NI lines of multiplets 4 and 3, the lines of multiplets 10 and 13 are all very weak and some are heavily blended (here and elsewhere in this paper we refer to a line as being "heavily blended" when the synthetic spectrum predicts that it is a minor contributor to a spectral feature). However the lines of multiplet 13 are consistent with our adopted abundance, while those of multiplet 10 indicate a higher abundance. Also the strongest line of multiplet 12 (131.9676 nm) points toward a higher N abundance ($\epsilon_N \approx -5.00$). The lines of multiplet 5 indicate an

abundance of -5.00, however the whole feature is poorly reproduced by our synthetic spectrum, it appears to be slightly red–shifted and has a complex structure which resembles very little the corresponding feature in ι Her. This pattern is exactly the same as that found by Castelli&Bonifacio in ι Her, thus suggesting that it is due to shortcomings in the models and atomic data rather than to stellar peculiarities.

We fail to reproduce the NII line at 130.0035, its central depth and width are roughly equal to that in ι Her, however since this line lies in the wing of SiI-I129.8892 the silicon deficiency of F86 places the continuum higher up in F86 than in ι Her; hence this line indicates that the N abundance is roughly the same in ι Her and F86.

BS give an upper limit of ϵ_N=-4.21 based on the non–detection of the NII line 399.5. This line is undetectable im our 16.5 Å/mm spectra; which, however does not place any constraint since our synthetic spectra predict that the line ought to be undetectable at this dispersion even with a solar N abundance. The line is rather weak and lies in the wing of H_ϵ, so that a slight error in the placement of the continuum would wipe it out.

Magnesium

Our adopted Mg abundance is based primarily on the MgII line at 173.4852, the resonance line of MgII at 123.9925 is also consistent with this abundance, but has a blending feature on the red wing which is not reproduced by our computation, we believe this to be an interstellar or circumstellar [3] component. The line at

[3] by circumstellar we mean, rather loosely, material which is present in the vicinity of the star. If F86 is an HB star we may expect material, which was ejected during the previous evolutionary phases, to be still in the star's vicinity.

175.3474 seems to point towards a more marked deficiency of Mg. The lines at 173.7613 and 173.7626 are affected by a reseaux mark. In the long–wavelength range of IUE the MgII resonance lines at 279.5528 and 280.2705 appear to be much stronger than our computed lines; however they are almost certainly contaminated by an interstellar component. On the other hand the strong line at 279.7998, which does not originate from the ground level, agrees with our computations if we assume a solar Mg abundance.

The MgII doublet at 448.1, both in our 8 Å/mm spectra and in our 16.6 Å/mm spectra is slightly weaker than the computations. The fact that our equivalent width is consistent with that measured by Glaspey *et al.*(1989) and Sargent& Searle (1967) (but not BS) suggests that the same sort of discrepancy would exist between our computation and their data. From this doublet BS deduce (assuming a $0 kms^{-1}$ microturbulent velocity) a slight Mg deficiency, which is totally consistent with our findings.

Aluminium

The Al lines show none of the anomalies displayed by C and N, with the exception of the resonance line of AlII 167.0787 where there is a redshifted strong sharp component, most probably interstellar. There could be also a very weak interstellar component of the AlIII resonance line at 185.4716, while no such component is detectable in the other line of multiplet 1, 186.2790. The line of AlII, multiplet 10 presents a sharp blending unidentified feature which is present also in ι Her . Since it is based on many lines the Al abundance ought to be quite accurate. BS deduced an upper limit of -5.21 from the non–detection of the AlIII lines 452.89 and 452.92, this upper limit is consistent with our present determination of -6.75. The above–mentioned lines are not detectable in our spectra and they are not predicted by our computed spectra.

Silicon

From the UV spectrum we deduce underabundance of 0.51 dex. This results clearly from the comparison with ι Her: The Si lines in F86 are systematically weaker than the corresponding lines in ι Her. Our result is somewhat at odds with the result of BS, since they deduced a silicon underabundance of 0.62 dex by assuming a 5kms^{-1} microturbulent velocity but an *overabundance* of 0.18 dex by assuming a 0kms^{-1} microturbulent velocity, as we do.

Of the silicon lines measured by SS and BS the two SiII lines of multiplet 1, 385.6018 and 386.2595 are not blended and so is the SiIII line of multiplet 2 at 455.2449. On the contrary the SiII line of multiplet 3 at 413.0894 is blended with SiII 413.0872 and PII 413.0790. The other SiII line of multiplet 3 at 412.8054 is blended with PII 412.7559 in our 16.5 Å/mm spectra. Our synthetic spectrum predicts that the PII line should be of comparable strength with the SiII line and it should be resolved from it in the 9 Å/mm photographic spectra used by BS (for which we assumed a resolving power $\Delta\lambda = 0.0135\text{nm}$).

The two lines of multiplet 1 lie between H_8 and H_9 and are contaminated by the wings of both hydrogen lines. Thus an accurate measurement of the equivalent widths of these lines is almost impossible due to the difficulty in the placement of the continuum. These two lines should not be used for abundance determinations. The SiII line of multiplet 2 is at the detection limit both in the spectra of BS and in ours. It is therefore not suitable for abundance determination. On the other hand the line at 412.8054 is suitable if one can measure its equivalent width from high dispersion spectra, where it can be resolved from the PII line 412.7559. Our synthetic spectrum predicts that the blending components of SiII 413.0894 should have a minor effect so that in practice also this line may be used to determine the Si abundance.

We used our adopted model and the equivalent widths of BS and SS to derive Si abundance from the four above–mentioned SiII lines. The results are displayed in table 6.9, together with the Si abundance derived from the equivalent widths given in table 6.4 .

As was foreseen there is a rather large scatter in the abundance determined from the two lines of multiplet 1, this is most likely due to differences in the placement of the continuum. On the other hand the line at 412.8054 yields an abundance which is consistent with our value derived from the UV, both using the equivalent width of BS and that of SS.

Table 6.5

Log of IUE observations

image	program id	aperture	t_{exp} (minutes)	obs date yr day hr min
SWP4616	MHD02	large	270	79 072 05 25
SWP15592	MHD07	large	293	81 333 14 54
SWP20127	GHFFB	large	245	83 153 09 93
LWR11155	JK559	large	127	81 208 01 44

Due to the high quantum efficiency in the red of the Thompson barrette used as a detector in the Aurelie spectrograph we have been able to detect two SiII lines of multiplet 2. The abundance determined from these two lines is perfectly consistent with our adopted value.

Table 6.4

Equivalent widths from optical spectra

λ	Ion	EW (pm)	* denotes an average of several measurements
385.6012	SiII	7.9	*
386.2595	SiII	3.9	*
386.763	HeI	2.8	*
393.3663	CaII	10.5	*
393.5962	FeII	0.7	*
400.9258	HeI	1.7	*
402.619	HeI	38.3	*
404.4576	PII	2.9	*
412.8054	SiII	9.7	
413.0894	SiII	8.2	
417.8483	PII	7.2	
422.2198	PIII	2.1	
423.3172	FeII	4.6	*
430.3176	FeII	5.0	*
438.7929	HeI	19.6	
439.0572	MgII	2.9	
441.6830	FeII	2.6	*
441.9596	FeIII	2.6	
442.0712	PII	3.7	
443.1019	FeIII	1.9	*
445.2472	PII	2.9	*
446.3027	PII	2.8	
446.8000	PII	4.8	
447.1480	HeI	30.8	
447.5270	PII	3.9	
448.1000	MgII	13.2	
449.9230	PII	2.2	
450.8288	FeII	1.7	
451.5339	FeII	1.4	*
452.2634	FeII	3.8	
453.0823	PII	1.6	*
454.9474	FeII	5.5	* (blend FeII 454.9192, TiII 454.9617)
455.2622	SiIII	2.0	*
458.3837	FeII	1.8	*
458.8032	PII	2.7	*
458.9846	PII	3.5	*
460.2069	PII	3.1	*
587.5	HeI	10.9	*
634.7109	SiII	8.5	*
636.7240	PII	2.4	*
637.1371	SiII	6.7	*
640.2246	NeI	2.4	*
645.6383	FeII	2.6	
645.9945	PII	3.9	
650.3392	PII	2.4	
650.7979	PII	2.5	
667.8154	HeI	6.6	

In the UV we did not use the SiII lines of multiplet 13.04 in the abundance analysis, since these lines are temperature sensitive (Singh& Castelli, 1991). The resonance lines of multiplet 4 (126.0422) and 2 (152.6707) show a probable interstellar component. Such a component is not present in any of the SiIII or SiIV lines. Two silicon lines show a blending feature on the red wing, which is unidentified and present also in the spectrum of ι Her : line 141.0214 of SiII, multiplet 13.02 and line 129.6726 of SiIII, multiplet 4.

Due to the large number of lines both in the visible and in the UV used to determine the silicon abundance, this value ought to be fairly accurate. Moreover we have been able to show that the discrepancy with the result of BS is entirely due to the adopted model atmosphere and not to differences in the observational data and/or equivalent widths.

Phosphorous

Phosphorous lines represent the most striking peculiarity in the spectrum of F86. There is no doubt that P is indeed overabundant by some large factor in the atmosphere of F86, given the many P lines identified both in the visible and in the UV, which are not seen in the spectra of normal stars, such as ι Her. However to quantify this overabundance is somewhat problematic due to the lack of a reliable set of gf values. BS found a large discrepancy in the P abundance determined from PII and PIII lines, they adopted the abundance determined from the PII lines because they placed more reliance on their oscillator strengths than on those of PIII. In fact the spectrum of F86, so rich in P lines, is an ideal ground to test the reliability of the relevant atomic data.

In Table 6.10 we give a list of identified P lines, both in the visible and UV. Many of the identified lines are very weak, but still detectable with the aid of

Table 6.6

T_{eff} and log g for F86 from the literature

T_{eff} (K)	log g	method	Reference
16600	3.8	Newell photometry / Mihalas (1966) models	Newell (1973)
17500	4.2	$H\gamma$,H_δ, Balmer discontinuity	Bascheck & Sargent (1976)
19600	4.4	Strömgren photometry / calibration of Hartoog & Cowley (1979)	Hartoog (1979)
18000	4.5	IUE low resolution spectra / Kurucz (1979) models	Hack (1979)
17000 — 18000	4.0 — 4.5	as above + Balmer discontinuity	Hack (1980)
14500	4.0	(m1,b-y) diagram / Kurucz (1979) models	Huenemoerder *et al.* (1984)
15300	-	(c1,b-y) diagram / Kurucz (1979) models	Huenemoerder *et al.* (1984)
14600	4.0	(m1,19-55) diagram / Kurucz (1979) models	Huenemoerder *et al.* (1984)
14500	-	(c1,19-55) diagram / Kurucz (1979) models	Huenemoerder *et al.* (1984)
15500	4.0	(m1,15-55) diagram / Kurucz (1979) models	Huenemoerder *et al.* (1984)
16500	-	(c1,15-55) diagram / Kurucz (1979) models	Huenemoerder *et al.* (1984)
14250	-	(BC, BC_{5370}) diagram / Kurucz (1979) models	Huenemoerder *et al.* (1984)
15500	-	UV Si II lines of mult. 13.04	Singh & Castelli (1992)

the synthetic spectrum; on the other hand many more lines are predicted by the synthetic spectrum but are not detectable in the observed spectra.

Table 6.7

Lines used to fix the abundances

Ion	M.	λ (nm)
B II	UV 1	136.2461
C I	UV 2	165.6267
	UV 3	156.0309
	UV 4	132.8834
	UV 4	132.9085
	UV 4	132.9100
	UV 5	128.0135
	UV 5	128.0333
C II	UV 1	133.4532
	UV 1	133.5663
	UV 1	133.5708
C III	UV 2	124.7383
O I	UV 2	130.4858
N I	UV 4	149.2625
	UV 9	174.2719
	UV 13	131.0540
Mg II		123.9925
		173.4852
Al II	UV 2	167.0787
	UV 4	185.8025
	UV 5	176.0106
	UV 5	176.3869
	UV 5	176.3952
	UV 5	176.5816
		135.0177
Al III	UV 1	185.4716
	UV 1	186.2790
		137.9670

Ion	M.	λ (nm)
Si II	UV 1	181.7451
	UV 3	130.4370
	UV 4	126.0422
	UV 4	126.4738
	UV 7	134.6884
	UV 7	135.0072
	UV 7	135.0516
	UV 7	135.2635
	UV 7	135.3721
	UV 8	124.6740
	UV 8.01	122.8612
	UV 8.01	122.8738
	UV 10	171.1304
	UV 13.02	140.9053
	UV 13.02	140.9899
	UV 13.02	141.0214
	UV 13.05	125.0091
	2	634.7109
	2	637.1371
Si III	UV 1	189.2030
	UV 4	129.4545
	UV 4	129.6726
	UV 4	129.8892
	UV 4	129.8946
	UV 4	130.1149
	UV 4	130.3323
	UV 10	131.2591
	UV 39	134.2351
	UV 39	134.2389
	UV 39	134.2432
Si IV	UV 1	139.3755
P I		137.9482
		149.1365

Ion	M.	λ (nm)
P II	UV 2	130.4492
	UV 2	130.4675
	UV 2	131.0703
	UV 2	130.1874
	UV 2	130.9874
		124.9830
		126.4470
		128.4329
		129.4648
		147.1189
		147.2103
		149.0439
		187.8319
P III		175.6800
Fe II		138.7219
		156.6822
		161.2806
		163.1128
		163.2667
		163.6331
		163.9401
		164.1762
		164.3578
		164.6185
		164.7163
		168.5954
		174.9358
		174.9602
		183.4965
		185.9746
		186.0053

Table 6.8

Abundances of F86

ELEMENT	*BASCHEK &SARGENT*	*THIS PAPER*	*SOLAR VALUES*
He	− 2.22	− 2.22	− 1.05
B	−	− 11.00	− 9.44
C	< −5.21	− 5.00	− 3.48
N	< −4.21	− 5.00	− 3.99
O	< −2.51	− 3.75	− 3.11
Mg	< −4.61	− 4.71	− 4.46
Al	< −5.21	− 6.75	− 5.57
Si	− 4.31	− 5.00	− 4.49
P	− 4.31	− 4.10	− 6.59
S	< −5.01	− 5.25	− 4.83
Ca	− 4.61	− 5.68	− 5.68
Sc	−	− 8.94	− 8.94
Ti	< −5.71	− 6.40	− 7.05
V	−	− 7.25	− 8.04
Cr	< −5.51	− 5.75	− 6.37
Mn	−	− 6.65	− 6.65
Fe	− 3.31	− 4.37	− 4.37
Co	−	− 7.12	− 7.12
Ni	−	− 5.79	− 5.79
Cu	−	− 5.90	− 7.83
Zn	−	− 7.00	− 7.44
Ga	< −5.41	− 9.16	− 9.16

The visible lines of P are all rather weak and thus their equivalent widths are more subject to errors. There are 8 lines which are in common among us, BS and SS.

Table 6.11 lists the P abundance deduced from the equivalent widths taken from the three papers, using our model and atomic data. If we take the mean value of the abundances determined from each set of equivalent widths we find

$$(\epsilon_{\rm P})_{\rm SS} \approx -4.79 \pm 0.29$$

$$(\epsilon_{\rm P})_{\rm BS} \approx -4.36 \pm 0.23$$

$$(\epsilon_{\rm P})_{our} \approx -4.76 \pm 0.42$$

Table 6.9

Abundances of Si from equivalent widths of visible lines

λ (nm)	ϵ_{Si} EW BS	ϵ_{Si} EW SS	ϵ_{Si} THIS PAPER
385.6018	-4.48	-5.50	-4.99
386.2595	-4.72	-5.38	-5.62
412.8054	-4.90	-5.75	-4.57
413.0894	-4.93	-5.16	-4.96
634.7109	-	-	-5.07
637.1371	-	-	-5.10

the errors quoted are simply the standard deviation from the mean. So, in spite of the large scatter in the abundance determined from the individual lines, our result is perfectly consistent with that derived from the equivalent widths of SS.

There is a difference, which is just significative, with the result derived from the equivalent widths of BS. It is so somewhat surprising that using the equivalent widths of BS and our model we get almost exactly the same abundance as BS, although their model is entirely different from our model. It is reasonable that the abundance determined from our equivalent widths show the largest scatter since all our spectra have a lower resolution than those of BS and SS.

We measured equivalent widths for several more P II lines in the visible–red region, a total of 17. The average value of the P abundance is $\epsilon_P = -4.99 \pm 0.48$. This is the value adopted also to compute the UV spectra.

Our adopted abundance reproduces well the lines given in Table 6.7, however the other lines given in Table 6.10 are very poorly reproduced. Also in the UV we

Table 6.10

Identified P lines

Ion	M.	λ (nm)
PI		137.3490
		137.6073
		137.7934
		137.9428
		149.1365
		167.1068
		167.2476
		167.9697
		177.4949
		178.2829
		178.7648
		190.7661
		154.8461
PII		123.1184
		124.9830
		126.4470
		127.8081
		128.4329
		128.9569
		129.4648
		130.1874
	2	130.4492
	2	130.4675
		130.5497
		130.9874
	2	131.0703
		131.4994
		145.2900
		147.1189
		147.2103
		147.3150
		148.4496
		148.9304
		149.0767
		149.0862
		149.4967
		149.6439
		149.7666

Ion	M.	λ (nm)
PII		150.6442
		150.6959
		152.1591
		152.1659
		152.2398
		152.2604
		152.4258
		153.4488
		153.6416
	1	154.2304
	1	153.2533
	1	153.5923
	2	154.3133
		180.5073
		180.6084
		180.6847
		182.8597
		183.6437
		183.7483
		185.9410
		187.6777
		187.8319
		187.9806
		194.5545
		404.4576
		406.2149
		406.4727
		406.5564
		412.7559
		417.8463
		438.5393
		445.2472
		446.3027
		446.8000
		447.5270
		448.3693
		449.9230
		453.0823
		458.8032

Ion	M.	λ (nm)
P II		458.9846
		460.2069
		442.0712
		455.4854
		455.8095
		636.7248
		643.5282
		645.9945
		650.3398
		650.7979
		671.3283
PIII		133.2813
	1	134.4326
	1	134.4850
	7	137.9912
	7	138.0464
	7	138.1094
	7	138.1648
		161.8629
		175.6800
		175.7628
		176.7820
		405.7312
		408.0089
		422.2198
		424.6720
PIV		146.7427

Table 6.11

P abundances from equivalent widths of visible lines

λ (nm)	ϵ EW SS	ϵ EW BS	ϵ EW (Tab 6.4) (gf MRB)	ϵ EW (Tab 6.4) (gf HI)	ident
417.8463	-5.01	-4.28	-4.34	-4.34	PII
422.2198	-	-5.21	-5.39		PIII
445.2472	-	-	-4.41		PII
442.0712	-4.83	-4.26	-4.65	-4.67	PII
446.8000	-4.27	-4.29	-3.95		PII
447.5270	-5.03	-4.51	-4.65		PII
449.9230	-4.70	-4.83	-5.08		PII
453.0283	-	-	-5.01		PII
458.8032	-5.26	-4.26	-5.32		PII
458.9846	-4.64	-3.98	-5.03		PII
460.2069	-	-	5.41		PII
636.7240	-	-	-5.03	-4.42	PII
645.9945	-	-	-5.40	-5.02	PII
650.3398	-	-	-5.94	-5.32	PII
650.7979	-	-	-5.90	-5.10	PII

find that the P overabundance deduced from the PIII lines is much smaller than that deduced from the PII lines, in agreement with the findings of BS.

This state of affairs is, clearly, not very satisfactory. We believe our P abundance to be only a rough estimate and an error of over 1 dex is possible. Our result is in close agreement with that of BS.

SS say that the P/Si ratio is higher than normal by a factor of 50, using our abundances this ratio is much higher than normal and is of the order of 10^3. This is mainly due to the fact that we determine Si to be underabundant, while both SS and BS give a Si abundance which is roughly solar.

Chlorine

There is only one Cl line in our spectra: The resonance line of ClI at 134.7240 nm . It is heavily blended with FeII 134.7265 nm and cannot be used to fix the Cl abundance. Since Cl overabundance has been reported in two HBB stars (PHL 25 and PHL 1434 ; Heber, 1990) it would be interesting to determine the Cl abundance in F86. Unfortunately we do not have at our disposal the spectral range around 480 nm where the ClII lines have been detected in the two above–mentioned stars.

Calcium

There are only two Ca lines in our spectra: the Ca II 183.8008 nm line in the UV an the Ca II K line in the visible. Both lines are well reproduced by our computations assuming solar abundances. Thus we take the Ca abundance to be solar. We disagree with BS who say that the Ca II K line is probably interstellar, quoting Cohen & Meloy (1976). We shall say more on this in the next section.

Gallium

In Pop I CP stars P overabundance is always accompanied by Ga overabundance. The resonance line of Ga III at 149.5045 nm would support an overabundance of $\approx$ 1 dex. However the other resonance line of Ga III at 153.4462 nm and the resonance line of Ga II at 141.4402 nm are consistent with a solar Ga abundance. The Ga III are heavily blended with P II lines, while the Ga II line is heavily blended with Fe II. No firm conclusion may be reached on the Ga abundance, but it is definitely not as enhanced as in typical Ga stars. To compute our synthetic spectra we adopted a solar Ga abundance.

Germanium

The resonance line of Ge II at 123.7072 nm is heavily blended with Ti III 123.7018 nm and Ti II 123.7062 nm. No conclusion may be drawn on Ge abundance. For the purpose of the computations we assumed a solar abundance.

Iron

From the UV spectrum iron appears to be essentially solar. This is readily seen in the comparison with ι Her: iron lines in F86 are more or less of the same strength as in ι Her. We believe the main cause of disagreement between observed and computed spectra for iron lines to be the inadequacy of the atomic data and the low S/N of the spectra.

In the visible spectra we measured the equivalent widths of 10 FeII and 2 FeIII lines. The average abundance from the FeII lines is $\epsilon_{Fe} = -4.28 \pm 0.44$ (the quoted error is just the standard deviation from the mean). The scatter is quite large, as should be expected, since most of the Fe lines are weak and large relative errors affect the measured equivalent widths; however the average value is in substantial agreement with our UV result. This is a comforting result since it supports our choice for the model–atmosphere parameters.

We used the equivalent widths of BS and our model and atomic data to derive the iron abundance. We find $\epsilon_{Fe} = 3.73 \pm 1.11$, which is in agreement with the value given in table 4 of BS. However the standard deviation from the mean is large. A similar result is obtained if we use the equivalent widthsof SS: $\epsilon_{Fe} = -3.31 \pm 1.00$. In the case of iron the discrepancy between us and BS is due to the different model and atomic data as well as to difference in the equivalent widths.

Krypton

Hack (1980)identified Kr I 123.58 nm, we believe this feature to be due to SiII, instead, since there is an almost identical feature in the spectrum of ι Her, as discussed by Castelli& Bonifacio (1990).

Mercury

Hack (1980) identified several Hg lines: for Hg II λ 164.996 , λ 133.176 , λ 132.173, λ 130.795 and all the strong lines of Hg III. We offer no alternatives for these identifications, all the lines are clearly present in our spectra and for several of them there is no corresponding feature in the spectrum of ι Her. If Hg were overabundant we would expect to observe HgII 398.4 nm, as is the case for the classical Hg–Mn stars, however no feature is detectable in our spectra at that wavelength.

6.6 Conclusions

The abundance pattern of F86 is quite puzzling. In figure 6.12 we show a plot of d (defined as $\log(element/N_{tot}) - \log(element/N_{tot})_{\odot}$) versus atomic number. One can distinguish at a glance two groups of elements: 1) light elements (up to S), all of which are underabundant with respect to the sun with the exception of P, which shows a large overabundance ; 2) Iron peak elements which are solar or overabundant.

The ratios [C/Fe] and [O/Fe] are all negative. In Pop II stars these ratios are positive and more so with decreasing [Fe/H] (Spite, 1992). The abundance pattern of F86 is also unlike that of Pop I MS stars, which, by far and large, have essentially solar abundances (Underhill, 1982). Also, surprisingly enough, it

is unlike that of peculiar B He-weak stars. The so-often quoted similarity with 3 Cen A is limited to the He-deficiency and P overabundance. The most noticeable differences are: C is solar in 3 Cen A while it is markedly deficient in F86; N is markedly overabundant in 3 Cen A, while it is definitely underabundant in F86; Si is overabundant in 3 Cen A, but underabundant by a large factor in F86; although we have not been able to determine the Ga abundance in F86 it is not overabundant by a factor of the order of 10^3 as it is in 3 Cen A (Jugaku & Sargent, 1963).

F86 still defies our attempts to unveil its nature. If we believe the "intrinsic" chemical composition of a star to be correlated with its kinematics, then the kinematics of F86 tells us that its "intrinsic" composition should have a very low metal content. In spite of this its surface composition, though peculiar, is more like that of a Pop I star than like that of a Pop II star. Since the abundance pattern of F86 is unlike that of other Bp He–weak stars we doubt that diffusion alone could account for it, unless a number of *ad hoc* hypothesis are made.

We found no conclusive evidence for the existence of circumstellar material, although there are two clues which point in this direction: 1) the non–zero reddening 2) the presence of numerous sharp unidentified features in the UV spectrum, which are shifted with respect to photospheric resonance lines. The non–zero reddening is at odds with the fact that we do not observe strong interstellar lines in the UV nor in the visible. This is also comforted by the results of Cohen & Meloy (1976) : these authors do not detect Na I lines at 588.9 nm and 589.5 nm on 35 Å/mm spectra and from 10 Å/mm spectra they give an equivalent width of 13.5 pm for the Ca II K line. This is not too different from the equivalent width we measure for the photospheric Ca II K line from our 16.5 Å/mm spectra. Although Cohen and Meloy do not list the plate material used they say they used

10 Å/mm plates taken at Palomar Mountain in 1966-67 and for F86 they say that the spectra were already measured by Sargent& Searle (1968) and Greenstein (1968). We suspect that three of these spectra were the very same used by BS, one of which was the same used by SS. We believe that the line which they measure as interstellar is instead the photospheric Ca II line. They measure the stellar radial velocity by using H_γ, H_δ, H_8 to H_11 and the radial velocity of the interstellar Ca II K line. For F86 they give $V_{LSR}(F86) = -12 kms^{-1}$ and $V_{LSR}(CaII) = -8 kms^{-1}$; the error attached to these measurements is $\pm 15 kms^{-1}$. Thus their measurements do not contradict our hypothesis that the only Ca II K line observable in the spectrum of F86 is indeed photospheric. Probably Cohen & Meloy assumed that F86 is metal–deficient, thus expecting the star to show no photospheric Ca II K line, contrary to the prediction of our computed spectrum. The observed Ca II K line is well reproduced assuming solar Ca abundance and appears to be at the same radial velocity as other photospheric lines.

Taken at face value this result tells us that the dust to gas ration in the line of sight of F86 is higher than along other lines of sight. Whether the dust, responsible for the reddening is confined to the vicinity of of the star or more or less homogeneously distributed along the line of sight, we cannot tell.

If F86 is an HB star we can expect material ejected from the star during the red–giant and subsequent phases, to be still present in the vicinity of the star. Yet no firm conclusion on this issue has been reached.

In view of the results discussed in the previous sections the most likely interpretation of F86 is that it is a halo HB star. Its chemical composition has been modified by some atmospheric phenomenon, like in known Pop I CP stars. We cannot tell whether the iron abundance is intrinsic or atmospheric. If it is intrinsic

it could imply a relationship of F86 with the metal–rich halo stars of Carney *et al.*(1990), mentioned in chapter 2.

One of the most important questions which one has to ask now is: how many blue HB stars show abundance anomalies and peculiar spectra like F86? The question may be addressed only by the study of a statistically significant number of blue HB stars. So far this has not been done because HB stars are are faint and a detailed analysis requires high resolution spectra with a large spectral coverage. This requires a lot of observing time on large telescopes. However, using the experience gained with F86 we plan to tackle this problem in the future as follows: use photometry and low resolution spectra to determine atmospheric parameters and reddening, use high resolution spectroscopy of selected regions in the visible to determine chemical abundances. These spectra will be compared with templates of normal stars, such as ι Her, and with synthetic spectra. Our hope is that this new data might help to cast new light also on F86 which is still mocking our efforts to understand its nature.

Chapter 7.

Abundance analysis of two metal–poor giants

7.1 Introduction

One of the most useful techniques for detecting metal–poor candidates has proven to be the use of objective–prism spectra, combined with the measurement of a line index from low resolution spectra. Metal–poor candidates are picked up amongst those which show a featureless continuum in the objective–prism spectra. A very succesful survey is that of Beers *et al.*(1985), who combine the objective–prism data with Ca II K line index. In the late 1980's P. Molaro, F. Castelli and I began a research program which was aimed at the determination of abundances for some of these extremely–metal-poor G–dwarfs. In the rest of the chapter I describe some of the results of this program, essentialy those which have been published in Bonifacio *et al.*(1990) and Molaro & Bonifacio (1990).

7.2 Observations and data reduction

The spectra were observed by P. Molaro at ESO La Silla in September 1988 with the 3.6 m telescope equipped with the Cassegrain Echelle Spectrograph (CASPEC, D'Odorico *et al.*, 1983). The detailed observations log is given in table 7.1. The nominal resolution was about 20000 and each frame had a coverage of about 90 nm. Th-Ar lamp spectra were taken before and after each exposure to be used for wavelength calibration. Flat–field exposures were taken at the beginning and end of each night.

The reduction of echelle spectra is considerably more complex than that of other spectra. Since this kind of spectrographs has a growing importance in astronomy I think it is worthwhile to describe here some of the reduction techniques.

Table 7.1

Star	Date	Range Å	λ_c Å	T_{exp} sec	S/N
CS 22885-96	26/9/88	4450-5450	4950	5400	30
	29/9/88	3800-4800	4300	5400	30
CS 22881-39	26/9/88	4300-5300	4800	5400	15

I shall make explicit reference to CASPEC spectra, although much of what I say applies to any echelle spectrograph with a CCD detector.

The basic theory of echelle grating spectrographs may be found in Schroeder (1967, 1970, 1987). The format of an echelle spectrogram is two–dimensional. Several orders are imaged onto the focal plane at the same time. Figure 7.1 shows an example of a CASPEC spectrum. Each order appears as a strip in the (x, y) plane. In what follows we shall assume that the x direction is aligned with the dispersion of the echelle grating, while the y direction is aligned with the dispersion of the cross-disperser, as in figure 7.1. One can always reduce to this case by rotating the image through a suitable angle.

Three characteristics of the spectrum in figure 7.1 are worth noting:

1) the orders are not parallel to the x axis, but have a non–zero slope;
2) the orders are curved in the (x, y) plane;
3) if the same spectral line appears in two succesive orders it shows different intensities.

Points 1) and 2) are due to two effects: a) the light of different wavelengths will be deviated by different angles in going through the cross-disperser; b) light of

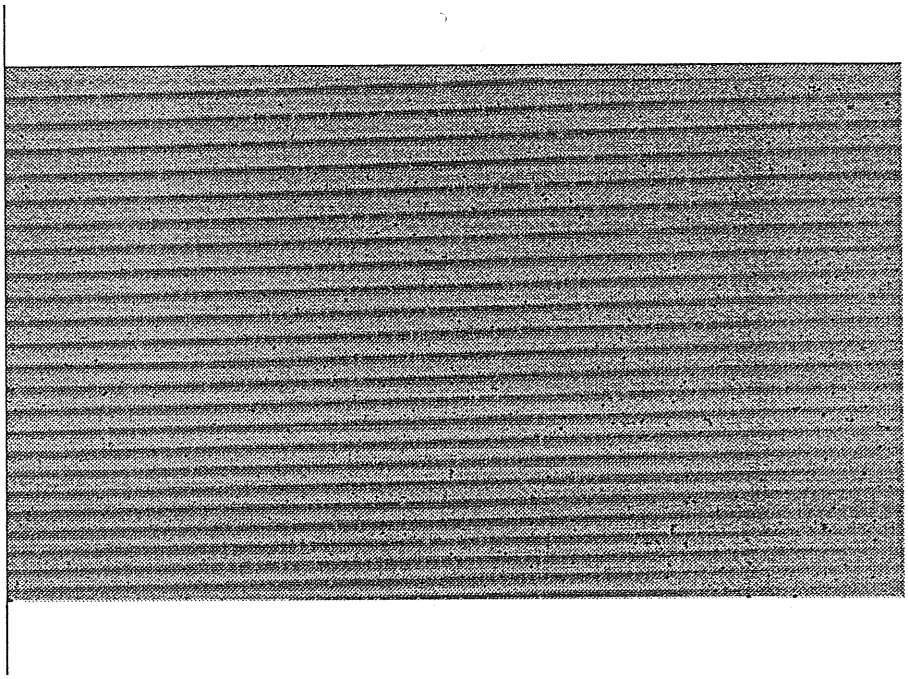

Fig 7.1 A grey scale plot of a CASPEC frame.

the same wavelength split in two consecutive orders will emerge from the echelle with different angles, thus the incidence angle on the cross-disperser (assuming post–dispersion, as in CASPEC) will be different. Naively one could imagine that by rotating the detector in the focal plane one could align the orders with the columns. However it is readily understood that effects a) and b) will both concur at making the orders non–parallel. Thus the slope of echelle orders is something we have to live with.

Point 3) is due to the fact that the blaze function of an echelle grating is very sharply peaked, so that it shows a considerable variation within one order.

A perspective plot of a part of an echelle frame is shown in figure 7.2, the z axis is the number of counts. The spatial profile of the order is called the

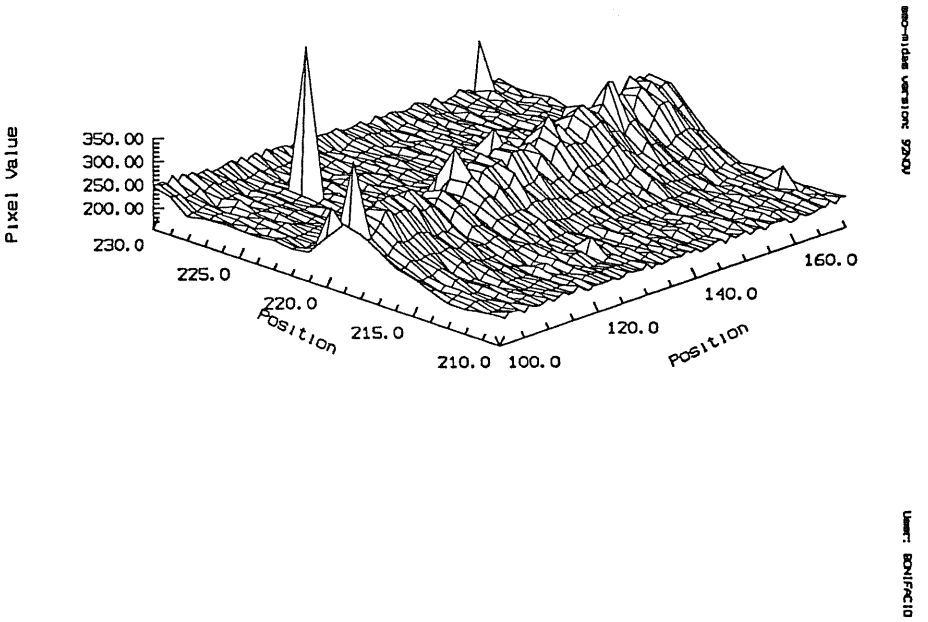

Fig 7.2 A perspective plot of a small portion of the CASPEC frame shown in figure 7.1.

cross-dispersion profile, since it depends essentially on the properties of the cross-disperser. The reduction of an echelle spectrum may be subdivided into the following steps.

1) order definition
2) background subtraction
3) division by the flat-field
4) order extraction
5) wavelength calibration
6) order merging
7) absolute flux calibration

Steps 3), 6) and 7) are optional. I shall discuss each step separately.

7.2.1 Order definition

In its most general form the problem of order definition amounts to determining k fuctions $f_m(x,y)$ which represent the m-th order spectrum of the astronomical source. One approach to the problem could be to take some parametric model for the above functions and do some sort of multivariate fit to the data using a χ^2, or similar, goodness–of–fit test. For instance assume that $f_m(x,y) = A_m(x)exp(-(\frac{y-\sum_1^N a_{mj}x^j}{\sigma(x)})^2)$, for each fixed x this is a gaussian in the y direction, moreover the centers of such gaussians lie on a polinomial of degree N in the (x,y) plane. The function $A(x)$ is essentially the blaze function. One would expect that some model of this sort ought to be capable of describing satisfactorily the cross–dispersion profile. The number of parameters to be estimated is about 10–20 for each order, whereas the number of points contained in the order is at least of the order of a few 10^3, so this approach seems feasable. However I do not know of any tool in standard image processing packages such as ESO–MIDAS or IRAF which implements this approach. I have tried to implement such a scheme with a home–made program, but the results are far from satisfactory and indeed worse than the relatively simple techniques described below. Although I have not yet fully analyzed the problem I think it mainly lies in the fact that astronomical spectra are characterized by low signal to noise ratios and sophisticated multivariate fit algorithms tend to be unstable under these conditions. In any case such fitting schemes require a major computational effort which is a drawback especially for large–format images.

If we do not require all the information contained in the spatial profile we may be content with an algorithm which detects the orders and finds the (x,y) loci of

the centers of each order. This may be done by simple thresholding or by more complex mathematical techniques, such as the Hough transform (Ballester, 1991). At the end one is able to construct a table which contains the order number and the coordinates of the central position of each order. The simplest description of the orders is then achieved by defining an order width and moving a rectangular slit of this width along the order. We shall come back to this when talking about order extraction.

7.2.2 Background subtraction

Within each order not all the signal present comes from the astronomical source, there is also other signal which we term generically as background and which must be subtracted. The background is the sum of many terms amongst them we wish to point out:

1) electronic bias, introduced to enhance charge transfer efficiency in the CCD
2) dark current, this is due to the thermal excitation of $e^{-}hole$ pairs
3) scattered light in the spectrograph
4) light from adiacent orders

Other sources of background may be present, such as a preflash in some types of CCD. A subtle source of background is the sky emission, which may be due both the earth's atmosphere and to astronomical sources which partially overlap our target and contaminate its spectrum (e.g. a star embedded in a nebula or a star in a cluster). For this latter sort of background there is no general way to subtract it and special solutions must be sought if its subtraction is considered to be important. These may require to take a spectrum of an empty sky area near the star. The four above–mentioned sources of background, however, may be dealt with in a standard way. Once we have defined the orders we have also

defined the inter–order regions. In such regions the counts are due exclusively to the background. One may assume the background to be a rather smooth surface, measure it at some selected points in the interorder region and then interpolate over the whole surface using some suitable scheme such as bicubic splines or low degree polynomials. Two points are worth mentioning here: first of all one must pay attention to select "good" places were to estimate the background, i.e. avoid CCD defects, ghost orders etc. ; in the second place one has at his disposal bias frames, which should contain only the elctronic bias and dark frames which should contain only bias plus dark current. One may be tempted to subtract bias and dark current before estimating the background, thus leaving only scattered light to be removed. Obviously the two procedures should yield identical results. We tried this several times and found indeed a perfect agreement between the two procedures. Usually we prefer to subtract the bias first, but not the dark current. This because in priciple there could be an additive fixed pattern noise which would not go away by flat–fielding but would be efficiently removed by subtracting the bias. Often several bias frames are available so that they can be averaged thus removing any random noise. This is not the case for dark frames which are ususally noisy and affected by cosmic hits. If dark current is important for a given CCD it is best to estimate it from the dark frame and subtract a constant from the image to avoid that the noise in the dark frame seriously degrade the scientific image.

7.2.3 Flat–fielding

The division by the flat–field is always recommended since it is the only way to remove effectively the pixel to pixel variations in the response of the CCD as well as CCD defects such as bad columns, hot spots etc. One of the most striking examples of the pixel to pixel variations is the so called "fringing" . This is due

to interference fringes which arise in the coating and/or in the silicon itself. The effect is quite large in the red ($\lambda > 500$ nm) but is usually neglegible for most purposes in the blue. For this reason many people consider this step optional. On the understanding that it is mainly perfomed to remove fringes people claim that it is unnecessary when dealing with blue spectra. The disadvantage of dividing by the flat–field is that we are introducing extra noise in our spectrum. My experience is that if many flat–fields are available, so that a low–noise mean flat–field may be computed, it is always advisable to divide by the flat–field, even in the blue. In most cases not only CCD defects and fringing are removed by this operation, but also the signature of the blaze function.

7.2.4 Order extraction

The step of order extraction is one of the most delicate of the entire procedure. How to perform it depends crucially on what has been done in the order–definition step. If the full cross–dispersion profile is available then one may compute, for each x , the integral of this profile in the y direction. One then obtains, for each order, a one dimensional spectrum. An alternative, but substantially equivalent, approach is to performed a so called "optimal" extraction, where the extracted spectrum is, for each x the weighted sum of several pixels in the y direction. The weights are computed in such a way as to take into account that the center of the order has a higher information content than the wings. Several such algorithms may be found in the literature. The one implemented in the ESO–MIDAS echelle reduction package is described in Mukai (1990). The simplest possible extraction is a box–car extraction in which for each x the counts of all pixels within a rectangular slit of fixed height and width 1 are summed up. Though crude, as it may be, this simple method gives ecellent results, provided that the orders are well followed in

the order–definition step and that the width of the slit is suitably chosen. Usually the "optimal" extraction methods require a fine tuning of key parameters which, in practice, is very difficult to obtain. We do not yet know of any fool–proof "optimal" extraction algorithm. For this reason we generally stick to box–car extraction.

7.2.5 Wavelength calibration

Once the spectrum has been extracted it may be wavelength calibrated. The first step in wavelength calibration is always to detect a certain number of emission lines on a lamp spectrum (for CASPEC one usually uses a Th-Ar lamp) with some sort of automatic procedure. Next one needs to identify a few of these lines. The lamp spectrum is then extracted and other lines are identified using the first identifications to derive a trial dispersion relation. Whenever a new line is identified an improved dispersion relation is derived and the whole process iterated. It is important to note that at this stage one tries to fit a "global" dispersion relation of the form $m\lambda = f(x, m)$, which is expected to hold on account of the general rpoperties of echelles (see Schroeder, 1967,1970). Once a sufficient number of lines has been identified in each order, single–order dispersions relations may be derived exactly as is done with a one–dimensional spectrum (see chapter 4 of my Magister Thesis). In case this does not happen (e.g. if an order contains only one or two detected lines), one has to be content with the global dispersion relation. In the latest version of the ESO–MIDAS echelle package it is sufficient to identify four lines on an echelle frame, the others are identified automatically.

7.2.6 Order merging

Once the spectrum is extracted and wavelength–calibrated one may either use the single orders as they stand or merge them in a single one dimensional

spectrum. This may be done only if the orders overlap in wavelength. This is not always the case. In CASPEC with the "long camera" the orders do not overlap in wavelength. If the orders do overlap one may devise some scheme by which, in the overlap region, the spectrum is a suitable weigthted sum of the spectra in the two orders. A merged spectrum is useful if one has a large wavelength coverage, then, if the spectrum is flux–calibrated, one gets information on the shape of the continuum. For line profile analysis and for the measurement of equivalent widths the merging is not particularly useful.

7.2.7 Absolute flux calibration

The idea behind absolute flux calibration is to observe a spectrophotometric standard star with the same spectrograph setting as our target star and use tabulated fluxes of the star to derive an instrumental response function. This response function may be used to flux calibrate the spectrum of our target star. A rather large uncertainty affects this flux. This is mainly due to two facts: 1) the amount of light lost at the slit depends crucially on the centering of the star on the slit, the quality of the guiding and the seeing, all these parameters may be different when observing the standard star and our target star, resulting in different slit losses 2) the transparence of the sky may vary because of atmospheric phenomena (e.g. a thin layer of clouds). However one may hope that neither of these effects contains strong colour terms, thus that the flux calibration is correct at least in a relative sense, giving the right shape of the continuum. Absolute flux calibration is seldom performed on high resolution spectra to recover the shape of the continuum, since they do not have a large spectral coverage. However it is often used as a method to rectify the spectra, especially when the divison by the flat–field has been omitted.

In the work I am describing here only the first five steps of the reduction have

been performed. The reduction was carried out in 1989 at ESO–Garching using ESO–MIDAS. The spectra were normalized to the continuum by fitting a spline through a set of interactively chosen points. This procedure is rather unambiguous for metal–poor stars given the few lines present.

7.3 Method of analysis

As usual the first step in the analysis is to select a representative model–atmosphere (again, as usual, we adopt a Kurucz model–atmosphere). Given the low metallicity of the stars under study we used model–atmospheres from the grid, or computed model–atmospheres, for which the abundances are scaled by a factor 10^{-3} with respect to the solar abundances. At the time of writing the 1990 paper the most recent version of the ATLAS code available in Trieste was version 8. The spectra of these stars are characterized by the presence of very few lines, most of them unblended; this makes rather starightforward both the definition of the continuum and the equivalent width measurement. We computed at first a synthetic spectrum from the adopted model, without changing the abundances. This was plotted superimposed to the observed spectrum and used for identification purposes. Next we measured equivalent widths using the interactive code BANDGEN, derived from the ELSPEC spectrogram processing package (Pasian *et al.*, 1982), in which the observed profile is fitted to a Gaussian or a Lorentzian using the Frazer & Suzuki (1966) method. Then we used our adopted model and the measured equivalent widths as input to the WIDTH code to determine the abundances. We used these results to select a new model which better satisfied the Fe I / Fe II ionization equilibrium (this requirement essentially fixes log g) and the independence of abundances from equivalent widths (this requirement fixes micro-

turbulence). The whole process was iterated until there was no significant change in the adopted model. The advantage of using equivalent widths to derive abundances is its speed over the method of computing synthetic spectra. We used the WIDTH code to estimate the effect on the derived abundances of slight changes in the model parameters. We focussed our attention on iron since it was represented by many lines. A change of 100 K in T_{eff} resulted in a change of $\approx$ .13 dex in the iron abundance (an increase in temperature produces an increase in derived abundance and vice versa). An increase in microuturbulence by 0.5 kms^{-1} leads to a decrease in derived iron abundance by about .15 dex. An increase in gravity by 0.1 dex results in an increase in the derived iron abundance of about 0.09 dex.

7.4 CS 22885-96

From the Johnson photometry given by Beers *et al.*(1985) and the Carney *et al.*(1987) calibration we derive T_{eff} = 5000 K . From the H' index, from the same source, calibrated as in Molaro & Castelli (1990) we derive T_{eff} = 4770 K. Our finally adopted temperature is T_{eff} = 4900 K. From the Fe I/ Fe II ionization equilibrium we derived a gravity of $\log g$ = 1.0. A microturbulent velocity of 2.0 kms^{-1} minimizes the scatter in the abundances derived from the equivalent widths of Fe I and Ti II lines. Thus our finally adopted model has the following parameters: T_{eff} = 4900 log g =1.0 ξ = 2.0 kms^{-1} .

The measured equivalent widths and derived abundances are listed in table 7.2. To determine the iron abundance we used 21 unblended Fe I lines, whose equivalent width exceeds 4.5 pm. We did not use weaker lines since their equivalent widths are affected by a large relative error, at the resolution of CASPEC, with the S/N of our spectra. The average iron abundance is [Fe/H]=-4.21 ± 0.20.

Table 7.2

			CS 22885-96		CS 22881-39	
Ion	λ (nm)	$\log gf$	EW (mÅ)	A	EW (mÅ)	A
NaI	588.9951	0.110	68	-9.74		
	589.5924	-0.190	59	-9.58		
MgI	517.2684	-0.402	125	-7.63	101	-6.79
	518.3604	-0.180	125	-7.86	178	-6.27
AlI	394.4006	-0.623	<80	-9.55		
	396.1520	-0.323	<80	-9.83		
CaI	422.6728	0.243	108	-9.54		
ScII	424.6822	0.322	83	-12.64		
TiII	390.0551	-0.450	30	-11.46		
	430.0056	-0.750	34	-11.07		
	430.1938	-1.430	30	-10.49		
	431.2871	-1.310	30	-10.59		
	439.5033	-0.650	51	-11.00	54	-10.48
	441.7719				42	-9.80
	444.3794	-0.810	28	-11.26	56	-10.29
	446.8507	-0.770	39	-11.03	73	-10.06
	450.1273	-0.860	39	-10.97	67	-10.06
	453.3969	-0.760	57	-10.62	66	-10.06
	454.9617	-0.450	43	-10.77	64	-9.99
	456.3761	-0.950	28	-10.97	64	-9.92
	457.1968	-0.530	39	-10.77	67	-9.97
	458.9958				52	-9.24
CrI	425.4332	-0.114	4.2	-10.76		

The dispersion around the above–given mean value is due to the errors in the equivalent widths measurements, errors on the atomic data and uncertainities in the models. If we combine quadratically this dispersion with the errors associated with the choice of model–parameters given in the previous section, we obtain an error of about 0.3 dex in the derived iron abundance. Note that for elements whose abundance is derived from a single transition, such as Ca, Cr or Sc the errors are potentially much larger. Our derived iron abundance is substantially lower than that deduced by Beers *et al.*(1985) from the Ca II K index ([Fe/H]=-3.5). We suspect that the discrepancy is due to the presence of Ca II interstellar absorption which contaminates the measured index. To support this view we note that our spectra contain rather strong Na I interstellar absorptions and the strength of the interstellar Ca II K line ought to be similar.

7.5 CS 22881-39

For this star we had at our disposal only one spectrum centered at about 480 nm and with a lower S/N, since the star is almost two magnitudes fainter than the one previuosly discussed. Both using the Johnson photometry and the H' index the temperature is about 6000 K. The Fe I/Fe II ionization equilibrium indicates a surface gravity of log g =1.0. To derive the microturbulent velocity we used the Ti II lines, which are the most numerous. A value of $\xi = 2.5$ kms^{-1} minimizes the scatter in the Ti abundances derived from these lines. From the Fe I lines we derive an iron abundance of [Fe/H]= -3.53 ± 0.30, which is consistent, within the errors, with the value of -3.80 determined by Beers (1987). Apart from Ti II Fe I and Fe II only Mg I had strong enough lines to be detected in our spectrum. All the equivalent widths and derived abundances are listed in table 7.2.

Table 7.2 (continued)

			CS 22885-96		CS 22881-39	
Ion	λ (nm)	$\log gf$	EW (mÅ)	A	EW (mÅ)	A
FeI	400.5241	-0.570	70	-8.43		
	406.3594	0.080	95	-8.05		
	407.1737	0.000	63	-9.12		
	413.2058	-0.634	50	-8.73		
	414.389	-0.440	30	-9.37		
	418.1754	-0.186	38	-8.01		
	420.2028	-0.697	41	-8.98		
	423.5943	-0.090	46	-8.43		
	425.0787	-0.691	68	-8.41		
	426.0473	0.129	62	-8.38		
	427.1759	-0.127	86	-8.66		
	429.4127	-0.930	55	-8.51		
	430.7905	0.030	91	-8.60		
	432.5762	0.000	70	-9.01	88	-7.76
	433.7048	-1.580	32	-8.20		
	437.5930	-3.031	43	-8.36		
	438.3544	0.160	99	-8.64	57	-8.51
	440.4750	-0.180	86	-8.55	65	-7.99
	441.5122	-0.580	50	-8.82	73	-7.43
	442.7309	-3.044	34	-8.45		
	448.2169	-3.501	29	-8.03		
	452.8613	-0.760	25	-8.48		
	453.1147	-2.080	38	-7.70		
	501.2067	-2.642	38	-7.90		
	522.7189	-0.969	48	-8.60		

Table 7.2 (continued)

			CS 22885-96		CS 22881-39	
Ion	λ (nm)	$\log gf$	EW (mÅ)	A	EW (mÅ)	A
FeI	526.9537	-1.321	83	-8.44	64	-7.79
	527.0357	-1.440	30	-8.40		
	532.8038	-1.466	71	-8.47		
	537.1489	-1.645	62	-8.40		
	539.7127	-1.933	48	-8.34		
	540.5774	-1.884	40	-8.54		
	542.9696	-1.879	47	-8.42		
	543.4523	-2.122	25	-8.53		
FeII	423.3172	-1.836	30	-8.53		
	458.3837	-1.802	23	-8.50		
	462.9339				46	-7.40
	492.3927	-1.559	3.0	-8.51	63	-7.84
	501.8440	-1.400	29	-8.70	101	-7.42
	516.9033	-1.303	30	-8.79	101	-7.53
	531.6615				50	-7.42
SrII	407.7709	0.167	<40	-14.57		
	421.5519	-0.145	<24	-14.61		
BaII	455.4029	0.170	<25	-14.68		

7.6 Discussion

As more and more stars metallicity in the range $-3.5 \leq$ [Fe/H] are subject to fine analysis (Molaro& Castelli, 1990; Molaro & Bonifacio, 1990; Norris *et al.*,1993

Molaro *et al.*,1993), it becomes clear that they are not rare weirds, but rather the brigth tail of a population of extremely low metallicity. Thus scenarios which require a peculiar origin or evolution for such stars appear less probable. One such scenario was suggested by Carney & Peterson (1981) to explain the metal–deficiency of G 64-12 : a relatively metal–rich gas cloud could be diluted by an infalling extragalactic metal–free cloud; stars formed out of this material would be extremely–metal–poor although coeval with more metal–rich stars. Although such a possibility is not ruled out, it seems difficult to admit that such a peculiar fate is shared by several stars at different galactic locations.

One of the most striking features of this low–metallicity population was pointed out by us in the 1990 paper (Molaro& Bonifacio, 1990): namely that the abundance pattern of these extreme objects is very much like like that of Pop II stars of much higher metallicity. Such a similarity was already noted by Bessel & Norris (1984) for CD$-38°245$. From this observation they deduced that the same kinds of objects are responsible for the chemical enrichment of all Pop II stars of any metallicity. In a simple picture, in which metallicity is a monotonically increasing function of age, this translates into the statement that the early Galaxy must have been pretty much like the present–day Galaxy.

Some of the abundance ratios are, however, different in extremely–metal–poor stars than in Pop II stars of higher metallicity. The ratio [Mg/Fe] shows an enhancement. As more stars are analyzed this statement rests on more solid ground. There is some scatter among the most metal–poor stars, however it may be considered as safely established that [Mg/Fe] shows an upturn below [Fe/H] $=3.0$, although the magnitude of this increase is highly uncertain. Some of the scatter could be real (i.e. not due to observational errors), if there where chemical inhomegeneities in the early Galaxy. In their sample of four extremely–metal–

poor giants Molaro *et al.*(1993) find a scatter of nearly two orders of magnitude in the abundance of the heavy elements Sr and Ba. Such a scatter cannot be produced by observational errors alone. It is tempting to identify the reason of this scatter with chemical inhomogeneities in the gas out of which these stars were formed.

Sodium is another exception, the ratio [Na/Mg] is nearly constant and equal to the solar value, down to [Fe/H]=-2.5 (Gratton & Sneden, 1988), however in the most metal–poor stars [Na/Mg] seems to be substantially less than zero. If Na is primarily produced during the explosive burning of C, then it should be overdeficient with respect to magnesium in metal–poor stars (Arnett, 1971). This is consistent with the observations. It is also instructive to look at the behaviour of [Al/Mg] (Bonifacio *et al.*, 1990; Molaro *et al.*, 1993), below [Fe/H]=-2.0 this ratio turns flat at the constant value of $\approx$ 1.0. Molaro *et al.*(1993) claim that this is a strong indication in favour of the presence of a primary component of Al, as predicted by the theories of explosive nucleosynthesis in metal–weak supernovae (Truran & Arnett, 1971 ; Woosley & Weaver , 1982).

It is clearly important to continue this work. As more determinations of abundances in extremely–metal–poorstars are performed these trends may be confirmed and defined quantitatively, thus providing precious constraints to theories of nucleosynthesis in the early Galaxy.

BIBLIOGRAPHY

Adams W.S., Joy A.H., Humason M.L. and Brayton A.M.:1935, *Astrophys. J.* **81**, 187

Adelman S.J.:1984, *M.N.R.A.S.* **206**, 637

Allen C.W. Astrophysical Quantities 1976 The Athlone Press – University of London

Aller L.H.: 1963 The Atmospheres of the Sun and the Stars, 2nd ed. (The Ronald Press Co., New York)

Allocchio C., Morossi C. and Ramella M.:1988 Private Communication

Alpher R.A., Bethe H. and Gamow G.:1948, *Phys. Rev.* **73**, 803

Alpher R.A. and Herman R.C.:1950, *Rev. Mod. Phys.* **22**, 153

Alpher R.A. and Herman R.C.:1953, *Ann. Rev. of Nucl. Sci.* **2,1**,

AndersE. and Grevesse N.: 1989 *Geochim. Cosmochim. Acta* **53**, 197

Applegate,J.H.,Hogan,C.J. and Scherrer,J.:1988, *Astrophys. J.* **329**, 572

Arnett W.D.:1971, *Astrophys. J.* **166**, 153

Artru M.C.:1986, *Astron. & Astrophys.* **168**, L5

Artru M.C. and Lanz T.:1987, *Astron. & Astrophys.* **182**, 273

Artru M.C.,Borsenberger J. and Lanz,T.:1989, *Astrophys. J. Suppl. Ser.* **80**, 17

Audouze J. and Tinsley B.M.:1976, *Ann. Rev. of Astron. and Astrophys.* **14**, 43

Auer L.H. and MIhalas D.:1973, *Astrophys. J. Suppl. Ser.* **25**, 433

Baade W.:1944, *Astrophys. J.* **100**, 137

Ballester P.:1991 in *Proceedings of the 3rd ESO/ST-ECF Data Analysis Workshop* p. 23

Balona L.A.:1984, *M.N.R.A.S.* **211**, 973

Barnard A.J., Cooper J. and Smith E.W.:1974, *J. Quant. Spectrosc. Radiat. Transfer* **14**, 1025

Barnett E.W. and McKeith C.D.:1988, *M.N.R.A.S.* **234**, 325

Baschek B. and Norris J.:1970, *Astrophys. J. Suppl. Ser.* **19**, 327

Baschek B. and Norris J.:1975, *Astrophys. J.* **199**, 694

Baschek B. and Sargent A.I.:1976, *Astron. & Astrophys.* **53**, 47

BeersT.C.:1987 in *Nearly Normal Galaxies, from the Planck Time to the Present* ed. S.M. Faber New York, Springer, p. 41

Beers T.C.,Preston G.W.and Shectman S.A.:1985, *Astron. J.* **90**, 2089

Bessell M.S. and Norris J.:1984, *Astrophys. J.* **285**, 622

Bethe H.:1939, *Phys. Rev.* **55**, 434

Berger J.:1963, *P.A.S.P.* **75**, 393

Berry H.G.,Bromander J.,Curtis L.J.and Buchta R.:1971, *Physica Scripta* **3**, 125

Beskow G. & Treffenberg L.:1947 *Arkiv f. Mat.,Astr. o. Fys.* **34A**, No.13

Beskow G. & Treffenberg L.:1947 *Arkiv f. Mat.,Astr. o. Fys.* **34A**, No.17

Blitz L. and Spergel D.N.:1991, *Astrophys. J.* **379**, 631

Boesgaard A.M. and Heacox W.D.:1978, *Astrophys. J.* **226**, 888

Bohlin R.C. and Grillmair C.J.:, *Astrophys. J. Suppl. Ser.* **1988**, 66209

Bohlin R.C.,Saavage B.D. and Drakes J.F.:1978, *Astrophys. J.* **224**, 132

Bond H.E.:1981, *Astrophys. J.* **248**, 606

Bondi H. and Gold T.:1948, *M.N.R.A.S.* **108**, 252

Bonifacio P.: 1989 "NORMA: A Program for the Normalisation of Spectra", Università degli Studi di Trieste, Dipartimento di Astronomia, Rapporto Interno 20-IV-1989

Bonifacio P.:1991 Thesis submitted for the degree of *Magister Philosophiae* at The International School for Advanced Studies – Trieste

Bonifacio P. and Castelli F.:1992 in Proceed. IAU Coll. 138 *Peculiar versus normal phenomena in A-type stars* eds. M. Dworetsky, F. Castelli and R. Faraggiana, ASP Conf. Series n. 44, p. 143

Bonifacio P.,Castelli F.,Molaro P.:1990, Proc. Elba Workshop on *The Chemical and Dynamical Evolution of Galaxies* September 1989,ESO preprint 693

Bonifacio P. , Castelli F. and Hack M.:1991 in Poster papers presented at the 145th Symp. of IAU *Evolution of Stars: The Photospheric Abundance Connection*, eds. G.Michaud, T. Tutukov and M.Bergevin, p.57

Blades J.C., Wheatley J.M., Panagia N., Grewing M., Pettini M. and Wamsteker W.:1988, *Astrophys. J.* **334**, 308

Bonsack and Wolff .:1980, *Astron. J.* **85**, 599

Breger M.:1976, *Astrophys. J.* **32**, 7

Burbidge G.R. and Burbidge E.M.:1955, *Astrophys. J. Suppl. Ser.* **1**, 431

Burbidge M.E., Burbidge G.R., Fowler W.A. and Hoyle F.:1957, *Rev. Mod. Phys.* **29**, 547 (B^2FH)

Burkert A., Truran J.W. and Hensler G.:1992, *Astrophys. J.* **391**, 651

Caloi V., Castellani V. and Tornambè A.:1978, *Astron. & Astrophys. Suppl. Ser.* **33**, 169

Cannon R.D.:1981 in Proc. I.A.U. Symp. 105 *Observational tests of the stellar evolution theory* eds. A. Maeder and A. Renzini, Dordrecht Reidel Pub. Co., The Netherlands, p. 123

Carlberg R.G., Dawson P.C., Hsu T. an Vandenberg D.A.:1985, *Astrophys. J.* **294**, 674

Carney B.W.:1983, *Astron. J.* **88**, 610

Carney B.W. and Latham D.W.:1987, *Astron. J.* **93**, 116

Carney B.W., Laird J.B., Latham D.W. and Kurucz R.L.:1987, *Astron. J.* **94**, 1066

Carney B.W., Latham D.W. and Laird J.B.:1990, *Astron. J.* **99**, 572

Carney B.W., Aguilar L., Latham D.W. and Laird J.B.:1990, *Astron. J.* **99**, 201

Carney B.W., Laird J.B., Latham D.W. and Kurucz R.L.:1987, *Astron. J.* **94**, 1066

Carney B.W. and Peterson R. C.:1981, *Astrophys. J.* **245**, 238

Carr B.J., Bond J.R. and Arnett W.D.:1984, *Astrophys. J.* **277**, 445

Castelli F.:1991, *Astron. & Astrophys.* **251**, 106

Castelli F. and Bonifacio P.:1990, *Astron. & Astrophys. Suppl. Ser.* **84**, 259

Cayrel R.:1986, *Astron. & Astrophys.* **168**, 81

Cester B.:1984 *Corso di Astrofisica*, Hoepli, Milano

Chamberlain J.W. and Aller L.H.:1951, *Astrophys. J.* **114**, 52

Chandrasekar S. *An Introduction to the study of stellar structure* :1939 , The University of Chicago Press, Chicago ; also 1957 Dover, New York

Chandrasekar S. and Henrich L.R.:1942, *Astrophys. J.* **95**, 288

Chiosi C. and Jones J.:1983 in *The Origin and Evolution of Galaxies* eds. B.J.T. Jones and J.E. Jones, Dodrecht Reidel Pub. Co., The Netherlands, p. 197

Chiosi C., Bertelli G. and Bressan A.:1992, *Ann. Rev. of Astron. and Astrophys.* **30**, 235

Cohen J.G. and Meloy D.A.:1975, *Astrophys. J.* **198**, 545

Cowan R.D.,Hobbs L.M. and York D.G.:1982, *Astrophys. J.* **257**, 373

Crawford D.L.:1978, *Astron. J.* **83**, 48

Crocker D.A., Rood R.T. and O'Connell R.W:1988, *Astrophys. J.* **332**, 236

Cugier H. and Hardrop J.:1988a, *Astron. & Astrophys.* **197**, 163

Cugier H. and Hardrop J.:1988b, *Astron. & Astrophys.* **202**, 101

Curtis L.J.,Martinson I. and Buchta R.:1971, *Physica Scripta* **3**, 197

Dicke R.H., Peebles P.J.E., Roll P.G. and Wilkinson T.D.:1965, *Astrophys. J.* **142**, 414

Deutsch A.:1947, *Astrophys. J.* **105**, 283

D'Odorico S., Enard D., Lizon J.L., Ljung B.,Nees W., Ponz D., Raffi G. and Tannè J.F.:1983, *The Messenger* **33**, 2

Dumont P.D., Biémont E. and Grevesse N.:1974, *J. Quant. Spectrosc. Radiat. Transfer* **14**, 1127

Edvardsson B., Andersen J., Gustafsson B., Lambert D.L., Nissen P.E. and Tomkin J.:1993, *Astron. & Astrophys.* **275**, 101

Eggen O.J., Lynden–Bell D. and Sandage A.:1962, *Astrophys. J.* **136**, 748 (ELS)

Faraggiana R. and Malagnini M.L.:1984, *Astron. & Astrophys.* **137**, 149

FitzGerald M.P.:1970, *Astron. & Astrophys.* **4**, 234

Frazer R.D.B. and Suzuki F.:1966 *Annal. Chem.* **38**, 1770

Freeman K.C.:1986 in Norman *et al.* (1986) p.227

Froese–Fischer C.:1977, *J. Phys. B* **10**, 1241

Gamow G.:1946, *Phys. Rev.* **70**, 572

Gillet D.: 1989 *La Lettre de l'OHP* **1**, 1

Gilmore G. and Reid I.N.:1983, *M.N.R.A.S.* **202**, 1025

Gilmore G. and Wyse R.F.G.:1985, *Astron. J.* **90**, 2015

Gilmore G., Wyse R.F.G. and Kuijken K.:1989, *Ann. Rev. of Astron. and Astrophys.* **27**, 555

Glaspey J.W., Michaud G., Moffat A.F.J. and Demers S.:1989, *Astrophys. J.* **339**, 926

Goldbach C., Martin M., Nollez G., Plomdeur P., Zimmermann J.B. and Babic D.:1986, *Astron. & Astrophys.* **161**, 47

Goldbach C., Martin M. and Nollez G.:1989, *Astron. & Astrophys.* **221**, 155

Goldbach C. and Nollez G.:1987, *Astron. & Astrophys.* **181**, 203

Goldbach C. and Nollez G.:1988, *Astron. & Astrophys.* **201**, 189

Gratton R.G and Sneden C.:1988, *Astron. & Astrophys.* **204**, 193

Gray D. F.:1976 *The Observation and analysis of stellar photospheres*, John Wiley & Sons, New York

Greenstein J.L.:1968, *Astrophys. J.* **152**, 431

Greenstein J.L. and Sargent A.I.:1974, *Astrophys. J. Suppl. Ser.* **28**, 157

Greenstein G.S., Truran J.W. and Cameron A.G.W.:1967, *Nature* **213**, 871

Grenon M.:1987, *J.of Astron. & Astrophys.* **8**, 123

Grenon M.:1989, *Astrophys & Sp. Sci.* **156**, 29

Grigsby J.A.:1991, *Astrophys. J.* **380**, 606

Grigsby J.A., Morrison N.D. and Anderson L.S.:1992, *Astrophys. J. Suppl. Ser.* **78**, 205

Gross P.G.:1973, *M.N.R.A.S.* **164**, 65

Hack M.:1979, *Astron. & Astrophys.* **74**, L4

Hack M.:1980, *Astron. & Astrophys.* **81**, L1

Hack M. and Stalio R.:1975 in *Physics of Ap–Stars* I.A.U. Coll. 32 eds W.W. Weiss, H. Jenker and H.J. Wood, Finsterle & CO.KG., Wien p. 555

Harris A.W. and Sonneborn G.: 1987 in "Exploring the universe with the IUE satellite " Y. Kondo ed., D. Reidel Publishing Company, Dodrecht . The Netherlands

Hartoog M.R.:1979, *Astrophys. J.* **231**, 161

Hauck B. and Mermilliod M.:1980, *Astron. & Astrophys. Suppl. Ser.* **40**, 1

Hauck B. and Mermilliod M.:1990, *Astron. & Astrophys. Suppl. Ser.* **86**, 107

Hayes D.S. and Latham D.W.:1975, *Astrophys. J.* **197**, 593

Heber U.:1983, *Astron. & Astrophys.* **118**, 39

Heber U.:1986, *Astron. & Astrophys.* **155**, 33

Heber U.:1990 - I.A.U. Symp. 145

Heber U., Hunger K., Jonas G., Kudritzki R.P.:1984, *Astron. & Astrophys.* **130**, 119

Heber U., Kudritzki R.P., Caloi V., Castellani V., Danziger J., Gilmozzi R.:1986, *Astron. & Astrophys.* **162**, 171

Helfer H.L., Wallerstein G. and Greenstein J.L.:1959, *Astrophys. J.* **129**, 700

Heintze J.R.W.:1973 I.A.U. Symp. 54 p.231

Hibbert A.:1988, *Physica Scripta* **38**, 37

Hoffleit D.:1982 "The Bright Star Catlogue" 4th edition, Yale University Observ., New Haven, Connecticut

Hoyle F.:1947, *M.N.R.A.S.* **106**, 343

Hoyle F.:1948, *M.N.R.A.S.* **108**, 372

Hoyle F., Burbidge G.R. and Narlikar J.V.:1993, *Astrophys. J.* **410**, 437

Hoyle F. and Shwarzschild M.:1955, *Astrophys. J. Suppl. Ser.* **2**, 1

Hoyle F. and Tayler R.J.:1964, *Nature* **203**, 1108

Huenemoerder D.P., de Boer K.S. and Code A.D.:1984, *Astron. J.* **89**, 851

Imhoff C.L.: 1984 " Record of the International Ultraviolet Explorer NASA/ESA/SERC Three Agency Coordination Meeting", Computer Science Corporation,CSC/TM-84/6042,pp. A139-A148

Jamar C.,Macau-Hercot D.,Monfils A.,Thompson G.I.,Houziaux L. and Wilson,R.: 1976 *Ultraviolet Bright-star Spectrophotometric Catalogue* ESA SR-27

Johnson H.L.:1958 *Lowell Obs. Bull.* **4**, 37

Jugaku J. and Sargent L.W.L.:1963, *Astrophys. J.* **138**, 90

Jones J.E.:1985, *P.A.S.P.* **97**, 593

Kane L.,McKeith C.D. and Dufton P.L.:1980, *Astron. & Astrophys.* **84**, 115

Kippenhahn R. and Thomas H.C.:1978, *Astron. & Astrophys.* **63**, 265

Keenan P.:1942, *Astrophys. J.* **96**, 101

Keenan P., Morgan W.W. and Münch G.:1948, *Astron. J.* **53,194,**

KleinO., Beskow G. and Treffenberg L.:1945 *Arkiv f. Mat.,Astr. o. Fys.* **33B**, 1

Klemola A.R.:1962, *Astron. J.* **67**, 740

Kohl J.L.,Parkinson W.H. and Withbroe G.L.:1977, *Astrophys. J.* **212**, L101

Korhonen T. and Reiz A.:1986, *Astron. & Astrophys. Suppl. Ser.* **64**, 487

Kron G.E. and Mayall N.U.:1960, *Astron. J.* **65**, 381

Kubiak M.:1973 *Acta Astron.* **23**, 23

Kurucz R.L.:1970 *SAO Special Rep.* **309**

Kurucz R.L.:1979, *Astrophys. J. Suppl. Ser.* **40**, 1

Kurucz R.L.:1981 *SAO Special Report* **390**

Kurucz R.L.:1988a, line lists on magnetic tapes

Kurucz R.L.:1988b, Reports on Astronomy, XX IAU General Assembly, Baltimore

Kurucz R.L. and Avrett E.H.:1981 *SAO Special Report* **391**

Kurucz R.L. and Peytremann E.:1975 *SAO Special Report 362*

Leckrone D.S.:1969 Ph.D. Thesis, U.C.L.A.

Leckrone D.S.:1971, *Astron. & Astrophys.* **11**, 387

Leckrone D.S.:1973, *Astrophys. J.* **185**, 577

Leckrone D.S.:1981, *Astrophys. J.* **250**, 687

Lennon D.J.:1983, *M.N.R.A.S.* **205**, 829

Lesh J.R.: 1979 in *Spectral Classification in the future* ed M.F. Mc Charthy *et al.*Specola Vaticana, Città del Vaticano, p.81

Lester J.B., Gray R.O. and Kurucz R.L.:1986, *Astrophys. J. Suppl. Ser.* **61**, 509

Lindblad B.:1922, *Astrophys. J.* **55**, 85

Luyten W.J.:1959 *Pub. Un. Minn. Obs.* "A Search for faint blue stars XVII"

Majewski S.R.: 1992a in The Stellar Populations of Galaxies I.A.U. Symp. 149, ed. Barbuy B. and Renzini A. , Kluwer Academic Publishers, Dordrecht, p. 61

Majewski S.R.:1992b, *Astrophys. J. Suppl. Ser.* **78**, 87

Mathis :1990, *Ann. Rev. of Astron. and Astrophys.* **28**, 37

Mayer M.G. and Teller E.:1949, *Phys. Rev.* **76**, 1226

Mayor M.:1976, *Astron. & Astrophys.* **48**, 301

Mazzali P.A., Lennon D.J., Pasian F., Bonifacio P. and Castellani V.: 1993 poster paper presented at IAU Symposium 162 *Pulsation Rotation and Mass Loss in Early–Type Stars* 4–8 ottobre 1993 Nice, France,– in press

Michaud G.:1970, *Astrophys. J.* **160**, 641

Michaud G.:1980, *Astron. J.* **85**, 589

Michaud G., Montmerle T., Cox A.N., Magee N.H., Hodson S.W. and Martel A.:1979, *Astrophys. J.* **234**, 206

Michaud G., Bergeron P., Heber U. and Wesemael F.:1989, *Astrophys. J.* **338**, 417

Miller M.H., Roig R.A. and Bengston R.D.:1971, *Phys. Rev. A* **4**, 1709

Molaro P. and Bonifacio P.:1990, *Astron. & Astrophys.* **236**, L5

Molaro P. and Castelli F.:1990, *Astron. & Astrophys.* **228**, 426

Molaro P., Castelli F. and Primas F.:1993 in *Origin and Evolution of the Elements* eds N. Prantzos, E. Vangioni-Flam and M. Cassè, Cambridge University Press, Cambridge, U.K.

Moon T.T.:1985 *Comm. from the Un. of London Obs.* 78

Moon T.T. and Dworetsky M.M.:1985, *M.N.R.A.S.* **217**, 305

Morgan W.W., Keenan P. and Kellman : 1943 *An Atlas of Stellar Spectra* Chicago University Press, Chicago.

Morgan W.W. and Mayall N.U.:1957, *P.A.S.P.* **69**, 291

Mukai K.:1990, *P.A.S.P.* **102**, 183

Napiwotzki R., Schönberner D. and Wenske V.:1993, *Astron. & Astrophys.* **268**, 653

Neckel Th. and Chini R.:1980, *Astron. & Astrophys. Suppl. Ser.* **39**, 411

Newell E.B., Rodgers A.W. and Searle L.:1969, *Astrophys. J.* **156**, 597

Newell E.B.:1973, *Astrophys. J. Suppl. Ser.* **26**, 37

Nissen P.E.:1989, *The Messenger* **58**, 40

Nissen P.E., Edvardsson B. and Gustafsson B.:1985 in *Production and Distribution of C. N and O elements: Proc. ESO Workshop* Garching, ESO, eds. Danziger I.J., Matteucci F. and Kjär K.

Norman C.A., Renzini A. and Tosi M. eds. 1986 *Stellar Populations* Cambridge University Press, Cambridge U.K.

Norris J.:1981, *Astrophys. J.* **248**, 177

Norris J.:1986, *Astrophys. J. Suppl. Ser.* **61**, 667

Norris J.E. and Ryan S.G.:1989, *Astrophys. J.* **340**, 739

Norris J. and Ryan S.:1989b, *Astrophys. J.* **336**, L17

Norris J.and Ryan S.:1991, *Astrophys. J.* **380**, 403

Norris J., Bessel M. and Pickles A.J.:1985, *Astrophys. J. Suppl. Ser.* **58**, 463

Norris J., Peterson R.C. and Beers T.C.:1993, *Astrophys. J.* **415**, 797

Nussbaumer H. and Storey P.J.:1981, *Astron. & Astrophys.* **96**, 91

Nussbaumer H. and Storey P.J.:1984, *Astron. & Astrophys.* **140**, 383

O'Connell D.J.K. ed. 1958 *Ricerche Astronomiche, Specola Vaticana, Volume 5 : Stellar Populations* North Holland Publishing Co., Amsterdam (reprinted from *Pontificiae Academiae Scientiarum Scripta Varia 16:* Semaine d'Etude sur le Problème des Populations Stellaires

Oke J.B. and Schild R.E.:1970, *Astrophys. J.* **161**, 1015

Oort J.H.:1926 *Pub. Kapteyn Astron. Lab.*, Groningen No. 40

Pagel B.E.J. and Edmunds M.G.:1981, *Ann. Rev. of Astron. and Astrophys.* **19**, 77

Penzias A.A. and Wilson R.W.:1965, *Astrophys. J.* **142**, 419

Peters G.J. and Aller L.H.:, *Astrophys. J.* **1970**, 159525

Peters G.J. and Polidan R.S.:1985 "Calibration of Fundamental Stellar Quantities", I.A.U. Symp. **111**, 121

Popper D.:1947, *Astrophys. J.* **105**, 204

Preston G.W., Shectman S.A. and Beers T.C.:1991, *Astrophys. J.* **375**, 121

Prialnik D. and Kovetz A.:1984, *Astrophys. J.* **281**, 367

Ramella M., Castelli F., Malagnini M.L., Morossi C., Pasian F.:1987, *Astron. & Astrophys. Suppl. Ser.* **69**, 1

Renzini A.:1977 in *Advanced Stages in Stellar Evolution* (Saas-Fee: 7th Course of the Swiss Society of Astronomy).

Relyea L.J. and Kurucz R.L.:1978, *Astrophys. J. Suppl. Ser.* **37**, 45

Rich R.M.:1986 *Ph. D. Thesis* at Caltech

Rich R.M.:1988, *Astron. J.* **95**, 828

Riddiford L. and Butler S.T.:1952 *Phil. Mag.* **43**, 447

Roman N.G.:1950, *Astrophys. J.* **112**, 554

Roman N.G.:1954, *Astron. J.* **59**, 307

Roman N.G.:1955, *Astrophys. J. Suppl. Ser.* **3**, 195

Rood R.T.:1970, *Astrophys. J.* **161**, 145

Rood R.T.:1972, *Astrophys. J.* **177**, 681

Rood R.T.:1973, *Astrophys. J.* **184**, 815

Sadakane K.,Takada M.,Jugaku J.:1983, *Astrophys. J.* **274**, 261

Sandage A.:1969, *Astrophys. J.* **158**, 1115

Sandage A.:1970, *Astrophys. J.* **162**, 841

Sandage A.:1981, *Astron. J.* **86**, 1643

Sandage A.:1986 1986 in Norman *et al.* (1986) p.29

Sandage A. and Fouts G.:1987, *Astron. J.* **93**, 74

Sandage A. and Wildey R.:1967, *Astrophys. J.* **150**, 469

Sanduleak N.:1989, *Astrophys. J. Suppl. Ser.* **71**, 713

Sargent W.L.W. and Searle L.:1967, *Astrophys. J.* **150**, L33

Sargent W.L.W. and Searle L.:1968, *Astrophys. J.* **152**, 443

Searle L. and Sargent W.L.W.:1972, *Astrophys. J.* **173**, 25

Searle L. and Zinn R.:1978, *Astrophys. J.* **225**, 357

Schild R.E., Peterson D.M. and Oke J.B.:1971, *Astrophys. J.* **166**, 95

Schmidt M.:1963, *Astrophys. J.* **137**, 758

Schneider H.:1992 in Proceed. IAU Coll. 138 *Peculiar versus normal phenomena in A-type stars* eds. M. Dworetsky, F. Castelli and R. Faraggiana, ASP Conf. Series n. 44, p. 592

Schroeder D.J.:1967, *Appl. Opt.* **6**, 1976

Schroeder D.J.:1970, *P.A.S.P.* **82**, 1253

Schroeder D.J.: 1987 *Astronomical Optics* Academic Press Inc., San Diego, California, USA

Schwarzschild M. and Schwarzschild B.:1950, *Astrophys. J.* **112**, 248

Schwarzschild M., Spitzer L. Jr. and Wildt R.:1951, *Astrophys. J.* **114**, 388

Singh J. and Castelli F.:1992, *Astron. & Astrophys.* **253**, 431

Spite M.:1992 in *The Stellar Populations of Galaxies* I.A.U. Symp. 149 eds. B. Barbuy and A. Renzini, Kluwer, Dordrecht p. 123

Sterne T.E.:1933, *M.N.R.A.S.* **93**, 736

Stetson P.B.:1991, *Astron. J.* **102**, 589

Straizys V. and Kurilene G.:1981, *Astrophys & Sp. Sci.* **80**, 353

Struve O.:1928, *Nature* **122**, 994

Suzuki S.:1929, *Proc. Phys. Math. Soc. Japan*

Swann W.F.G.:1933, *Phys. Rev.* **43**, 447

Sweigart A.V.:1987, *Astrophys. J. Suppl. Ser.* **65**, 95

Takada-Hidai M.,Sadakane K. and Jugaku J.:1986, *Astrophys. J.* **304**, 425

Talbot R.J. and Arnett W.D.:1970, *Astrophys. J.* **170**, 409

Thompson G.I., Nandy K., Jamar C., Monfils A., Houziaux L., Carnochan D.J., Wilson R.: 1978 *Catalogue of Stellar Ultraviolet Fluxes*, The Science Research Council.

Tolman R.G.:1922, *J. Am. Chem. Soc.* **44**, 1902

Trimble V.:1975, *Rev. Mod. Phys.* **47**, 877

Truran J.W.:1986 in *Nucleosynthesis and its implications on Nuclear and Particle Physics* eds. Adouze & Mathieu, Reidel, Dordrecht p. 97

Truran J.W. and Arnett W.D.:1971, *Astrophys. J. Suppl. Ser.* **11**, 430

Twarog B.:1980, *Astrophys. J.* **242**, 242

Twarog B.:1980b, *Astrophys. J. Suppl. Ser.* **44**, 1

Underhill A. and Doazan V.:1982 *B stars with and without emission lines* - Monograph Series on non–thermal phenomena in stellar atmospheres, NASA SP-456

Underhill A.B., Divan L., Prevot- Burnichon M.L. and Doazan, V:1979, *M.N.R.A.S.* **189**, Microfiche MN 189/1

Upson II W.L. and Rogerson Jr.,J.B.:1980, *Astrophys. J. Suppl. Ser.* **42**, 175

Van Albada G.B.:1947, *Astrophys. J.* **105**, 393

van den Bergh S.:1962, *Astron. J.* **67**, 486

van den Bergh S.:1967, *Astron. J.* **72**, 70

Van der Kruit P. and Searle L.:1982, *Astron. & Astrophys.* **157**, 230

Voels S.A., Bohannan B., Abbot D.C. and Hummer D.G.:1989, *Astrophys. J.* **340**, 1073

Wagoner R.V., Fowler A. and Hoyle F.:1967, *Astrophys. J.* **148**, 3

Wamsteker W., Driessen C., Muñoz J.R., Hassal B.J.M., Pasian F., Barylak M., Russo G., Egret D., Murray J., Talavera A., Heck A.:1989, *Astron. & Astrophys.*

Suppl. Ser. **79**, 110

Westerlund P.E.:1964, *M.N.R.A.S.* **127**, 83

Whitelock P.A.:1991 in *Confrontation Between Stellar Evolution and Pulsation* eds C. Cacciari and G. Clementini, p.365

Wiese W.L. and Martin G.A.:1980, NSRDS-NBS 68 Part II

Wiese W.L.,Smith M.W. and Glennon,B.M.:1966,NSRDS-NBS 4 Ω

Wolf B. and Reitermann A.:1989 *Recent Developments of Magellanic Cloud Research* (Paris 9-11 May 1989), K.S. de Boer, F. Spite, G. Stasinka Eds.; p.23

Woosley S.E. and Weaver T.A.: 1982 in *Supernovae, A Survey of Current Research* eds. M.J. Rees and R.J. Stoneham Reidel, Dordrecht p. 79

Wyse R.F.G. and Gilmore G.:1986, *Astron. J.* **91**, 855

Zinn R.:1980, *Astrophys. J.* **241**, 602

Zinn R.:1985, *Astrophys. J.* **293**, 424

Zinn R.:1986 1986 in Norman *et al.* (1986) p.73